APTD-1172

PB 210 819

Final Report *February 1972*

EVALUATION OF THE APRAC-1A URBAN DIFFUSION MODEL FOR CARBON MONOXIDE

By: F. L. LUDWIG and WALTER F. DABBERDT

Prepared for:

COORDINATING RESEARCH COUNCIL
30 ROCKEFELLER PLAZA
NEW YORK, N.Y. 10020

ENVIRONMENTAL PROTECTION AGENCY
DIVISION OF METEOROLOGY
RESEARCH TRIANGLE PARK, NORTH CAROLINA 27711

CONTRACT CAPA-3-68(1-69)

STANFORD RESEARCH INSTITUTE
Menlo Park, California 94025 · U.S.A.

Reproduced by
NATIONAL TECHNICAL
INFORMATION SERVICE
U.S. Department of Commerce
Springfield VA 22151

162

STANFORD RESEARCH INSTITUTE
Menlo Park, California 94025 · U.S.A.

Final Report

February 1972

EVALUATION OF THE APRAC-1A URBAN DIFFUSION MODEL FOR CARBON MONOXIDE

By: F. L. LUDWIG and WALTER F. DABBERDT

Prepared for:

COORDINATING RESEARCH COUNCIL
30 ROCKEFELLER PLAZA
NEW YORK, N.Y. 10020

ENVIRONMENTAL PROTECTION AGENCY
DIVISION OF METEOROLOGY
RESEARCH TRIANGLE PARK, NORTH CAROLINA 27711

CONTRACT CAPA-3-68(1-69)

SRI Project 8563

Approved by:

R. T. H. COLLIS, *Director*
Atmospheric Sciences Laboratory

R. L. LEADABRAND, *Executive Director*
Electronics and Radio Sciences Division

BIBLIOGRAPHIC DATA SHEET	1. Report No. APTD-1172	2.	3. Recipient's Accession No.
4. Title and Subtitle: Evaluation of the APRAC-1A Urban Diffusion Model for Carbon Monoxide			5. Report Date: February 1972 6.
7. Author(s): F. L. Ludwig and Walter F. Dabberdt			8. Performing Organization Rept. No.
9. Performing Organization Name and Address: STANFORD RESEARCH INSTITUTE, Menlo Park, California 94025			10. Project/Task/Work Unit No. 11. Contract/Grant No. CAPA-3-68(1-69)
12. Sponsoring Organization Name and Address: COORDINATING RESEARCH COUNCIL, 30 Rockefeller Plaza, New York, N. Y. 10020 and ENVIRONMENTAL PROTECTION AGENCY, Division of Meteorology, Research Triangle Park, N. C.			13. Type of Report & Period Covered 14.
15. Supplementary Notes			

16. Abstracts: An experimental program was conducted in St. Louis during the period August through October 1971, for the further development and testing of a practical, multipurpose urban diffusion model (APRAC-1A) for carbon monoxide to determine whether earlier (1970) findings in San Jose, California could be generalized to larger cities with highly developed urban cores. Two adjacent downtown street canyons were instrumented to obtain measurements of CO concentration at 30 points and winds at eight. The instrumented canyons are at right angles to each other and have aspect (height-to-width) ratios of 1.5 and 2.0; these are significantly larger than the value of 0.7 of the site studied earlier in San Jose. Wind, temperature, and CO were also measured to a height of 130 m above the site on a television tower. Helicopter-and van-borne instrumentation was used to supplement data collected with the automated street-canyon instrumentation system. The model was revised to improve the specification of atmospheric stability and small-scale street-canyon effects. The distribution of CO in the street canyon indicates the presence of a single-cell, helical circulation in the deep St. Louis street canyons under cross-street, roof-level flow conditions; the same pattern was found in the shallow San Jose canyon. Carbon monoxide measurements made along the street to within 10 m of the intersection indicate that the street-effects formulation should be applicable in this region. The observed concentrations of CO were simulated with root-mean-square errors of 3-4 ppm. This is half the uncertainty that had been encountered when the model was applied to St. Louis prior to refinements of the stability and diffusion formulations and without the street-effects model. Linear regression (calibration) would reduce the differences by an additional 1 ppm. Median and 90-percentile concentrations were specified within 2-3 ppm by the current model; these errors would be halved by the use of calibrated values.

17. Key Words and Document Analysis 17a. Descriptors

Air pollution
Urban areas
Atmospheric diffusion
Mathematical models
Carbon monoxide
Streets
Wind (meteorology)
Temperature
Aircraft
Mobile equipment
Stability
Field tests
Motor vehicles
Exhaust emissions
Highways

17b. Identifiers/Open-Ended Terms

17c. COSATI Field/Group 13B

Details of illustrations in this document may be better studied on microfiche

18. Availability Statement: Unlimited	19. Security Class (This Report) UNCLASSIFIED	21. No. of Pages 168 162
11	20. Security Class (This Page) UNCLASSIFIED	22. Price 6.00 - 0.95

ABSTRACT

Stanford Research Institute carried out an experimental program in St. Louis during the period August through October 1971, for the further development and testing of a practical, multipurpose urban diffusion model (APRAC-1A) for carbon monoxide to determine whether earlier (1970) SRI findings in San Jose, California could be generalized to larger cities with highly developed urban cores. Two adjacent downtown street canyons were instrumented to obtain measurements of CO concentration at 30 points and winds at eight. The instrumented canyons are at right angles to each other and have aspect (height-to-width) ratios of 1.5 and 2.0; these are significantly larger than the value of 0.7 of the site studied earlier in San Jose. Wind, temperature, and CO were also measured to a height of 130 m above the site on a television tower. Helicopter- and van-borne instrumentation was used to supplement data collected with the automated street-canyon instrumentation system.

The data collected generally confirm the findings of the earlier studies, and only minor revisions of the model were required to improve the specification of atmospheric stability and small-scale street-canyon effects. The distribution of CO in the street canyon indicates the presence of a single-cell, helical circulation in the deep St. Louis street canyons under cross-street, roof-level flow conditions; the same pattern was found in the shallow San Jose canyon. Carbon monoxide measurements made along the street to within 10 m of the intersection indicate that the street-effects formulation should be applicable in this region.

The model was applied using only routinely available meteorological and traffic data. Concentrations were calculated for four locations in the canyons and two at roof level. These calculations were compared with about 600 hour-averaged observations for each location. The observed concentrations of CO were simulated with root-mean-square errors of 3-4 ppm. This is half the uncertainty that had been encountered when the model was applied to St. Louis prior to refinements of the stability and diffusion formulations and without the street-effects model. Linear regression (calibration) would reduce the differences by an additional 1 ppm. Median and 90-percentile concentrations were specified within 2-3 ppm by the current model; these errors would be halved by the use of calibrated values.

It is felt that the APRAC-1A model is now suitable for practical applications.

CONTENTS

ABSTRACT iii

LIST OF ILLUSTRATIONS vii

LIST OF TABLES xi

PROGRAM SUMMARY xiii

ACKNOWLEDGMENTS xix

I INTRODUCTION 1

II EXPERIMENTAL PROGRAM 3

A. General Approach 3

1. Experimental Evaluation of the Submodels . . . 3
2. Experimental Evaluation of the Composite Model 7

B. Description of the Field Program 8

1. Experimental Area 8
2. Instrumentation and Operations 13
3. Data from Other Sources 29

C. Preparation and Analysis of Data 29

1. Mobile Systems 29
2. Street Canyon 31
3. Weather Service Data 34

III EVALUATION OF THE MODEL 37

A. Mixing Height Submodel 37

B. Stability 45

Preceding page blank

CONTENTS (Concluded)

C. Emissions Submodel. 55

1. Traffic Volumes 56
2. Traffic Speeds. 58
3. Emissions Formula 60

D. Winds 73

E. Street Canyon 76

F. Freeway 94

IV PERFORMANCE OF THE MODEL. 101

V CONCLUDING REMARKS. 113

Appendix A--GENERAL DESCRIPTION OF THE MODEL

Appendix B--LIST OF SYMBOLS

REFERENCES

ILLUSTRATIONS

Figure 1	Aerial View of St. Louis Central Business District. . .	9
Figure 2	Intersection Used for Street Canyon Experiments	10
Figure 3	Map of the Area in the Immediate Vicinity of the Locust-Broadway Street Canyon Experiment.	11
Figure 4	Locations of Van and Helicopter Routes and Vertical Sounding Area	12
Figure 5	Freeway Measurement Site, Highway 40 at Forest Park, St. Louis	16
Figure 6	Location of Street Canyon Sensors and Air Inlets. . . .	18
Figure 7	Equipment in Boatmen's Building	19
Figure 8	Organization of Data Acquisition System as Used in St. Louis.	23
Figure 9	Schematic Diagram of Data Collection Sequence	25
Figure 10	Comparisons of Calculated and Observed Mixing Heights	39
Figure 11	Variations of Calculated and Lidar-Observed Mixing Heights with Time.	42
Figure 12	Normalized Concentration as a Function of Stability and Mixing Height	44
Figure 13	Diurnal Emission Patterns for St. Louis	57
Figure 14	Space and Time Variation of CO Concentration over Downtown St. Louis, 31 August 1971.	63
Figure 15	St. Louis Suburban Temperature Profiles	64

Figure 16	Carbon Monoxide Mass Budget Analysis, St. Louis 0800 CDT, 31 August 1971.	67
Figure 17	Carbon Monoxide Mass Budget Analysis, St. Louis 1730 CDT, 23 August 1971.	68
Figure 18	Space Variation of CO over Downtown St. Louis, and Suburban Temperature Profile.	70
Figure 19	Carbon Monoxide Mass Budget Analysis, St. Louis 0730 CDT, 24 August 1971.	71
Figure 20	Carbon Monoxide Mass Budget Analysis, St. Louis 0730 CDT, 24 August 1971.	72
Figure 21	Distribution of CO Concentration in Broadway Street Canyon	78
Figure 22	Distribution of CO Concentration in Locust Street Canyon	80
Figure 23	Locations of Along-Street CO Measurement Sites. . . .	88
Figure 24	Comparison of Along-Street CO Concentrations with Midblock Observations of CO and Winds.	88
Figure 25	Temporal Variation of CO Concentration Adjacent to the Downwind Edge of the Six-Lane Daniel Boone Expressway at Forest Park, St. Louis.	96
Figure 26	Distribution of CO Concentration at 3-m Height Downwind of the Daniel Boone Expressway at Forest Park, St. Louis.	97
Figure 27	Height Variation of CO Concentration Adjacent to the Downwind Edge of the Six-Lane Daniel Boone Expressway at Forest Park, St. Louis.	98
Figure 28	Observed and Calculated CO Concentrations at 4 m. . .	103

Figure 29	Scatter Diagram Showing Observed CO Concentrations Versus Those Calculated with Model.	107
Figure 30	Cumulative Frequency Distributions of Hourly CO Concentrations on Broadway.	110
Figure 31	Cumulative Frequency Distributions of Hourly CO Concentrations on Locust.	111
Figure A-1	Vertical Diffusion According to Gaussian Formulation	A-5
Figure A-2	Vertical Diffusion as a Function of Travel Distance and Stability Category, as Revised for Urban Conditions.	A-5
Figure A-3	Diagram of Segments Used for Spatial Partitioning of Emissions.	A-7
Figure A-4	Computer Display of Traffic Links for Chicago	A-9
Figure A-5	Calculated and Observed CO Concentrations for a Midblock Location in San Jose	A-16
Figure A-6	Observed and Calculated CO Concentrations at the Cincinnati CAMP Station, 14-20 December 1964.	A-17
Figure A-7	Calculated St. Louis CAMP Station CO Concentration Frequency Distribution for 1965 Traffic Conditions--Weekday, Saturday, and Sunday Hours	A-18
Figure A-8	Calculated St. Louis CAMP Station CO Concentration Frequency Distribution for 1990 Traffic Conditions--1-Hour, 8-Hour, and 24-Hour Averages.	A-19
Figure A-9	Calculated St. Louis Concentration Patterns for Two Grid Sizes.	A-21
Figure A-10	Calculated CO Concentrations in St. Louis for Historical and Forecast Traffic Conditions.	A-22

TABLES

Table 1	The Relationship of Stability Category to Standard Deviation of Wind Direction, σ_θ	6
Table 2	Helicopter and Van Operating Periods	15
Table 3	Resolution Limitations Imposed by the Analog-to-Digital Converter	27
Table 4	Approximate Number of Hours of Usable Data Obtained from the Street Canyon Instrumentation	28
Table 5	Percent Occurrence of Various Combinations of Wind Direction Variability and Turner Stability Class	47
Table 6	Joint Occurrence of Turner's Net Radiation Index and Observed Insolation	48
Table 7	Joint Occurrence of Insolation Classes (after Ludwig et al., 1970) and Observed Insolation	49
Table 8	Joint Occurrence of Revised Insolation Classes and Observed Insolation	50
Table 9	Revised Stability Categories	51
Table 10	Percent Occurrence of Various Combinations of Wind Direction Variability and Revised Model Stability Class	52
Table 11	Percent Occurrence of Various Combinations of Wind Direction Variability and Revised Stability Class with Urban Fetch	53
Table 12	Percent Occurrence of Various Combinations of Wind Direction Variability and Revised Stability Class with Nonurban Fetch	54

Preceding page blank

TABLES (Concluded)

Table 13	Average Vehicle Speeds in Downtown St. Louis During the Period 24 August to 2 September 1971. . . .	59
Table 14	Vehicle Speeds for St. Louis	61
Table 15	Carbon Monoxide and Wind Data for Budget Analyses. . .	66
Table A-1	Values of α for Cars Produced After 1970	A-10

PROGRAM SUMMARY

During this research program, the APRAC-1A urban diffusion model was developed to simulate carbon monoxide (CO) concentrations from readily available meteorological and traffic data. The model is based on existing experimental data and previous research results. Carbon monoxide concentrations calculated with the model were initially compared with measured data from Continuous Air Monitoring Program (CAMP) stations; the calculated and observed values often differed significantly in magnitude, although they had similar trends. An extensive measurement program was undertaken in San Jose, California to determine the causes of the discrepancies between calculated and observed concentrations. It was found that local effects in street canyons and around buildings sometimes caused CO concentrations to vary as much as a factor of 3 from one side of the street to the other. It was obvious that these effects must be accounted for if the model were to avoid large errors. One of the principal accomplishments of the research in San Jose was the development of a new submodel to describe street-canyon effects. The submodel substantially improved the agreement between observations and calculations. The San Jose program also uncovered and corrected other shortcomings of the original model. These changes resulted in more realistic specification of atmospheric stability and turbulent diffusion in urban areas.

San Jose is a moderate-sized city, and questions arose as to the general applicability of the results to larger cities with taller buildings. To answer this question another extensive measurement program was undertaken in St. Louis. The results of that program are discussed in this report.

One of the primary concerns of the St. Louis research has been the evaluation of the performance of the street effects submodel in street

canyons deeper than those studied in San Jose. In the earlier work it was found that roof-level winds blowing across a street canyon will cause a helical circulation in the canyon. At street level the cross-street air movement is opposite to the roof-level wind direction, causing a downflow of relatively clean air in front of the "downwind" buildings that face the roof-level wind, and an upflow across the street. The resulting street-level CO concentrations in front of the downwind buildings may be significantly less than those observed across the street.

We wished to investigate whether the helical circulation found in the relatively shallow San Jose street canyon (with a height-to-width ratio of about 0.7) was typical of circulations in the deeper street canyons of larger cities; wind tunnel studies had suggested that under light wind and low turbulence conditions a double-helical circulation might develop (e.g., Chang et al., 1971).* To test the generality of the San Jose observations, two street canyons, with height-to-width ratios of about 1.5 and 2, were instrumented in St. Louis, so that CO concentrations could be measured on both sides of each street at five heights, from 4 m to roof level. Concentrations were also measured in midstreet at about 7 m and at roof level at about 35 m. Winds in the street canyon were measured on either side, at roof level and at 4-1/2 m. Larger-scale airflow and CO concentrations in the area were monitored with instrumentation up to a height of 130 m on a television transmitting tower on top of a building at the intersection of the two streets. These data are available on magnetic tape from the National Climatic Center, Asheville, North Carolina.

The data collected show that a single-helix circulation is found in the deep street canyons of St. Louis and that the simple model developed from the San Jose data is fundamentally correct for these deeper canyons. Some slight modifications were required to account for the entrainment of

* References are given at the end of the report.

recirculating polluted air in the downward-flowing part of the helical circulation. There had been evidence of this entrainment in the San Jose data also. In the revised version of the street canyon submodel, the air is presumed to begin its downward flow at roof level concentration. Carbon monoxide is then added so that the concentration increase is linear with decreasing height. At street level the original and revised models give the same concentration. That concentration is based on "box model" reasoning, i.e., the CO concentration is inversely proportional to street width and wind speed, and directly proportional to the emissions in the street canyon. For the upwind side of the street, no changes were required in the street effects model. It is still based on box model reasoning; the volume into which the emissions can be mixed is limited by the helical circulation that transports street emissions toward the buildings. As the air moves from the source, the volume into which the pollutants are mixed increases, so the concentration is taken to be inversely proportional to the straight-line distance from the receptor and the nearest traffic lane.

The data indicate that the helical circulation develops when the roof level winds are at an angle of more than 30^{o} to the street directions. When the winds are more nearly parallel to the street, cross street gradients were found to be small. For winds parallel to the street, the street canyon effects submodel describes the vertical gradients as an average of the two expressions used when the winds are blowing across the street. The small changes that were made in the street model have improved its ability to predict the CO gradients in the street canyons. Observations made at street level with mobile equipment indicate that the street-canyon submodel is applicable through most of the block, at least to within about 10 m of the intersection.

The submodel used to calculate atmospheric stability was revised to give results that are more consistent with the fluctuations of wind

direction observed on the television tower. During the evaluation of the stability model, it was found that for a given stability type, there was appreciably greater fluctuation in wind direction when the air had an urban fetch than when it had a nonurban fetch. This fact lends support to the revisions made during an earlier phase of the program that effectively increased diffusion rates in the urban situation as compared to the rural.

Model calculations of mixing depth were compared with lidar (laser radar) observations of the aerosol layer from a concurrent program sponsored by the National Science Foundation, and with radiosonde measurements of the temperature profile near the downtown center. It was concluded from these comparisons that the mixing depth submodel does about as well as is possible using routinely available data.

Helicopter and van measurements of CO concentrations around the downtown area were combined with wind speed measurements so that a mass budget analysis could be performed to estimate the rate of CO emissions by traffic in the study area. The emissions model was also applied to the same area and the results were compared. Uncertainties in the wind field, possible changes in CO emission rates during the measurement periods, and uncertainties in traffic amounts all contribute to the difficulties in making reliable comparisons, but the results should be good enough to uncover serious deficiencies in the model. On the average, the three cases analyzed in St. Louis and the four earlier cases from San Jose show agreement within a factor of 2 between the two methods. With the data currently available there does not seem to be sufficient justification for changing the submodel.

The revisions and additions that have been made in the model since it was originally formulated have substantially improved its performance. When the revised model was applied in St. Louis and compared with observed hour-average CO concentrations, the root-mean-square difference (RMSD)

between the calculated and observed values ranged from 2.6 to 3.9 ppm depending on the particular observation site. This is about half the uncertainty of the original model when it was applied to this same city. If the calculated and observed data are fit by linear regression, the corresponding RMSD's are reduced to values between 1.6 and 3.3 ppm. The correlation coefficients between calculated and observed CO have been improved substantially. They are now in the range 0.4 to 0.7, as opposed to the 0.2-to-0.4 range found before revision.

The ability of the model to specify frequency distributions of concentration is good. Median and 90-percentile concentrations are specified within about 2 and 3 ppm of the observed values, respectively. Use of regression relationships derived from the observed concentrations and those calculated with the model reduces the error in specifying median and 90-percentile concentrations to about 1.3 ppm.

The APRAC-1A model is now sufficiently accurate that it can be used for planning purposes, and a users manual has been prepared (Mancuso and Ludwig, 1972). Some improvements and extensions are still desirable, including better specification of emissions and a new submodel to describe the effects that take place in the immediate vicinity of a freeway.

ACKNOWLEDGMENTS

The authors appreciate the support provided by the Coordinating Research Council and the Air Pollution Control Office (EPA) and the assistance furnished by the representatives of these agencies on the CAPA-3 monitoring committee: J. F. Black (Chairman), A. P. Altshuller, J. M. Colucci, R. P. Doelling, C. R. Hosler, W. B. Johnson, R. G. Larson, F. J. Mason, J. J. Mitchell, J. S. Seward, I. Solomon, and A. E. Zengel.

The authors are grateful to a number of SRI personnel for their assistance. E. Uthe provided the lidar data used in the evaluation of the computations of mixing depth. E. L. Younker, F. H. Burch, and W. B. Guthoerl were responsible for the design and construction of the computerized data collection system. B. Wheeler and T. Humphrey did the programming for the minicomputer. During the field operations in St. Louis, R. Allen, A. H. Smith, W. Guthoerl, J. Kealoha, N. Nielsen, L. Salas, A. Pijma, and S. Mueller gave assistance. G. L. Williams, H. Shigeishi, R. Trudeau, A. H. Smith, R. Hadfield, A. Imada, J. Kealoha, and L. Salas assisted in various aspects of data reduction and analysis. V. Small, M. Kucinski, E. Cox, S. Hanson, M. Taylor, and P. Monti all aided in the preparation of this and other project reports.

The authors are also grateful to the owners and managers of the buildings where our equipment was located: the Boatmen's Bank Building, the First National Bank Building in St. Louis, and the Federal Reserve Bank. Mr. Robinson, Manager of the Boatmen's Bank Building, and his staff were particularly helpful. The personnel of Fostaire Helicopter Service were extremely cooperative in the help that they provided in mounting our equipment and providing storage space.

Preceding page blank

The personnel of several government agencies were particularly helpful in providing access to their data. These included G. Brancato and the National Weather Service station staff at Lambert Field, D. Wuerch of the Environmental Monitoring Support Unit, C. Copley and the staff of the St. Louis Air Pollution Control Commission, the St. Louis Department of Streets, and the Missouri Department of Highways.

Mrs. Doris Wallace of McDonnell Douglas Automation Company was helpful in expediting the analysis of our data.

I INTRODUCTION

The long-term objective of this research program is the development of a methodology for predicting the concentrations of motor-vehicle-generated air pollutants throughout an urban area as a function of local meteorology and the distribution of traffic. The resulting methodology is intended to be used as a tool in planning activities for the prediction of the pollution patterns in any urban region that will result from planned traffic changes or predicted growth and also as an operational tool for short-term prediction.

The achievement of the long-term objective set forth in the preceding paragraph requires that several intermediate objectives be satisfied. In this program we have undertaken the development of a mathematical model of the transport and diffusion of a relatively inert automotive pollutant, carbon monoxide. The nature of the model has been governed by the desire to make it a useful planning tool for application in a variety of cities. We have attempted to develop a model whose data requirements are neither elaborate nor esoteric, but are readily satisfied by routine observations

This program of research is envisioned as having four major steps:

(1) Developing a practical urban diffusion model for carbon monoxide

(2) Testing and improving the model as much as possible with special experimental programs

(3) Extending the applicability of the model: to reactive pollutants, to smaller computational

facilities, to direct coupling with traffic or economic models, etc.

(4) Further testing of the model in its extended applications.

At this time the second step has been completed. Within the practical constraints mentioned above, we believe that the model does as well as is possible with present knowledge. Furthermore, it is organized in a modular fashion so that new developments in urban meteorology, such as better data or better techniques for specifying mixing height and other parameters, can be incorporated relatively easily.

This report is primarily devoted to the description of the final phases of the testing and improvement process. The model development and the earlier stages of the testing and improvement have been covered in detail in two reports already issued (Ludwig et al.,1970; Johnson et al.,1971). Some things are repeated here to provide background for the descriptions of the extensive field program conducted in St. Louis and for the treatment and interpretation of the data resulting from that field program.

This report documents the final technical evaluation of the model that has been developed under this program. It has been given the name APRAC-1A, a nomenclature intended to acknowledge both the role of the sponsoring committee and the fact that this is the first version of what could be a series of more comprehensive or more specialized models.

II EXPERIMENTAL PROGRAM

A. General Approach

The purpose of the experimental program has been to provide the data necessary to evaluate the performance of the diffusion model and its components. To do this, it has been necessary to obtain special measurements that can be compared, either directly or indirectly, with the values of the various parameters derived by the model from generally available input information. Appendix A reviews the ways in which the model treats the available information. The first parts of this section describe the approaches used to evaluate the model's components, and the necessary measurements. These are followed by a discussion of the field program that was undertaken to provide some of the required data.

An earlier report described a prior experimental program that we conducted in San Jose, California (Johnson et al., 1971). Inasmuch as the experimental program described here generally extends that work to a larger city (St. Louis), it has not been necessary to repeat much of the detailed information presented in the earlier report and its Appendices. The techniques and equipment used in the two cases were similar.

1. Experimental Evaluation of the Submodels

a. Emissions

Evaluation of the emission submodel required some method of determining the rate at which CO is generated in the urban area. This method should be independent of traffic measurements, because traffic

measurements are the fundamental data source used by the model. The method chosen is based on the fact that the net flux of some conservative property or material through a closed surface is equal to the total rate at which that property or material is generated within the volume enclosed by the surface. In practice we have had to make some reasonable assumptions. These are:

(1) Carbon monoxide is conserved during its residence time in the volume studied.
(2) The mean wind varies only in the vertical through the volume studied.
(3) The net horizontal turbulent flux of CO is negligible compared to its transport by the mean wind.
(4) Vertical transport of CO through the top of the studied volume is negligible.

The conservative nature (inertness) of CO has been established for the relatively short periods involved in the experimental program (Junge, 1963). The area that was studied was reasonably homogeneous and only about 1 km on a side, so the assumption of horizontal uniformity of the wind should be justified. The third assumption depends on there being no gradient of emissions or turbulence across the penetrable boundaries of the volume. This is generally true for the scale of the experiments. For measurements with a resolution of a city block or so, the distribution of CO sources in the area studied can be considered to be reasonably uniform, as can the turbulence field.

The final assumption is valid because the observations show that the vertical gradients of CO are quite small at the top of the studied volume (about 335 m), so the turbulent fluxes of the material must be relatively small. The vertical transport by mean motions is also small because the mean vertical motions themselves are usually small.

The two measurements required to determine the net flux of CO from a selected volume under the specified assumptions are the wind field and the CO concentration at the boundaries of that volume. Because of the assumed horizontal uniformity of the wind field, the U.S. Weather Service's Environmental Meteorological Support Unit (EMSU) profile data obtained at the Arch were sufficient. If we choose a volume with vertical sides, then the distribution of CO needs to be measured only on those sides, because our assumptions allow no flux of CO through the top of the volume, and the physical presence of the ground surface prevents fluxes through the bottom.

In summary, the approach outlined above requires measurements of winds at various levels above the surface. It also requires measurements of CO concentrations on the vertical surfaces of some chosen volume, in our case, a rectangular box. The methods used to obtain these measurements are described later.

b. Atmospheric Stability

The stability of the atmosphere describes the intensity and direction of the flux of sensible and latent heat in conjunction with the momentum flux; as such, it is related to the structure of the turbulence and hence can be used to describe the nature of the diffusion process.

Stability categories can, in turn, be determined from the variability of the wind direction. According to Gifford (see Slade, 1968, Chapter 3), the stability categories used in the model calculations are related to the standard deviation of the wind direction σ_θ as shown in Table 1. The values of σ_θ shown in the table are those that would be calculated from data collected over a period of about 10 minutes to an hour. Each wind direction value in the total sample should represent the average wind direction over a very short period such as a few seconds. Since typical wind vanes tend to have response times of a few seconds, "instantaneous" values from such instruments will be suitable for deter-

Table 1

THE RELATIONSHIP OF STABILITY CATEGORY
TO STANDARD DEVIATION OF WIND DIRECTION, σ_θ

σ_θ Degrees	Stability Category
25	1, extremely unstable
20	2, moderately unstable
15	3, slightly unstable
10	4, neutral
5	5, slightly stable
2.5	6, moderately stable

mination of the values of σ_θ required by Table 1. Stability values from the submodel can be compared with measured values of σ_θ to assess the submodel's performance in terms of an independent parameter.

The submodel's ability to determine the stability category from readily available meteorological information depends in part on the determination of daytime surface heating, using observations of opaque cloud cover and solar elevation. The model's estimates of insolation can be checked against measurements of the radiative power received at the surface. Such measurements are helpful in determining the source of possible inaccuracies in the procedures used to determine stability category.

c. Mixing Height

As used in the model, the mixing height is that height to which surface-generated materials can reach; it is the upper boundary of the mixing layer. This concept of mixing height suggests one method for its determination. If this concept is satisfied, then the upper boundary of the mixing layer should be marked by a sharp decrease with

height in surface-generated pollutants. Measurements of the vertical distribution of pollutants, such as CO or particulates, that are released within the mixing layer can help define the extent of that mixing layer.

Another commonly employed approach to the determination of mixing height makes use of the distribution of temperature in the vertical. The top of the mixing layer is often marked by a layer of increased atmospheric stability, which in turn is characterized by an increase in value of the rate of change of temperature with height, dT/dz.

d. Street Canyon Effects

Unlike the preceding items, the distribution of carbon monoxide in street canyons is directly observable. Testing the street canyon effects requires that we observe these effects and see if they agree with the results of the parameterization that has been devised. The CO concentrations and airflows in and around the street canyons must be measured with considerable detail and accuracy.

2. Experimental Evaluation of the Composite Model

After the individual components of the model have been tested, then the composite must be tested. This is straightforward. The questions to be answered are:

1) How accurately does the model calculate CO concentrations for specific times and places?
2) How accurately does the model reproduce the concentration frequency distribution for given locations?

To answer the above questions, we must provide accurate measurements of CO concentrations and the information necessary to make the calculations with the model.

B. Description of the Field Program

On the preceding pages, we have described the general approaches that we have used to evaluate the model and its components. The types of data necessary for the application of the approaches have been discussed. The following pages describe the program that was undertaken in St. Louis to obtain the necessary data.

1. Experimental Area

St. Louis was chosen as the area in which to extend the experimental program that was begun in San Jose. St. Louis has the primary requisites that were sought. It is significantly larger than San Jose, has a well-developed downtown area with deep street canyons, and is relatively free of unusual and complicating topographical features that might mask fundamental problems in the model. Furthermore, a significant number of studies of urban diffusion and local meteorology had already been conducted there (e.g., Stanford Aerosol Laboratory, 1953, Pooler, 1966; McElroy and Pooler, 1968; and Wuerch, 1970, 1971); these represented a considerable source of information that might be useful in the interpretation of our own data. Finally, there were several other studies of urban meteorology planned for St. Louis at about the same time as our field program and thus there was the possibility of obtaining some additional data that might not otherwise have been available.

Within St. Louis we sought an area of deep street canyons with relatively uniform building heights, in which we could collect the data necessary to evaluate the street effects submodel. For this we chose the area near the corner of Locust Street and Broadway in the central business district. Figure 1 is an aerial photograph of the central business district; Figure 2 is a closer view of the intersection used for the street effects studies. A map of the nearby areas is given in Figure 3 ; this shows approximate building heights (in standard-height "floors").

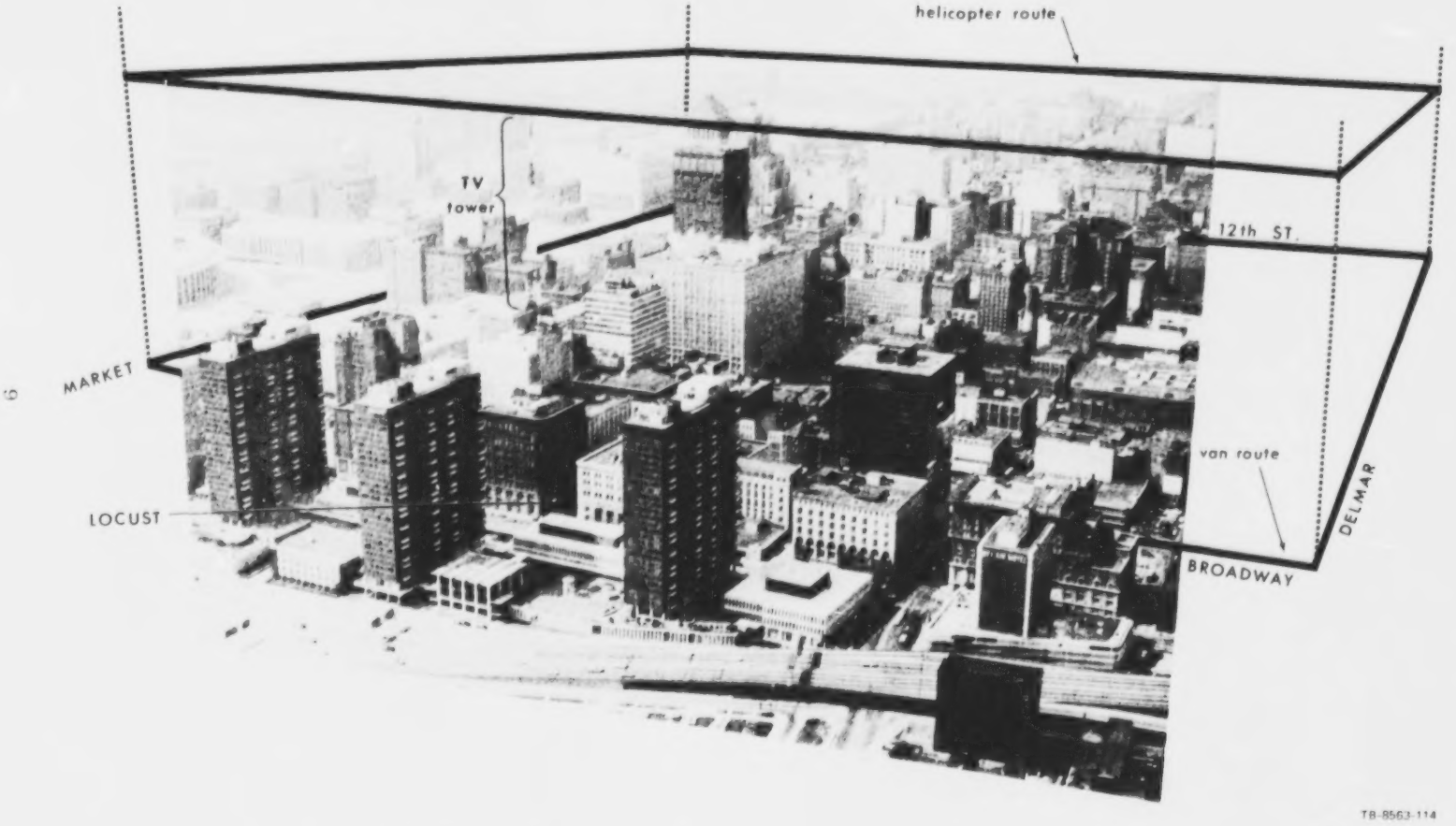

FIGURE 1 AERIAL VIEW OF ST. LOUIS CENTRAL BUSINESS DISTRICT

FIGURE 2 INTERSECTION USED FOR STREET CANYON EXPERIMENTS

The chosen location was instrumented to study two street canyons, at right angles to each other. One of the buildings at the selected site also had the television transmission tower shown in Figure 1; it extended to about 160 m above street level. This allowed us to measure winds, temperatures, and CO concentrations well away from the street effects.

As indicated in earlier sections, evaluation of some of the models required vertical profiles of temperature and pollutant concentrations. Evaluation of the emissions submodel required measurements of CO at various levels around the perimeter of some area with significant CO sources. The area chosen is shown on the map in Figure 4. It surrounds the area shown in Figure 1. The map and photograph are marked to show the route followed by an instrumented van and helicopter during the experiments designed to determine emission rates. The rectangular

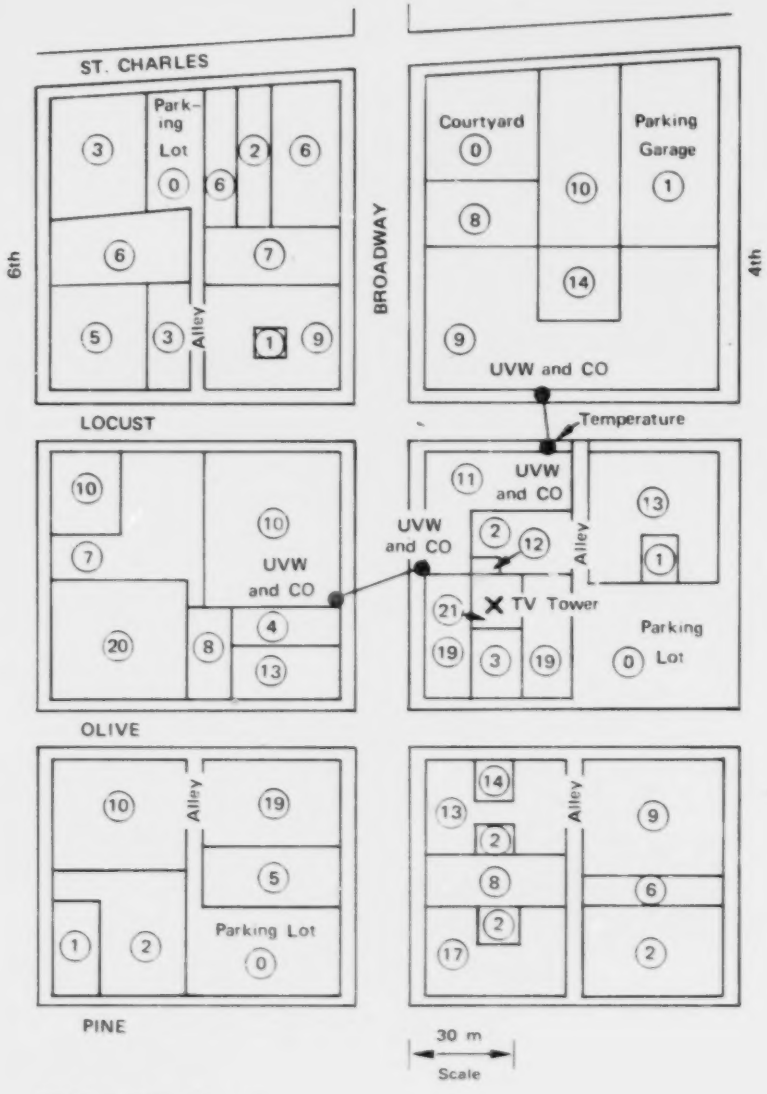

Circled numbers are
approximate number of floors.

TA-8563-110

FIGURE 3 MAP OF THE AREA IN THE IMMEDIATE VICINITY OF THE LOCUST-BROADWAY STREET CANYON EXPERIMENT

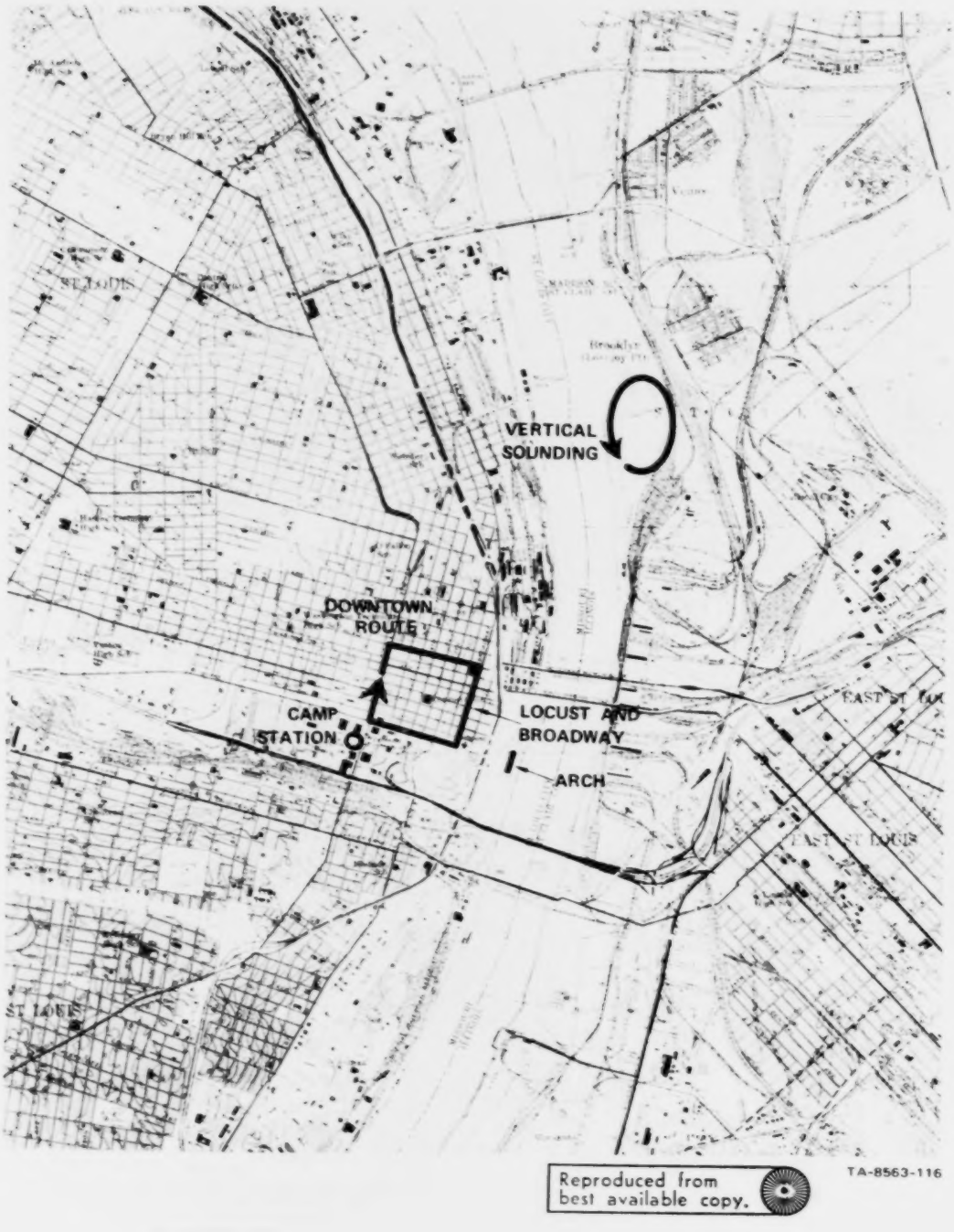

FIGURE 4 LOCATIONS OF VAN AND HELICOPTER ROUTES AND VERTICAL SOUNDING AREA

route surrounds the downtown area and has the street experiment site along the east edge, which permits the incorporation of data from that instrumentation with those from the mobile units.

Figure 4 also shows the area over which the instrumented helicopter measured vertical profiles of CO concentration and temperature, and the Gateway Arch which serves as a launch site for twice-daily balloon releases by the National Weather Service's Environmental Meteorological Support Unit (EMSU). These balloon soundings provided temperature, humidity, and wind profile measurements up to 3 km. The figure shows that all locations are within a few kilometers of each other.

2. Instrumentation and Operations

a. Mobile

A helicopter and a van were instrumented to measure CO concentration and temperature. The equipment has already been described in detail elsewhere (Johnson et al., 1971), and so only the general characteristics will be described here. For the CO measurements, filtered air was drawn through a few meters of polyethylene tubing from the front of the vehicle. By having inlets at the front, interferences from the helicopter's downwash or the van's exhaust were avoided when the vehicles were moving forward. The CO analyzers used in the van and in the Bell helicopter were manufactured by the Bacharach Instrument Co.* In these instruments the sampled air is passed through a bed of heated mercuric oxide; any CO present reduces the oxide and releases mercury vapor which can be quantitatively detected through its spectral absorption of ultraviolet radiation.

Temperatures were measured using radiation shielded thermistors. The data were recorded on strip charts, along with marks made by the operator to identify certain locations or significant events.

---

* 2300 Leghorn Ave., Mountain View, California 94040.

The CO analyzers were generally calibrated with gases of known CO concentration (0 and 11 ppm for the helicopter, 0 and 21 ppm for the van) before and after an experiment. It took about 45 minutes to an hour to complete an experiment. During this time, the van was driven around the rectangular route shown in Figures 1 and 4. The helicopter crossed to the east side of the Mississippi River and then climbed upward in the area shown by the spiral in Figure 4. During this period, the operator kept the CO analyzer flow rate constant and marked the charts at height intervals of 50 feet, as determined from the helicopter altimeter.

After completing the vertical sounding to about 610 m, the helicopter recrossed the river and began its first circuit of the route from the northeast corner at a height of 115 m. At the end of that circuit the helicopter circled and gained altitude over the area north of the route, while the operator adjusted the instrument in preparation for the second circuit at a height of 150 m. This routine was repeated at heights of 215, 275, and 335 m.

Most of the mobile measurements were made during the latter part of August 1971, a period during which other groups were conducting atmospheric studies (Changnon, 1971), e.g., of airflow over the city and the vertical distribution of atmospheric aerosols. We attempted to collect data during the morning, evening, and midday periods of heavy traffic, as well as the forenoon and afternoon periods in between. Table 2 shows the approximate time intervals during which data were collected for use in evaluating the emissions submodel.

In addition to the mobile measurements that were made in conjunction with the helicopter flights, the van was also used to make special observations downtown and in the vicinity of a heavily traveled highway. Carbon monoxide measurements were made at a variety of locations

Table 2

HELICOPTER AND VAN OPERATING PERIODS
(Central Daylight Time)

Date	Morning	Forenoon	Midday	Afternoon	Evening
23 Aug 71		0905-0955			1730-1820
24 Aug 71	0730-0820		1145-1235	1430-1520	1630-1720
28 Aug 71	0730-0820	0930-1020	1145-1235	1445-1535	1630-1720
31 Aug 71	0730-1820	0930-1020	1145-1235		1630-1720
1 Sept 71			1100-1150	1330-1420	1630-1720
2 Sept 71	0730-0820	0930-1020	1145-1235	1430-1520	1630-1720

on Locust Street and Broadway to examine along-street variations of CO with respect to the continuous observations at the fixed sampling sites. Because of local traffic regulations, the van could not be parked during the rush periods and so the observations were usually made between 0900 and 1600 CDT. As an additional check, the van was also operated at the Continuous Air Monitoring Project (CAMP) station at the intersection of 12th and Clark Streets (see Figure 4 and the discussions in Ludwig et al., 1970). Local contamination by the van itself for these stationary applications was avoided because the instrumentation is powered by storage batteries and it is not necessary to run the engine; a more detailed description of the van system is given by Johnson et al. (1971).

The van borne instrumentation system was also used to make measurements for basic studies of the diffusion of CO in the immediate vicinity of a freeway. An area in Forest Park, shown in Figure 5, was chosen for these studies. With the prevailing summertime wind flow from the south, the air moves progressively from a well-mixed region with no

concentrated CO sources over the six-lane Daniel Boone Expressway and into the adjacent Forest Park area. Measurements were made during the early morning hours during the peak freeway traffic period, and traffic within the park did not influence the local concentration. The measurements were of four types: (1) time series at a fixed point, (2) vertical profiles to 11-m height, (3) horizontal profiles to 200 m downwind of the freeway, and (4) horizontal traverses throughout the park.

b. Fixed Installation, Street Canyon

Location of Equipment. Photographs of the street canyon experimental site have already been presented in Figures 1 and 2. A diagram of the location of the various street canyon sensors and air sampling inlets is shown in Figure 6. These locations have also been indicated in Figure 3. Air sampling inlets were placed at fifteen locations in each of the two street canyons and at five heights on the

FIGURE 5 FREEWAY MEASUREMENT SITE, HIGHWAY 40 AT FOREST PARK, ST. LOUIS

tower seen in Figure 6. The inlets on the tower were at about 85, 93, 100, 116, and 131 m above street level. The base of the television tower was about 70 m above street level.

Three-component wind sensors were located at the top and bottom of the vertical arrays in the street canyons, as shown in Figure 6. Propeller-vane wind sensors were placed at two levels on the tower, 90 m and 131 m above the street. Temperature profile measurements (five-level) were made on the south side of the Locust Street canyon at the same heights as, and adjacent to, the CO profile, and also on the tower at 86, 95, 101, 116, and 130 m above the street. Two traffic counters were used to count the vehicles that passed on the two streets where the equipment was located.

The CO analyzer used with the air sampling inlets on the TV tower was located in a room just below the base of the tower. The electronics required to process the tower wind and temperature signals were also located in this room. All the rest of the electronic equipment and CO analyzers were located in a room on the tenth floor of the Boatmen's Building (Figure 7). As can be seen in Figure 2, the tubing and cables from the air inlets and the wind, temperature, and traffic sensors in the two street canyons were brought to this central location for signal conditioning, processing, recording, and preliminary analysis.

Carbon Monoxide. Nondispersive infrared analyzers were used to measure the CO concentrations.* They have a 40-inch-long absorption cell and use an optical filter to remove the effects of of water vapor interference. They have a sensitivity of about 0.5 ppm. It was necessary to calibrate the instruments twice daily. The room at the foot of the television tower was not air-conditioned, and more frequent

*Beckman Instruments, Model 315-AL.

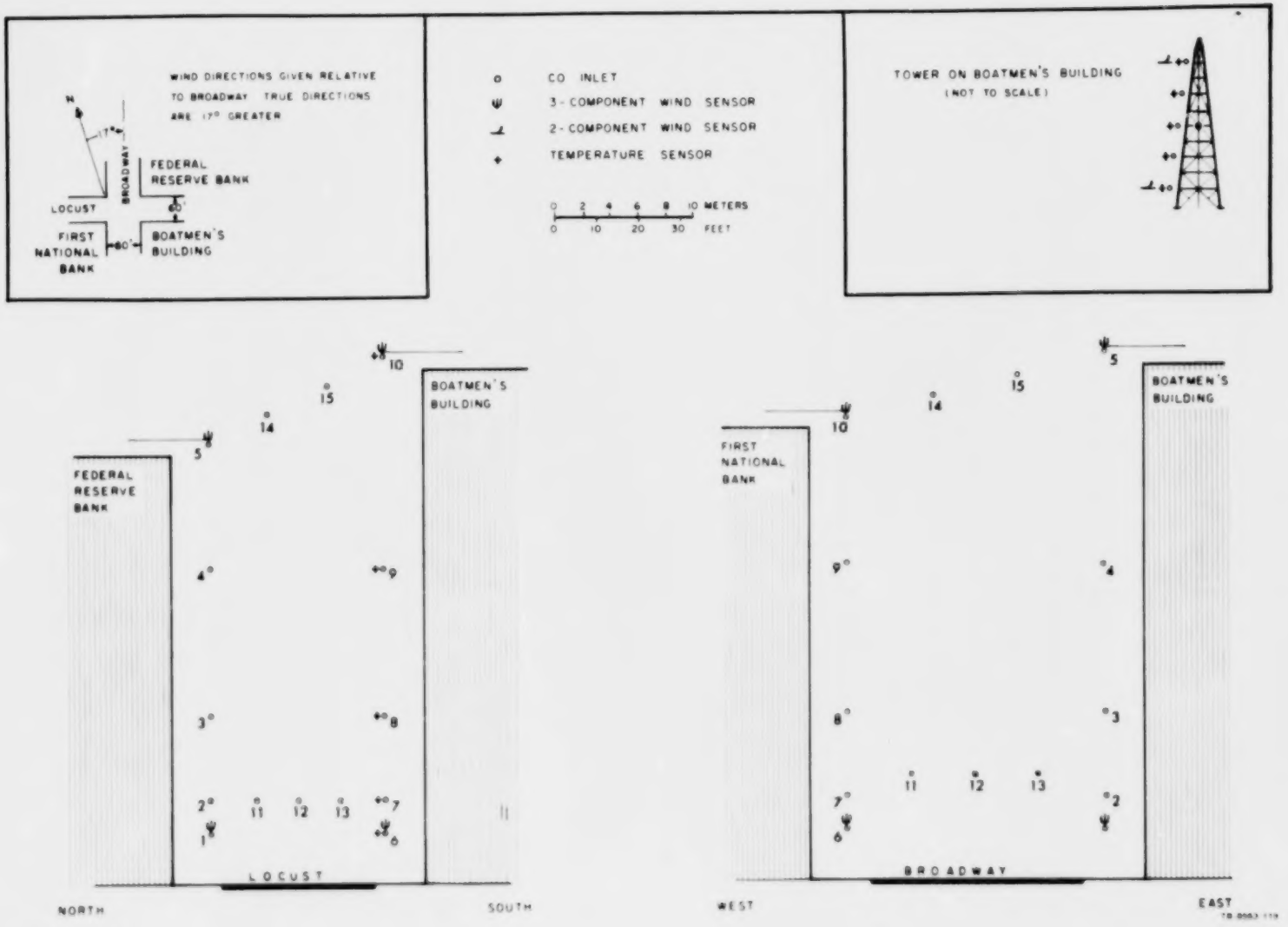

FIGURE 6 LOCATION OF STREET CANYON SENSORS AND AIR INLETS

FIGURE 7 EQUIPMENT IN BOATMEN'S BUILDING

calibrations were required for that instrument. Zero adjustments were made using high purity helium. The span was adjusted using a mixture of 21-ppm CO in nitrogen prepared and analyzed by the Matheson Company. All instruments were calibrated with gases from the same sources. Air was brought to the analyzers from the various sampling points through 1/4-inch-ID polyethylene tubing. Tests conducted earlier (Johnson et al., 1971) indicated that polyethylene tubing as used on this program does not interfere with the CO measurements. Filters at the tubing inlets removed particulates that might affect CO analyzer operation. The tubing lengths ranged from 40 m to 100 m; tests showed that air entering the longest tube reached the CO analyzer in about 20 seconds. The air sampling inlets were connected in groups of five to manifold systems. Each manifold system used computer-controlled solenoid-actuated valves to switch the CO analyzer from one inlet to another. The four levels that were not being sampled at any given time were continually purged with an auxiliary pump. Thus, the CO analyzer pump did not need to exhaust dead air from the tubing when air from a new level was switched to the instrument.

Wind. Three-component winds were measured at two levels on the four vertical arrays: at 4.5 m height and just above the roof level; the sensors protruded 3 m from the buildings. Each instrument* used three orthogonally oriented, low-inertia propellers to measure three wind components (u,v,w).

Winds on the tower were measured with propeller and vane type sensors.** The propellers on these instruments, like those on the three-component sensors, have a low starting speed, about 0.2 m s^{-1}.

*R. M. Young Co. Model 27002/27302

**R. M. Young Co. Model 35002-35402/35602

Vertical Temperature Gradient. Platinum wire resistance elements* were used to measure vertical temperature gradients. These elements were mounted in 0.125-inch stainless steel tubes. These tubes were housed in radiation shields of silvered, double-walled glass cylinders similar to Dewar flasks and were ventilated at a rate of about 5 m s^{-1}.** The time constant of the aspirated, steel-housed sensor was about 40 seconds. Temperature differences of as little as 0.01°C between sensors could be detected.

Traffic Counters. The capability to count traffic and record the counts with the other data was added to the system used for our earlier studies in San Jose (Johnson et al., 1971). Vehicle passage is sensed by contact closure in a pneumatically operated switch (like those used in gasoline stations to alert the operator of the presence of a customer). These closures are detected by a buffer circuit with 80-millisecond response time and then counted by an 8-stage binary counter. This digital number is converted to an analog voltage by a commercially available digital-to-analog converter.*** The traffic count is accumulated for approximately 90 seconds and then entered into the system. Within 0.3 second, the counter is reset and the count for the next time interval is started. A maximum of 127 vehicles can be counted in 90 seconds. At a speed of 10 m s^{-1} (22 mph), separate vehicles can be detected i they are spaced at least 80 cm apart.

Control and Data Acquisition System. A small general-purpose computer**** with a magnetic tape recorder controlled the data

*Rosemount Engineering Model 104 MK-57-BB-CC

**R. M. Young Co. Model 43404

***Zeltex Co.

****Data General Corp., NOVA.

collection and CO analyzer manifold switching operations. Nine separate remote units accepted commands from the computer via a 20-mA dc circuit, digitized the voltage inputs from the sensors, and transmitted the data back to the computer via another 20-mA dc circuit. The computer was connected to the two dc circuits through a line coupler. The organization of the various components of the data acquisition system is shown schematically in Figure 8. The system has been described in detail in an appendix of an earlier report (Johnson et al., 1971).

The computer sends a command message, consisting of two characters, to all the remote units. The first character is an address code that is recognized by only one remote unit. On recognition of the address code, the activated remote unit sends its data message to the computer. The second character of the command message (inlet code) indicates which inlet is to be opened by those units controlling the air sampling inlet manifolds. The data message returned to the computer from the remote unit consists of the inlet code stored at the time of the preceding command, followed sequentially by the digitized data from the sensors connected to that unit. The data message ends with the identifying character of that control unit. Each measurement was transmitted as a 7-bit binary number plus even parity.

After the computer received the complete message, it checked the identification code to verify that it corresponded to the address that was transmitted. Then another unit was commanded to report. The timing of command messages was derived from the computer's real-time clock in a programmed sequence. The sequence for the St. Louis experiment (shown schematically in Figure 9) was as follows: The three-component winds were sampled for about 8 seconds, or about 2 times each; these data were recorded on magnetic tape. This was followed by the sampling of about 2 seconds of temperature and traffic data. This, in turn, was followed by 44 seconds of CO concentrations and tower winds--

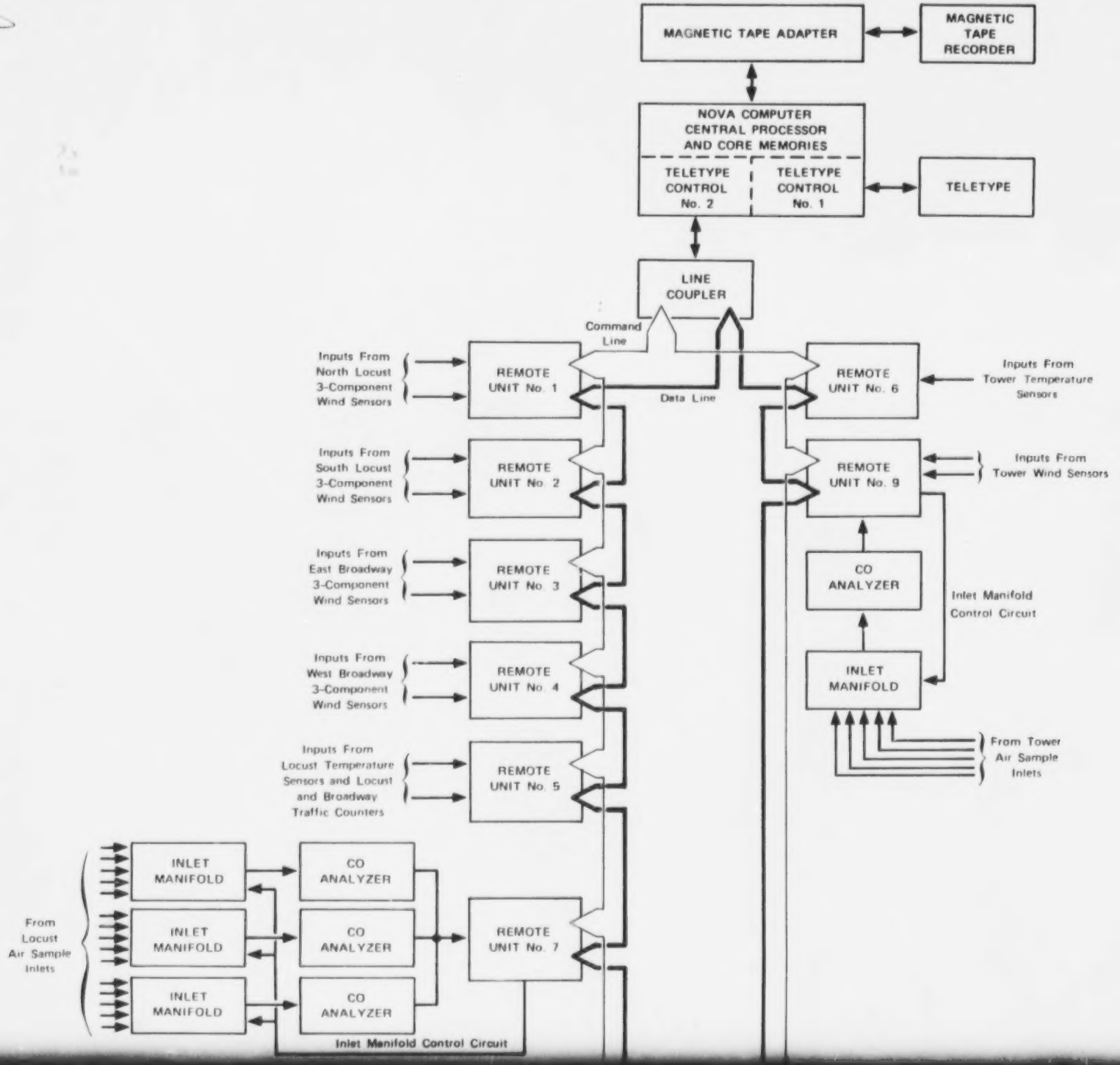
MAGNETIC TAPE ADAPTER
MAGNETIC TAPE RECORDER
NOVA COMPUTER CENTRAL PROCESSOR AND CORE MEMORIES
TELETYPE CONTROL No. 2
TELETYPE CONTROL No. 1
TELETYPE
LINE COUPLER
Command Line
Data Line
Inputs From North Locust 3-Component Wind Sensors
REMOTE UNIT No. 1
Inputs From South Locust 3-Component Wind Sensors
REMOTE UNIT No. 2
Inputs From East Broadway 3-Component Wind Sensors
REMOTE UNIT No. 3
Inputs From West Broadway 3-Component Wind Sensors
REMOTE UNIT No. 4
Inputs From Locust Temperature Sensors and Locust and Broadway Traffic Counters
REMOTE UNIT No. 5
REMOTE UNIT No. 6
Inputs From Tower Temperature Sensors
REMOTE UNIT No. 9
Inputs From Tower Wind Sensors
CO ANALYZER
Inlet Manifold Control Circuit
INLET MANIFOLD
From Tower Air Sample Inlets
From Locust Air Sample Inlets
INLET MANIFOLD
INLET MANIFOLD
INLET MANIFOLD
CO ANALYZER
CO ANALYZER
CO ANALYZER
REMOTE UNIT No. 7
Inlet Manifold Control Circuit

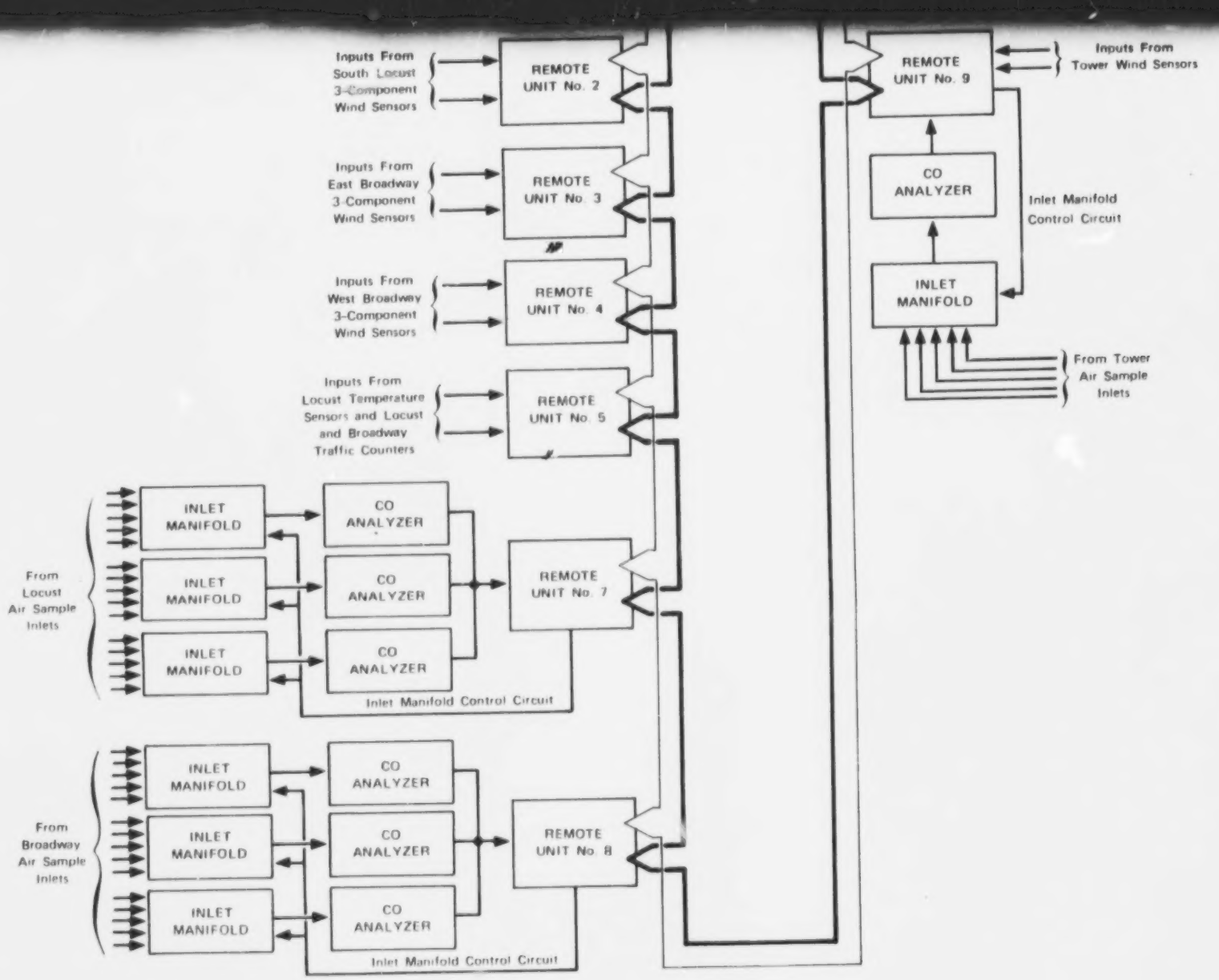

NOTE Remote units 6 and 9 were located in room below TV tower, other equipment were located in a room on the tenth floor of the Boatmen's Building.

T8-8563-111R

FIGURE 8 ORGANIZATION OF DATA ACQUISITION SYSTEM AS USED IN ST. LOUIS

Preceding page blank

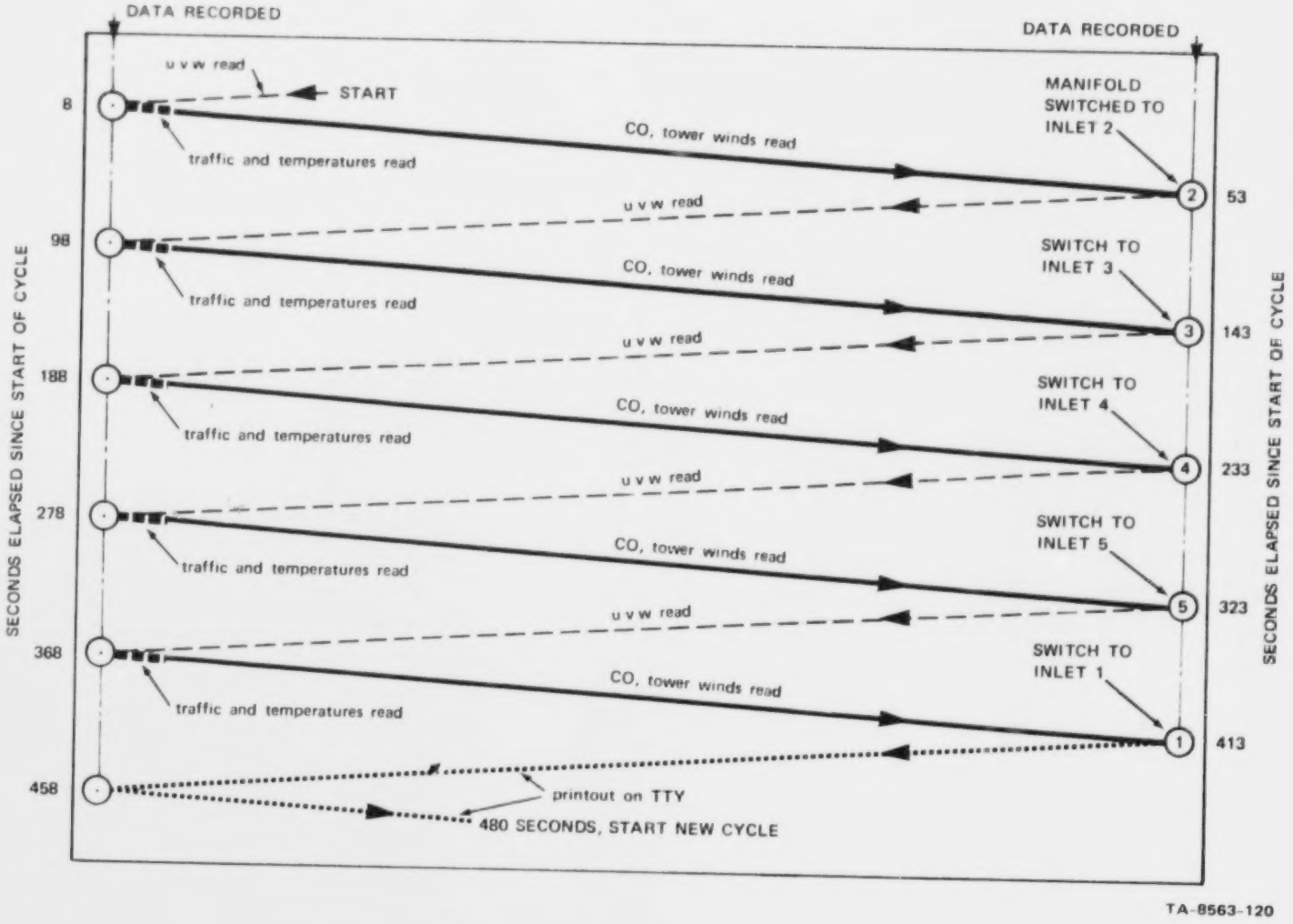

TA-8563-120

FIGURE 9 SCHEMATIC DIAGRAM OF DATA COLLECTION SEQUENCE

about 16 values of each. At the last sampling of the CO data, the inlet manifold valves were switched to another level, and the accumulated data were recorded on magnetic tape. The three-component winds were read for 44 seconds (about ten times each), then traffic and CO again. After the CO values had been recorded for the fifth time, average values of all parameters (except traffic) for the preceding 7 minutes were displayed on a teletype, so that equipment performance could be monitored. The complete sampling cycle began anew after the teletype printout.

The digitizing of the data for transmission, processing, and recording imposed certain resolution limits on the observations. We have tried to keep these consistent with the accuracies of the sensors. Table 3 summarizes the resolution imposed by the analog-to-digital conversion for the various parameters.

Operations. The equipment for the street experiment was shipped to St. Louis and installed during the early weeks of August 1971. The system was tested and the necessary calibrations were completed; some limited data collection began August 26. This was before all the installation was complete on Locust Street. (Data from the tower sensors were recorded on the teletypewriter commencing August 23 in order to support the mobile measurement program.) We continued to collect data while making the final installations, which were completed by September 2, 1971. The next few days were spent checking to see that the equipment was all operating properly, in anticipation of starting round-the-clock data collection.

On the afternoon of September 5, a lightning strike on the tower atop the Boatmen's Building did extensive damage to the system. Data collection was not resumed until September 12, and then only on a limited basis. Repair work continued during the following week and by September 19 the system was returned to near normal operation. There were malfunctions of various pieces of equipment

Table 3

RESOLUTION LIMITATIONS IMPOSED BY THE ANALOG-TO-DIGITAL CONVERTER

Parameter	Range	Resolution
Wind components	-20.3 to +20.3 m s^{-1}	0.16 m s^{-1}
Wind speed	0 to 20.3 m s^{-1}	0.16 m s^{-1}
Wind direction	0 to 360^{o}	3^{o}
Temperature difference	-1 to +1^{o}C	0.008^{o}C
Carbon monoxide concentration	0 to 50 ppm	0.4 ppm
Traffic count	0 to 127 vehicles	1 vehicle

during the ensuing weeks and many of these appeared to be related to the damage sustained September 5.

We had originally planned to operate the traffic counters 24 hours per day, but we encountered some difficulties. The hoses that stretch across the street were damaged by street sweepers during the night on several occasions, so it was necessary to bring them in during the late night and early morning hours. Calls to the Street Department and wrapping the hoses with high visibility tape minimized the problem, so that traffic data were successfully collected during the early morning hours on many days during the last three weeks of operation.

Table 4 summarizes the hours of data collection for the street experiment. Data collection began August 26 and ended October 15. The equipment was taken down, packed, and returned to California during the last weeks of October and early November.

Table 4

APPROXIMATE NUMBER OF HOURS OF USABLE
DATA OBTAINED FROM THE STREET CANYON INSTRUMENTATION

Date	N. Locust UVW	S. Locust UVW	East Broadway UVW	West Broadway UVW	Tower Winds	Locust Temp.	Tower Temp	N. Locust CO	S. Locust CO	Mid-Locust CO	East Broadway CO	West Broadway CO	Mid-Broadway CO	Tower CO	Locust Traffic	Broadway Traffic
Aug 26	4	11	11	11	11	11	11	3	3	3	11	11	11	11	4	4
27	13	13	13	13	13	13	13	13	13	13	13	13	13	0	9	9
28	13	13	13	13	13	9	13	9	9	9	13	13	12	8	13	13
29	12	12	12	12	12	12	12	12	12	12	12	12	12	11	10	10
30	13	13	13	13	13	13	13	13	13	13	13	13	13	13	12	12
31	14	14	14	14	14	14	14	14	14	14	14	14	14	14	12	12
Sep 1	17	17	17	17	16	17	17	17	17	17	17	17	17	17	15	15
2	16	16	16	9	16	16	16	16	16	16	14	16	16	14	15	15
3	16	16	16	16	15	16	15	16	16	16	16	16	16	16	13	13
4	14	14	14	14	14	14	14	14	14	14	14	14	14	14	13	13
5	6	6	6	6	3	6	6	3	6	6	0	6	5	6	6	6
12	5	0	5	5	0	0	0	0	5	0	5	5	5	5	0	0
13	10	0	18	18	0	9	9	11	18	9	11	17	17	10	7	7
14	0	0	18	18	0	18	0	14	16	15	13	16	13	12	16	16
15	12	12	24	24	0	24	0	23	24	24	24	24	24	8	15	15
16	24	24	24	24	0	24	0	20	24	20	24	14	24	24	17	17
17	24	24	24	24	7	24	7	22	24	0	24	0	24	12	16	16
18	16	16	16	16	16	16	16	16	16	6	16	6	16	16	0	0
19	24	24	24	24	24	24	24	24	24	24	24	24	24	24	14	14
20	20	20	20	20	20	20	20	20	20	20	20	20	20	19	20	20
21	24	24	24	24	24	18	24	14	24	22	16	19	19	16	16	16
22	24	24	24	24	24	24	24	24	24	24	14	24	24	24	24	24
23	24	24	24	24	24	24	24	19	23	18	24	24	24	11	24	24
24	24	24	24	24	24	24	24	17	24	22	24	17	24	9	12	12
25	11	11	11	11	11	11	11	11	11	4	11	11	11	0	13	13
30	12	12	12	12	12	12	12	12	12	12	11	12	12	1	12	12
Oct 1	21	21	21	21	21	21	21	21	20	21	15	21	21	21	9	9
2	23	23	23	23	23	23	23	17	23	16	23	23	23	15	16	16
3	15	15	15	15	15	15	15	9	15	9	15	15	15	15	24	24
4	23	23	23	23	23	23	23	18	23	18	23	23	23	20	21	21
5	24	24	24	24	24	24	24	24	24	24	24	24	24	22	16	16
6	22	22	22	22	22	22	22	22	22	15	22	22	22	21	13	13
7	16	16	16	16	16	16	16	15	16	16	16	16	16	16	8	8
8	24	24	24	24	24	24	24	24	24	24	24	24	24	24	18	18
9	13	13	13	13	13	13	13	13	13	13	13	13	13	13	13	13
10	24	24	24	24	24	24	24	24	24	24	24	24	24	24	24	24
11	24	24	24	24	24	24	24	24	5	24	24	24	24	24	24	24
12	24	24	24	24	24	24	24	24	0	24	24	24	24	24	24	24
13	24	24	24	24	24	24	24	24	12	24	24	24	24	24	22	22
14	24	24	24	24	10	24	20	24	24	24	24	24	24	9	24	24
15	11	11	11	11	0	11	9	11	11	11	11	11	11	0	10	10
Totals	704	696	719	742	613	725	645	671	675	640	704	690	736	587	594	594

3. Data from Other Sources

a. Meteorological

Conventional meteorological surface observations are taken at Lambert Field, about 22 km northwest of the downtown area. Rawinsonde measurements are made twice daily, nominally at 0500 and 1700 CDT, 110 km east of St. Louis at Salem, Illinois. Special urban soundings are taken by the National Weather Service at the Arch, about 700 m southeast of Locust Street and Broadway. These soundings are made Monday through Friday twice daily at about 0700 and 1230 CDT.

In addition to the conventional National Weather Service data mentioned in the preceding paragraph, there were a number of special meteorological measurements during the summer in connection with the METROMEX program (Chagnon, 1971). These measurements included detailed pilot balloon studies of winds and lidar soundings of the depth of the polluted layer. The lidar measurements have been quite useful in the evaluation of the mixing depth submodel.

b. Air Pollution

Air pollution measurements are made at several locations in the St. Louis area by the St. Louis Pollution Control Commission. There is also a station of the Continuous Air Monitoring Program (CAMP) in St. Louis. Data from these sources have been used only minimally in this study, largely because of the difficulties in integrating them with the project's magnetic tape data records.

C. Preparation and Analysis of Data

1. Mobile Systems

The van and helicopter instrumentation systems employed identical sensors for the measurement of air temperature and carbon monoxide concentration; details are given in an earlier report by Johnson et al.

(1971). The voltage outputs of the sensors were amplified and recorded on strip chart recorders in both systems, while the van system also used an instrumentation magnetic tape recorder (H-P Model 3960A*) in parallel as a backup device.

Preceding and following each helicopter flight, calibration checks were made of the CO analyzer electronic reference signals as well as the outputs from zero (high purity nitrogen) and span (10-ppm CO) gases. In-flight checks of the reference signal and zero gas were also made. This provided a reasonably comprehensive history of instrument performance during the course of each flight. Atmospheric mixing serves to filter small-scale variations of both temperature and CO, and so it was possible to obtain representative profiles by relatively low-frequency digitization of the analog chart record: For the vertical profiles, 15-m increments were used to 150 m height and 30-m increments at higher levels; 140-m intervals were used along the horizontal traverses. The digital chart values and the pre-, post-, and in-flight calibration and check data were entered into a Wang 720/702 Programmable Calculator/Plotter** for processing and display. All input and identification data were displayed in addition to the calculated value and its location. For the traverse data, segment averages were automatically computed and listed.

The van data were processed somewhat differently because of the larger and more frequent fluctuations that occur near to the earth's surface and also near the CO sources. When the van operated in a mobile configuration, spatial averages were required over specific route segments, while time averages were required when the van was stationary. One-hour

---

* Hewlett-Packard, Palo Alto, California

** Wang Laboratories, Inc., Tewksbury, Massachusetts

averages (compatible with fixed-station values) were used while studying along-street variations in the Locust and Broadway street canyons. The chart records were marked to identify the periods,and a simple, graphical average was computed. Calibration data were applied as with the helicopter analysis.

Observations at the freeway site were both limited and of a special, nonroutine nature and so an alternative procedure was used. The analog chart record was digitized so that both the mean and standard deviation of the observed CO concentrations could be computed.

The data records on magnetic tape served as a backup for those periods when the chart recorder failed. The data were then retrieved by one of two methods, depending on the purpose of the observations. For most cases, the analog output from the tape recorder was used to generate a new chart record which was analyzed by the methods described above. For statistical studies of fine-scale fluctuations, the analog data were input to a probability density analyzer which digitizes the signal at a prescribed rate and stores the data in the form of a probability density histogram. The "density" is then transferred automatically through a hardware interface to the programmable calculator which can analyze the data to obtain the mean, variance, skewness, and kurtosis of the distribution. This procedure was not used routinely, but provided a check on the mean values determined by more conventional arithmetic or graphical averaging.

2. Street Canyon

The street canyon data are quite extensive, and it was necessary to perform some editing and condensation. The data handling began by translating the binary data as originally recorded to the binary-coded decimal used for subsequent processing. During this preliminary processing, hourly average values were calculated for the various measured parameters along with standard deviations. Although these averages did not include some of the corrections employed in later processing, they did allow us

to assess the quality of the data that had been recorded on magnetic tape and make necessary corrections. Some of the preliminary processing was done in St. Louis using the facilities of the McDonnell Douglas Corporation. This allowed the staff in St. Louis to check equipment operation quite rapidly.

During the translation of the tapes the recorded voltages were converted to engineering units. Next, corrections were made for drift in the output of the CO analyzers. The following procedure was adopted. The true CO readings were assumed to be represented by

$$(CO)_{true} = c + d(CO)_{read} \quad . \tag{1}$$

Immediately following calibration, the values of c and d were taken to be 0 and 1, respectively, because the calibration results in the reading of the true concentration. During calibration the reading of the instrument before adjustment was recorded while it was sampling CO-free gas. This reading was used as -c for the period just prior to the calibration time. Before adjusting the span setting the change in reading was determined when a gas of known CO concentration (21 ppm) was introduced to replace the CO-free gas. For the period just prior to calibration, the factor d equaled the ratio of the change in reading that should have been observed for the calibration gas to the change that actually was observed. Between calibrations, the values of c and d were assumed to change linearly with time.

When the recorded CO concentrations were corrected, some data were eliminated. These included cases where adjustments may have been made while instruments were still on line. Actually, most equipment remained on line all the time; the recorded data included a "mode code" (see Johnson et al., 1971, Appendix A) whose value specified whether data were good or were to be ignored. Switches on the equipment changed the mode code values appropriately, but sometimes the switches were set improperly. Generally, these cases were discovered and noted in the

station log. It was at this point that the appropriate corrections were made in the recorded figures.

Next, the data were consolidated into a master tape similar to the summary tape described in Appendix D of the Comprehensive Report (Johnson et al., 1971). Although this tape is similar to that described in the earlier report, there are differences. On the St. Louis summary tape, carbon monoxide observations have been summarized in much the same way as the wind components were summarized on the earlier tape; i.e., for each period, the sum of the observed values, the sum of the squares of the observed values, and the number of measured values for each inlet are recorded. On this new tape we have also included sums of the cubes of observed CO readings so that skewness of the frequency distribution of observed values can be determined if desired. Wind component summaries are also included, as before.

There are other differences between the current summary tape and the earlier one. Each record of the earlier version summarized the data collected during a 5-minute period; the St. Louis data tape records cover 7-minute periods, because of the longer sampling cycle. We have reduced the considerable redundancy of the earlier summary; e.g. the date appeared numerous times in a single record. Also some of the identification numbers for CO analyzer inlets that were previously recorded explicitly are now implicit in the formatting of the records.

The summary records for St. Louis contain traffic data that are quite useful in interpreting the data. We have also included standard deviations of the wind directions measured on the tower. These have been related to the stability categories, as suggested elsewhere (Pasquill, 1961, or Slade, 1968). The standard deviations were determined by first calculating the vector-average wind direction and then the root-mean-square deviation between the individual wind directions and this average.

Some of the traffic data contained in the records were not measured. The traffic flow data for those periods when measurements were not available were based on the available measured values for the same hour of the day and day of the week. The observed traffic data indicate that there are variations in hourly averaged traffic of about 10 to 20 percent about the average.

Copies of the summary tape are available to interested persons from the National Climatic Center in Asheville, North Carolina.

The summary tape has been used for the calculation of all the averages presented in subsequent sections of this report. Hourly averages were calculated for the entire period and these have been used for comparisons with values determined from the model and its components. The data for each 7-minute period have also been stratified according to the values of different parameters. For instance, averages were calculated for all those cases where certain combinations of wind speed and wind direction (as measured by the TV tower instrumentation) were observed. The averages of these stratified data have helped us to analyze the importance of different variables.

3. Weather Service Data

The hourly meteorological data obtained from the National Weather Service have been used primarily for the application of the diffusion model and its submodels. The information from records of hourly observations for the period August 20 to October 15, 1971 at Lambert Field was copied at the Weather Service office. The data copied included those necessary for use with the model, i.e., wind speed and direction, temperature, and opaque cloud cover. Eventually the data needed by the model were transferred to punched cards.

The significant levels of the Salem, Illinois rawinsonde station were obtained in punch card form from the National Climatic

Center in Asheville, North Carolina. These cards could be used directly by the model.

The low level sounding data were copied at the National Weather Service Office in St. Louis. These sounding data are not the type that the model was designed to use. However, they have provided good, independent estimates of the atmospheric mixing height over the downtown area for comparison with mixing heights determined by the model using Salem, Illinois data.

III EVALUATION OF THE MODEL

The diffusion model is composed of a number of submodels. This design allows us to check the performance of these submodels individually and to make improvements where necessary without disrupting the overall structure. In the following sections the outputs of the most important submodels are compared with data specially collected during this program or with other independent sources of data. Weaknesses are diagnosed and improvements made where possible.

A. Mixing Height Submodel

The mixing height submodel has three distinct parts. First, there is the part that calculates the mixing height for the early morning hours. Second is that part that calculates the maximum mixing height during the day, and finally is the routine that interpolates to obtain values for the other hours of the day.

Both morning and afternoon mixing heights are based on the nearest radiosonde temperature profile that is collected at about dawn. Both are determined from the intersection of this sounding and the dry adiabat that passes through the temperature at the surface. For the afternoon mixing height, the maximum temperature measured at the airport is used. For the morning value, the downtown urban temperature is determined using the sounding and an empirical relation developed by Ludwig et al. (1970). The rationale underlying the model comes from the fact that the lapse rate within a well mixed layer will be adiabatic in the absence of condensation. The afternoon mixing height calculations also assume no change in the temperatures above the mixing layer during the period following the morning sounding.

Preceding page blank

The interpolation during daylight hours is based directly on the surface temperature variations, and the rationale is the same as discussed above. During the hours from midnight until dawn, the mixing height is taken to remain constant at its predawn value. This is based on observations that the urban heat island is generally stable, with relatively constant urban-rural temperature differences (Ludwig and Kealoha, 1968). From sundown through midnight, time-based interpolation is used.

In this section, the different parts of the model will be evaluated using different sources of independent data. Several days of lidar data collected on another SRI project* were available and probably provide the best check on all aspects of the model. The lidar mixing height was determined as the level where there was a sudden decrease in backscattered energy. This sudden decrease corresponds to a drop in aerosol concentration. Since most of the aerosol particles are generated at the surface, the lidar is essentially measuring the height to which they and other pollutants are mixed. This is a direct measurement of the parameter.

Figure 10(a) shows values of mixing height determined from lidar observations plotted against the values calculated from the model using the morning sounding taken at Salem, Illinois and hourly temperatures from Lambert Field. The figure shows that the model tends to overestimate midday values and underestimate dawn values. Of the 19 cases available, 16 (84 percent) calculated values are within a factor of 2 of the lidar observations and 12 (63 percent) are within a factor of 1.5.

Temperature soundings made in the urban area are another source of independent mixing depth measurements. Using the fact that the mixing layer should be characterized by lapse rates near the adiabatic

---

*National Science Foundation Grant GA 30435, "Lidar Observation in St. Louis."

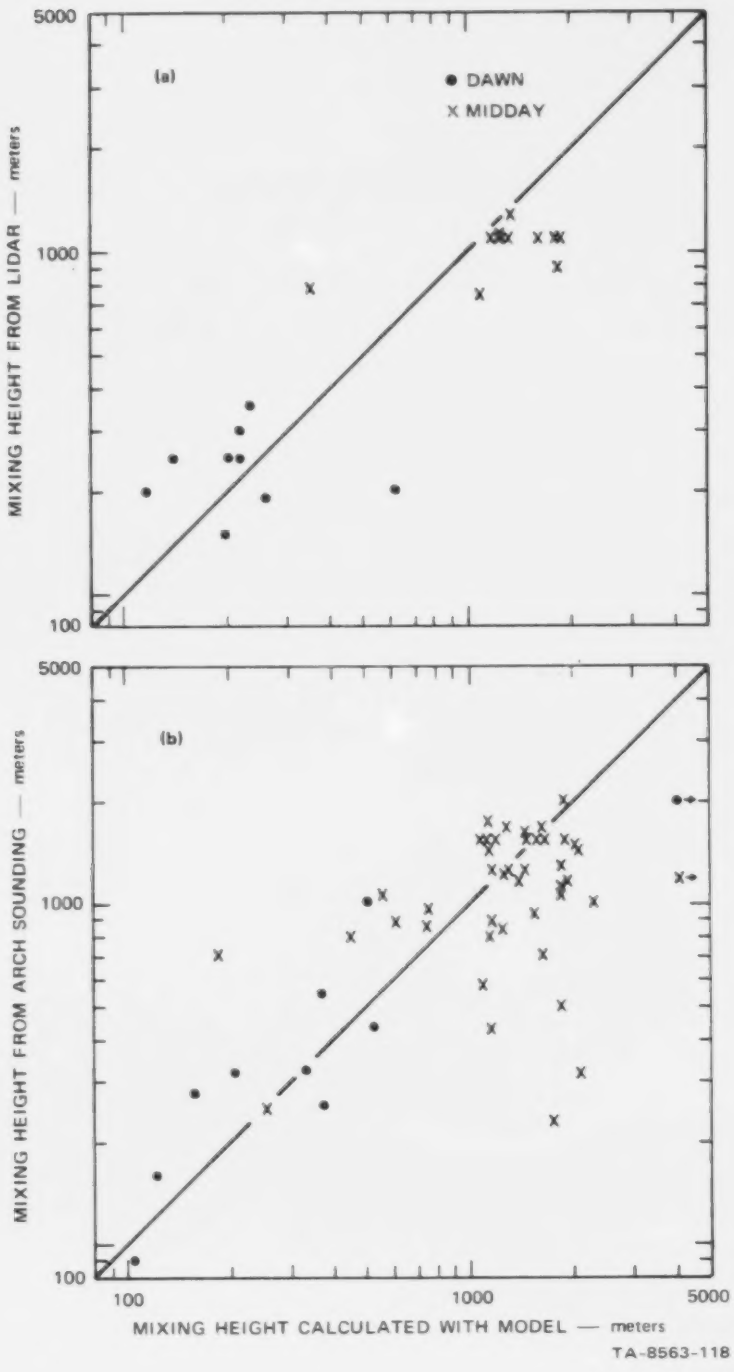

FIGURE 10 COMPARISONS OF CALCULATED AND OBSERVED MIXING HEIGHTS

(0.01° C m^{-1}), the top of the mixing layer should be marked by a significant deviation from this value. The objective method that was used to define the mixing depth selected the bottom of that layer where the lapse rate falls below 75 percent of the adiabatic. This criterion was applied to 43 EMSU soundings taken near midday at the St. Louis Gateway Arch during the months of August, September, and October 1971. The lowest 100 meters were ignored because it was felt that that layer was too likely to be affected by local heating and hence not representative.

The soundings taken at dawn were often affected by the local surface cooling in the park area surrounding the launch site. Thus most of these soundings were typified by an inversion beginning at the surface and extending to heights of 200 to 750 m. It was assumed that the mixing layer over the urbanized area was within that inversion layer. There were 33 such cases and the mixing height determined from the model was less than the height of the top of the inversion in all but three cases. In the worst of these exceptions, the model specified an 800-m mixing height, 280 m above the inversion top.

There were ten soundings that could be used to determine mixing depth at dawn, i.e., they had either no surface inversion or only a very shallow one. For these soundings the mixing height was taken to be the bottom of the lowest elevated stable layer. The mixing heights obtained using this criterion and the midday mixing heights obtained by the objective technique described earlier are plotted in Figure 10(b) versus the corresponding values specified by the model. The agreement is generally good. In 83 percent of the cases the model values are within a factor of 2 of the values obtained from the sounding; in 68 percent the agreement is within a factor of 1.5. This is comparable to the results that Wuerch (1970) obtained when predicting midday mixing depths using the dawn sounding at the Arch (as opposed to the Salem, Illinois sounding) and the midday surface temperature at the Arch (as opposed to

the Lambert Field surface temperature). Thus it appears that the model does about as well with routine data as is likely to be possible.

Continuous lidar measurements of the mixing height during four August days were used to evaluate the interpolation scheme used by the model. The mixing heights from the two sources are compared in Figure 11. The first three days had relatively few clouds that attenuated the insolation, while the fourth day shown was overcast for most of the morning and early afternoon hours. As a result surface temperatures rose rather rapidly after sunrise on the first three days. Therefore, the calculated value of mixing height increased rapidly because the interpolation scheme is based on surface temperature. The lidar observations show a much slower increase in mixing height during these hours. It is apparent, and reasonable, that the postdawn morning mixing height, which is a product of solar heating, responds to that heating with considerable lag. The model should probably include a provision of this sort, but at present the available theory and experimental information are both inadequate to formulate such a feature with confidence that it would be generally applicable.

On August 23 and 24 the lidar observations continue into the evening hours and another feature of the mixing layer behavior is evident. As cooling at the lowest layers begins in the late afternoon and early evening, a stable layer develops near the surface. This stable layer caps the mixing, so the transition from the afternoon to the evening mixing heights is nearly discontinuous; there is an abrupt drop. The performance of the model could undoubtedly be improved if this behavior were included in the interpolation scheme. Unfortunately, the available theory and experimental data again do not permit this to be incorporated at this time.

The interpolation scheme used by the model does a good job of showing the diurnal mixing height trend on the overcast day, August 25.

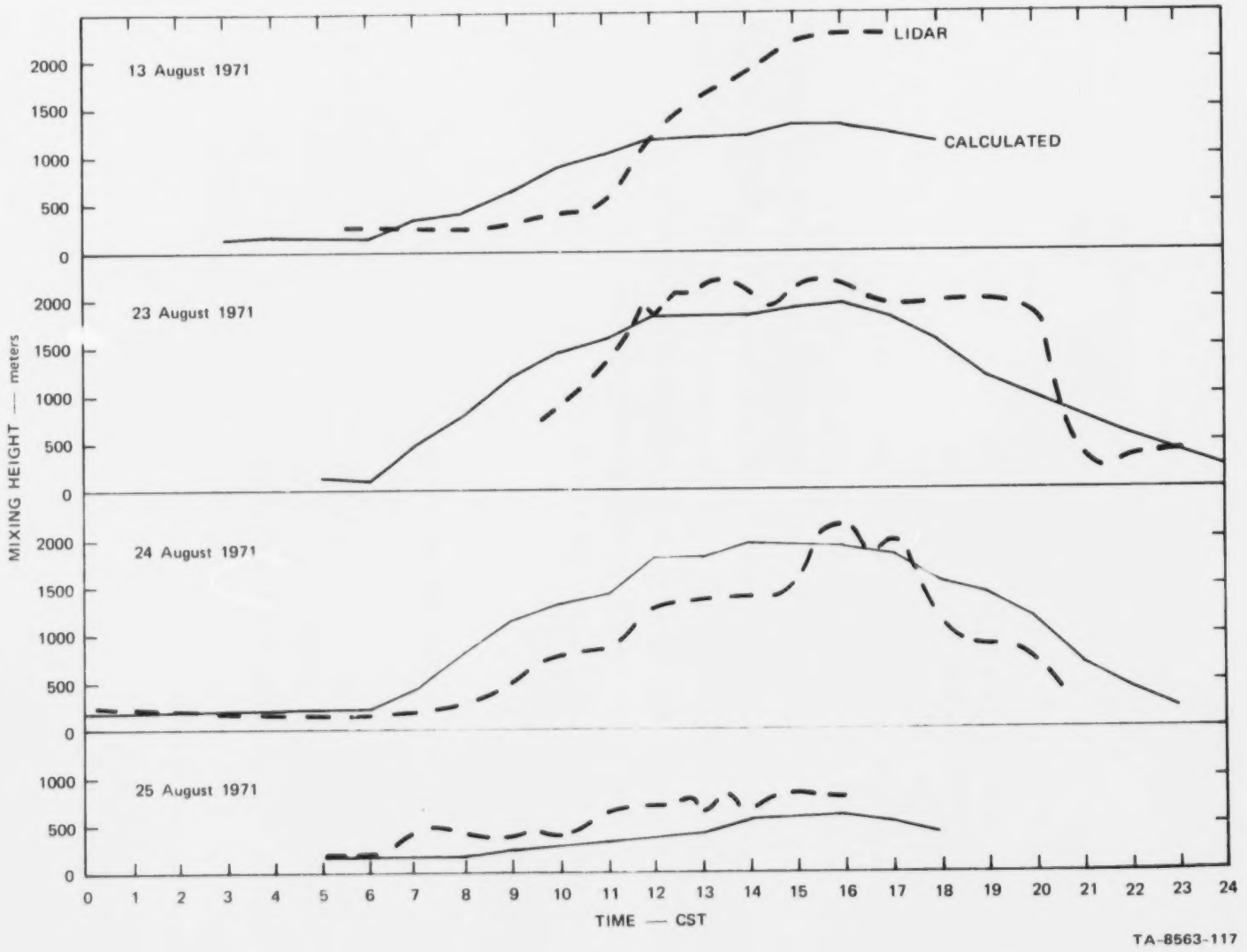

FIGURE 11 VARIATIONS OF CALCULATED AND LIDAR-OBSERVED MIXING HEIGHTS WITH TIME

Thus any future modifications of the mixing height submodel designed to reflect the morning lag in the response of mixing to solar heating should probably be made dependent on the rate of change of temperature or on the insolation strength. Since the latter is already determined in the stability submodel, it might be the most convenient. The abrupt evening mixing height decline is probably dependent on rate of cooling and hence cloud cover, although we do not have the data to confirm this.

The sensitivity of the model to mixing height variations has been discussed in an earlier report (Ludwig et al., 1970). Since that discussion, the functions used to describe the variability of σ_z with stability and travel distance have been changed (Johnson et al., 1971), and this somewhat changes the model's sensitivity to mixing height. The results are qualitatively the same as before, but differ slightly in detail. Figure 12 shows normalized concentration as a function of mixing height and stability class, using the new σ_z functions. Figure 12(a) assumes source strength to be uniform and equal to 1 from the receptor to 32 km upwind, where it becomes zero. The average concentration is the same in Figure 12(b), but decreases linearly from 2 at the receptor to zero at 32 km. The latter case is more nearly like the source field surrounding a receptor at the center of the city.

For small mixing heights the concentration will be nearly proportional to the reciprocal of the mixing height. As the mixing height increases, the dependence of concentration on it is reduced. The dependence is less pronounced for the more stable cases and for the more realistic source field. This is because the mixing height dependence is the result of those parts of the calculation based on the box model. The Gaussian model is used for calculations of concentrations due to emissions from segments close to the receptor. The box model, if used at all, applies to the farther segments. In the linearly decreasing source

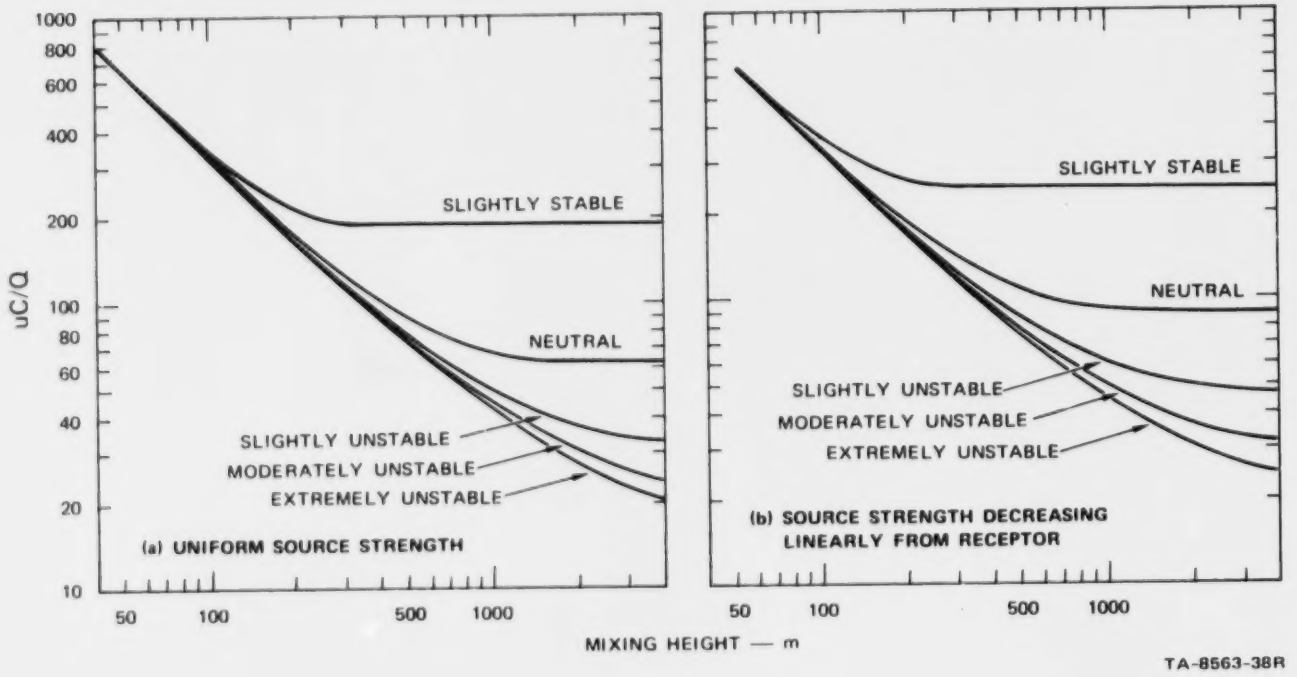

FIGURE 12 NORMALIZED CONCENTRATION AS A FUNCTION OF STABILITY AND MIXING HEIGHT

configuration the emission rates in the more distant segments are less than those in segments close to the receptor. Thus, the contributions that the box model makes to the results are smaller than those for the uniform area case. This decreases the effect of mixing depths upon the normalized concentrations. The results displayed in Figure 12 suggest that, for some values of mixing depth, the results obtained from the model are nearly independent of stability and, for certain stability types, changes in the mixing depth produce no changes in the results, if the mixing depth is sufficiently large. Thus, the model's dependence on mixing height will always be less than proportional to the reciprocal of the mixing height. The effects of mixing height are further reduced when the street canyon model is included. Since the concentrations contributed by local sources and street canyon effects are independent of mixing height and are often as large or larger than the concentrations arising from more distant sources, the percentage effects of mixing height will be further reduced.

The above discussion is not intended to minimize the importance of improving the mixing depth submodel. It should be realized though that mixing depth errors do not translate directly into concentration errors. The uncertainty factor of 1.5 in mixing height probably results in uncertainties in street canyon concentrations of only about 20 percent or less.

B. Stability

The purpose of the stability submodel is to specify the variations of the vertical dispersion parameter σ_z with travel distance. The model's selection of stability category depends on the radiative balance at the surface and the low-level wind speed, as suggested by Pasquill (1961). Radiative balance is deduced from hourly cloud cover observations and the solar elevation angle. As we have already noted, fluctuations of wind direction are also related to the Pasquill stability categories (Slade, 1968).

Standard deviations of the wind directions observed on the tower were determined for 7-minute observation periods. These standard deviations were calculated as the root-mean-square difference between about 75 individual observations and the vector average direction for the period. These 7-minute standard deviations may be slightly smaller than values obtained for the recommended 10 minute to 1 hour sampling periods. The 7-minute standard deviations were averaged over an hour period and compared with the stability categories determined from Turner's (1964) algorithm, using hourly meteorological observations from the National Weather Service at Lambert Field. Table 5 is a contingency table based on more than 690 cases. It shows percentage of occurrence of various combinations of Turner stability class and the corresponding values based on wind direction variability. In nearly 80 percent of the cases the two agree within one class. The table shows that Turner's algorithm has a bias such that it tends to define the stability as somewhat greater than actually observed in this urban location. This is not surprising because the city's roughness is likely to cause greater standard deviations of wind direction than would be expected in rural areas from which the data were obtained to define stability classes in terms of wind direction variations.

In earlier phases of this program, an attempt was made to develop a simpler method for determining stability. The approach taken was to specify the level of daytime insolation in terms of the insolation parameter Φ, described by the following equation:

$$\Phi = (1 - 0.5\ N) \sin \alpha \quad , \qquad (2)$$

where N is the fraction of the sky covered by opaque clouds and α is the solar elevation angle. Originally we classified the daytime insolation so that the categories covered equal ranges of the value of Φ, e.g., less than 0.33 was slight insolation, greater than 0.67, strong. During this

Table 5

PERCENT OCCURRENCE OF VARIOUS COMBINATIONS OF WIND DIRECTION VARIABILITY AND TURNER STABILITY CLASS

Stability Class	Standard Deviation of Wind Direction (Degrees) and Corresponding Stability Class					
	> 22.55	17.55-22.55	12.55-17.55	7.55-12.55	3.75-7.55	< 3.75
	Extremely Unstable	Moderately Unstable	Slightly Unstable	Neutral	Slightly Stable	Moderately Stable
Extremely Unstable 1	0.1	0.1	0.1	0.0	0.0	0.0
Moderately Unstable 2	2.0	0.4	1.2	0.1	0.0	0.0
Slightly Unstable 3	4.2	1.6	4.9	1.2	0.3	0.3
Neutral 4	3.5	5.1	15.9	20.8	7.2	0.6
Slightly Stable 5	0.7	1.0	2.5	11.8	11.0	3.5
Moderately Stable 6			Not used for urban cases			

program, 141 hours of pyrheliograph data were collected to check the suitability of these categories. The categories, strong, moderate, and slight insolation, were originally defined by Pasquill (1961). Strong insolation was defined as "...sunny midday conditions in mid-summer in England." According to Chandler (1965), the corresponding value of insolation measured at Kew Observatory is 1.0 cal cm^{-2} min^{-1}. Using this as a guide the following insolation classes would fit Pasquill's definition of strong insolation:

slight insolation: < 0.4 cal cm^{-2} min^{-1}

moderate insolation: $0.4 - 0.8$

strong insolation: > 0.8 .

However, Pasquill has also specified slight insolation to be typical sunny, midwinter, midday conditions, which would be about 0.6 cal cm^{-2} min^{-1} according to Chandler. This seems inconsistent, in that its use would result in a very large class for slight radiation and a very small moderate insolation class. The class intervals given above seem more reasonable and lead to reasonably good agreement with Turner's insolation categories based on solar elevation, cloud height, and sky cover, as shown in Table 6. This contingency table shows the relative frequencies of

Table 6

JOINT OCCURRENCE OF TURNER'S NET RADIATION INDEX AND OBSERVED INSOLATION

Turner Net Radiation Index	Insolation, Cal cm^{-2} min^{-1}		
	< 0.4	$0.4 - 0.8$	≥ 0.8
0 or 1	29.8%	19.9%	5.0%
2	2.1%	24.1%	9.9%
3	0.7%	2.8%	5.7%

various combinations of measured insolation, classed as above, and Turner's net radiation index. As can be seen from the table, there are a substantial number of instances where moderate or strong insolation is observed but given a low radiation index by Turner's algorithm. This generally occurs during overcast conditions. The method tends to overestimate the effect of low overcast clouds on the insolation.

Table 7 shows the results of cross classifying measured insolation with equal intervals of Φ. This table shows that these intervals of Φ generally lead to greater underestimates of insolation than does Turner's algorithm. This suggests that the Φ categories should be revised. It would seem reasonable to use a classification system for Φ that was closely related to the classes of observed insolation. Maximum tropical

Table 7

JOINT OCCURRENCE OF INSOLATION CLASSES
(after Ludwig et al., 1970) AND OBSERVED INSOLATION

Φ	Insolation, Cal cm^{-2} min^{-1}		
	< 0.4	0.4 - 0.8	≥ 0.8
< 0.33	27.7%	6.4%	0.0%
0.33 - 0.66	5.0%	37.6%	18.4%
> 0.66	0%	2.8%	2.1%

sea level insolation is about 1.5 cal cm^{-2} min^{-1} (derived from Smithsonian Meteorological Tables, 1951). We have already concluded that the lower bound of the strong insolation class is at a value slightly more than half this maximum possible. Therefore, a value of Φ, slightly more than half its maximum possible value, should be appropriate for a class boundary. Table 8 shows the results obtained when the class intervals of Φ are revised accordingly. The revised categories result in very good agreement

Table 8

JOINT OCCURRENCE OF REVISED INSOLATION CLASSES AND OBSERVED INSOLATION

Φ	Insolation, Cal cm^{-2} min^{-1}		
	< 0.4	$0.4 - 0.8$	≥ 0.8
< 0.3	27.0%	2.8%	0.0%
$0.3 - 0.55$	5.7%	35.5%	7.1%
> 0.55	0.0%	8.5%	13.5%

with the measured insolation. Accordingly, the stability submodel has been changed to incorporate these new insolation categories:

slight insolation: $\Phi < 0.3$

moderate insolation: $0.3 \leq \Phi \leq 0.55$

strong insolation: $\Phi > 0.55$

Another revision, based on Pasquill's (1961) article, has also been incorporated. Now, overcast (opaque cloud cover $\geq 9/10$) conditions, night or day, are taken to have neutral stability. Neutral stability also prevails during the day when the sun is within 15^{o} of the horizon. The 15^{o} solar elevation criterion has replaced the earlier one (Johnson et al.,1971) based on number of hours before sunset or after sunrise. The two are virtually identical in their effect. Table 9 below summarizes the revised criteria used in the stability submodel. The revised model was applied to the hourly meteorological data from Lambert Field so that it could be compared with the wind direction standard deviations as was done with Turner's stability categories. Table 10 shows the results of this comparison. Reference to Tables 5 and 10 shows that the stabilities obtained with the revised submodel are in somewhat better agreement with the wind variabilities than are the Turner values. More than 87 percent

Table 9

REVISED STABILITY CATEGORIES

Surface Winds (knots)	Daytime Solar Elevation Angle > 15°			Opaque Cloud Cover ≥ 9/10, Day or Night or Solar Elevation Angle ≤ 15°	Nighttime	
	Strong Insolation	Moderate Insolation	Slight Insolation		≥ 5/10 Clouds	≤ 4/10 Clouds
≤ 3	1	2	2	4	5	5
3-6	1	2	3	4	4	5
6-10	2	3	3	4	4	4
10-12	3	3	4	4	4	4
≥ 13	3	4	4	4	4	4

of the stabilities determined by the revised submodel were within one category of those based on wind observations; with Turner's method 80 percent of the cases were within one category. There is a slight bias in this method, in the direction that would be expected for urban wind direction fluctuations.

It was expected that the wind direction fluctuations prevailing during a given stability condition, as determined by the model, would vary according to the roughness of the underlying surface. To test this, the data were stratified according to wind direction. The experimental location is near the eastern edge of the central business district, with generally open areas farther to the east, as can be seen in Figures 1 and 4. Thus winds with a component across Broadway from the east would have a considerably smoother upwind fetch than those with a component across Broadway from the west.

The wind direction measured at the upper level of the tower was used to stratify the data according to whether there was an upwind urban fetch (326 hours of data) or a nonurban fetch (309 hours). Tables 11 and 12 summarize the results. The difference between the two is rather striking.

Table 10

PERCENT OCCURRENCE OF VARIOUS COMBINATIONS OF WIND DIRECTION VARIABILITY AND REVISED MODEL STABILITY CLASS

Stability Class	Standard Deviation of Wind Direction (Degrees) and Corresponding Stability Class					
	> 22.55	17.55-22.55	12.55-17.55	7.55-12.55	3.75-7.55	< 3.75
	Extremely Unstable	Moderately Unstable	Slightly Unstable	Neutral	Slightly Stable	Moderately Stable
Extremely Unstable 1	2.9	0.9	1.1	0.3	0.0	0.0
Moderately Unstable 2	3.6	1.4	5.0	1.0	0.3	0.1
Slightly Unstable 3	2.0	2.6	7.5	5.2	0.3	0.0
Neutral 4	1.0	2.9	9.8	21.4	10.8	1.1
Slightly Stable 5	0.9	0.7	1.4	6.2	6.6	3.0
Moderately Stable 6			Not used for urban cases			

Table 11

PERCENT OCCURRENCE OF VARIOUS COMBINATIONS OF WIND DIRECTION VARIABILITY AND REVISED STABILITY CLASS WITH URBAN FETCH

Stability Class	Standard Deviation of Wind Direction (Degrees) and Corresponding Stability Class					
	> 22.55	17.55-22.55	12.55-17.55	7.55-12.55	3.75-7.55	< 3.75
	Extremely Unstable	Moderately Unstable	Slightly Unstable	Neutral	Slightly Stable	Moderately Stable
Extremely Unstable 1	1.8	0.3	0.3	0.0	0.0	0.0
Moderately Unstable 2	4.0	0.9	1.8	0.6	0.0	0.0
Slightly Unstable 3	3.4	3.1	10.7	4.3	0.0	0.0
Neutral 4	1.2	3.1	13.5	25.5	4.9	0.0
Slightly Stable 5	1.2	0.6	1.2	7.1	7.7	2.8
Moderately Stable 6			Not used for urban cases			

Table 12

PERCENT OCCURRENCE OF VARIOUS COMBINATIONS OF WIND DIRECTION VARIABILITY AND REVISED STABILITY CLASS WITH NONURBAN FETCH

Stability Class	Standard Deviation of Wind Direction (Degrees) and Corresponding Stability Class					
	> 22.55	17.55-22.55	12.55-17.55	7.55-12.55	3.75-7.55	< 3.75
	Extremely Unstable	Moderately Unstable	Slightly Unstable	Neutral	Slightly Stable	Moderately Stable
Extremely Unstable 1	2.9	1.3	1.6	0.3	0.0	0.0
Moderately Unstable 2	3.2	2.3	7.8	1.3	0.3	0.3
Slightly Unstable 3	1.0	1.3	4.9	6.1	0.6	0.0
Neutral 4	1.0	1.6	4.2	18.1	16.5	2.6
Slightly Stable 5	0.6	1.0	1.3	6.5	7.4	3.9
Moderately Stable 6			Not used for urban cases			

With an urban fetch more than 88 percent of the cases have wind variabilities within one category of that predicted from the hourly meteorological observations by the revised stability model; however, the bias is quite pronounced. In only 15 percent of the cases is the wind variability less than predicted; in more than 38 percent it is greater.

For the nonurban fetch cases the situation is nearly reversed. More than 86 percent of the cases are still within one category of that predicted, but almost 43 percent have wind direction variability less than the appropriate value. Less than 22 percent have greater variability. There is little question that the rougher urban surface causes significantly greater wind direction fluctuations and hence more rapid diffusion than is found over the smoother areas. These results, at least qualitatively, support the adoption of different σ_z functions for urban and rural modeling. This was done in the previous report for this project (Johnson et al., 1971), and the functions derived in that report to fit urban conditions will continue to be used in the model. The results of these studies suggest that future investigations of the effects on diffusion of different types of urban and rural surfaces could be quite profitable. However, at present, the combination of the revised stability model and the urban σ_z functions seems to be a very good compromise for use in urbanized areas.

C. Emissions Submodel

There are at least three potential sources of error in calculating the emissions from the traffic data. These are: (1) inaccurate estimates of hourly traffic volume, (2) inaccurate estimates of average vehicular speeds on the links, and (3) an inappropriate equation relating emission rates to the preceding two factors. These factors were all considered in the preceding report (Johnson et al., 1971), but data collected in St. Louis makes their reconsideration worthwhile.

1. Traffic Volumes

The detailed traffic data from San Jose indicated that the traffic on any given street link, for a given hour of the day, does not vary much from one weekday to another. The standard deviations of day-to-day values of half-hour traffic volumes in downtown San Jose at a given time of day were found to range from about 5 to 15 percent of the average volume. The St. Louis data collected at the street canyon experimental site showed somewhat greater variability, but this may only reflect the fact that a new freeway was opened at the southern edge of the downtown section at about the time the experiment started, so traffic patterns may have been in a state of flux. In any event, the conclusion reached in San Jose that the variability of 24-hour traffic volumes is less than 15 percent still seems reasonable. This could not be checked accurately because of previously mentioned difficulties in collecting overnight traffic data.

However, enough data were collected to construct mean diurnal traffic cycles that we believe are more reliable than our earlier sources. The results are shown in Figure 13 where they are compared with two weekday cycles obtained from other sources. The curve marked "original" is a composite diurnal emission cycle that has been used with the model. The curve marked "statistically determined" was derived from observed CO data at the St. Louis Continuous Air Monitoring Program (CAMP) Station, using a least-squares approach to give the best agreement between model calculations and observed values. It is not a traffic cycle, but an emission cycle. The corresponding traffic cycle would show lower peaks, because emissions per vehicle mile are increased by the slower speeds that accompany rush hour traffic. Similarly, off-peak traffic volumes are greater than those shown for emissions by the curves.

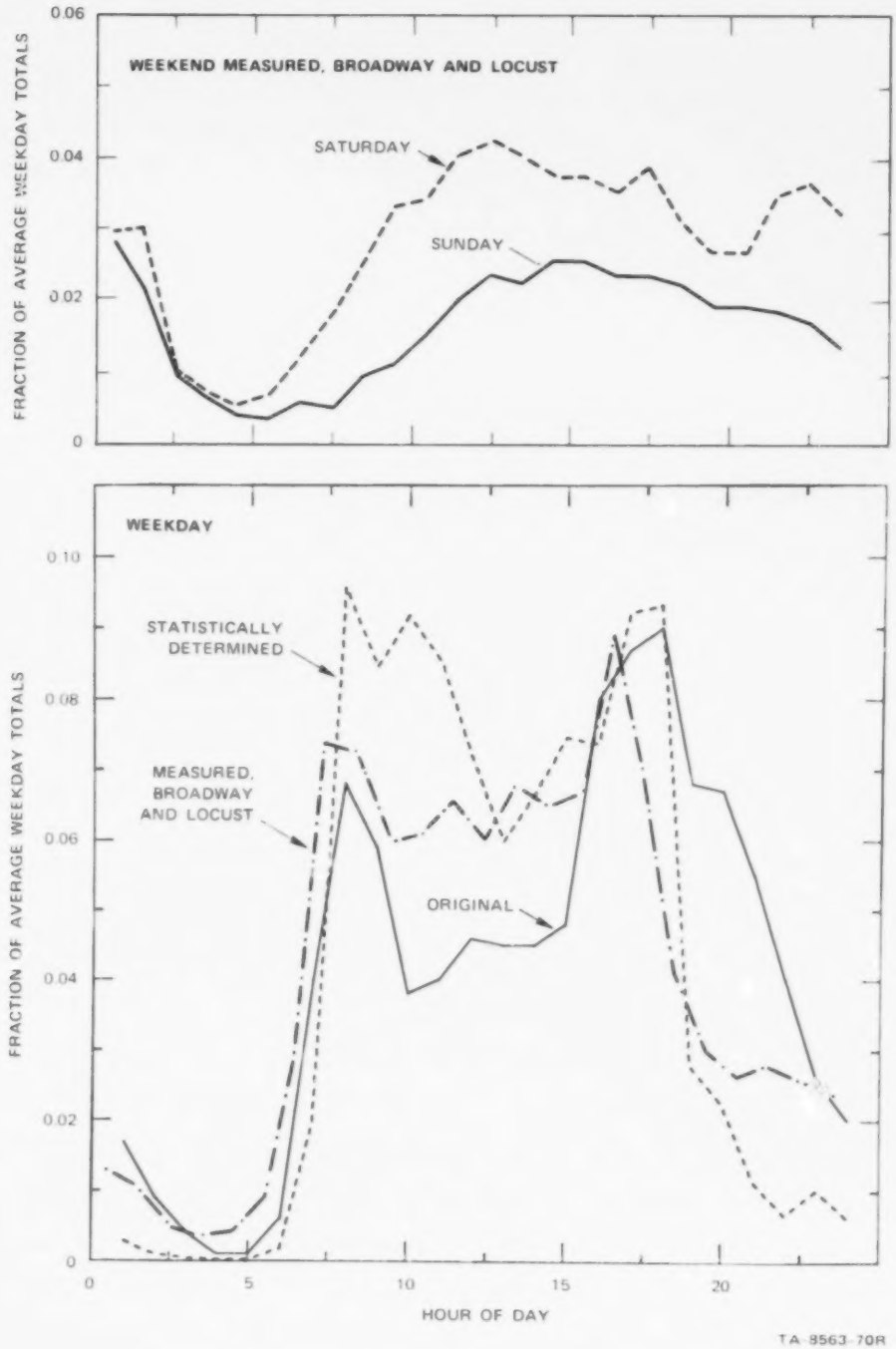

FIGURE 13 DIURNAL EMISSION PATTERNS FOR ST. LOUIS

The traffic cycle derived from the combined data collected on Locust and Broadway during the project is also shown in the figure. The measured cycle shows the high midday traffic that was implied by the statistically determined curve, but the morning and afternoon peaks are not so large. The predawn traffic is also greater than expected.

Saturday and Sunday traffic cycles are also shown in Figure 13. These curves are expressed in terms of fractions of total weekday traffic. Therefore, the sums of the fractions for each hour do not total one. The total Saturday traffic is about 67 percent of the weekday totals. The total Sunday traffic is about 40 percent of the weekday value.

The model has been revised to apply the weekday traffic cycle measured during this project to all the downtown streets and to the street canyon submodel (see Section III-E). The data collected on two days in San Jose (Johnson et al.,1971) showed very much the same general daytime trends as those displayed in this St. Louis data. It therefore seems reasonable to adopt this diurnal cycle for downtown traffic in general,in lieu of any better information. However, it is recommended that the model use local data if they are available.

2. Traffic Speeds

During the course of the mobile CO measurement program, an accurate log was kept of the movement of the van in the downtown area. Travel times along the route segments were noted to the closest 0.1 minute; the average segment length was 0.71 km. Observations were made on five days and during five different periods on each day: (1) early morning rush (0730-0830 CDT), (2) midmorning (0930-1030), (3) noon (1145-1245), (4) afternoon (1430-1530), and (5) evening rush (1630-1730). An average of five circuits were made each period around the downtown loop illustrated in Figure 4. The route has its fair share of lights, stop signs, crosswalks, and heavy traffic and is quite typical of traffic

Table 13

AVERAGE VEHICLE SPEEDS (mi h^{-1}) IN DOWNTOWN ST. LOUIS
DURING THE PERIOD 24 AUGUST TO 2 SEPTEMBER 1970

Period (CDT)	Broadway		Market		12th		Delmar		Average Period Speed
	Ave. Speed	No. of Cases	Ave. Speed	No. of Cases	Ave. Speed	No. of Cases	Ave. Speed	No. of Cases	
0730 - 0830	9.2	25	8.9	24	9.6	24	8.6	22	9.1
0930 - 1030	10.1	20	7.8	20	9.6	20	7.5	20	8.8
1145 - 1245	9.7	18	7.8	18	8.7	18	8.0	16	8.5
1430 - 1530	10.0	23	9.0	23	10.5	22	7.8	21	9.3
1630 - 1730	8.8	22	9.0	22	8.6	22	7.5	20	8.5
Average Segment Speed	9.1		8.5		9.4		7.8		8.8

flow in the central business district. Average speeds for the various periods and route segments are given in Table 13. When the uncertainty in the segment time is considered together with the overall average van speed of 8.8 mph, the uncertainty in the individual computed speeds is on the order of 3 percent or 0.3 mph.

The downtown average speed of 8.8 mi h^{-1} is less than the 14.1 mi h^{-1} average determined earlier (Johnson et al., 1971) for San Jose and considerably less than the assumed St. Louis suburban arterial speed of 20 mi h^{-1}. In practice, these localized speed values are quite easy to obtain and it is recommended in using the model that they be measured in the area of interest in view of the variations in traffic conditions among cities and the sensitivity of the model to them. The traffic speeds appropriate for application of the model in St. Louis are summarized in Table 14.

Although we have obtained refined values of vehicle speeds, we have not collected data under this program that can be used for evaluation of the speed-dependence of the emissions submodel. The model is relatively sensitive to errors in speed, particularly at low values. The overall performance of the model indicates that the emissions calculations are reasonable, but additional work is desirable to thoroughly evaluate the current submodel as well as possible alternatives.

3. Emissions Formula

The validation of the emissions submodel has centered on the evaluation of the predicted emissions [using Eq. (A4) in Appendix A] with independent measurements of the parameter. Traffic speeds were obtained in the manner described in the preceding section. Daily traffic volume in the downtown area was determined from Missouri State Highway Department (1970) data. Estimates of hourly averages were derived from Figure 13. Vehicular emissions could not be measured directly, but were computed on the basis of a CO mass budget analysis using surface (van) and aerial (helicopter) measurements around a 0.7-km square encompassing much of the St. Louis downtown area.

Table 14

VEHICLE SPEEDS FOR ST. LOUIS

Traffic Link Type	Average Off-Peak* Vehicle Speed (mi h^{-1})
Freeway:	
Downtown	43
Suburban	53
Arterial:	
Downtown	9
Suburban	20
Local	12

* Peak-hour speeds are assumed to equal 85 percent of the off-peak values.

A major difficulty in applying the budget technique is the definition of the wind field within and over the downtown district. One is faced with the dilemma that the largest concentrations and gradients of CO concentration are found near the lower boundary which, however, is beneath the zero-plane displacement height of the vertical wind profile. The mean areal wind structure up to a level of approximately 75 m is difficult, if not impossible, to define. Furthermore, the air in moving from the relatively smooth suburban and rural environs to the aerodynamically rough urban core undergoes marked horizontal and vertical accelerations. Therefore, the three-dimensional structure of the urban wind field is poorly defined and variable in both time and space.

Wind measurements available for the analysis are of two types: (1) the twice-daily profiles obtained at the EMSU station located 0.8 km to the southeast of the center of the study area, and (2) continuous

observations at the 90-m and 131-m levels on the specially instrumented tower on the east side of the study area. The EMSU data were used to describe the vertical wind structure for those analyses made near the times of the soundings. For lack of more detailed data and knowledge on low-level urban wind structure, the effective horizontal transport of CO in the lowermost stratum was taken as the average of the transport at the bottom and top of the layer. The same procedure was used for the upper strata. The mean vertical CO flux at the 335-m level was assumed to be zero; the net horizontal flux of the uppermost layer is then equal to the vertical flux through the bottom level of that layer. By working down to the surface, the vertical CO-flux profile is obtained as well as the areal average of surface emissions. These can then be compared with submodel predictions from the traffic data.

Of necessity, a streamlined procedure was necessary when EMSU wind data were not available. For these cases the tower winds were used and it was assumed that the transport in the lowermost stratum could be estimated by using an effective layer wind equal to two-thirds of the 90-m observation. Winds in the upper layers were assumed to be constant and equal to the value of the 130-m tower observation. These assumptions are necessarily coarse, but probably result in a minimum probability for biasing the computations.

An example of a sequence of concentration profiles obtained by the helicopter on 31 August is illustrated in Figure 14; corresponding vertical suburban temperature profiles are shown in Figure 15. Because of the assumptions on the wind structure discussed above, it is practical to analyze only those cases with relatively shallow mixing depths and high concentrations aloft in order to minimize the influence of the surface (van) observations on the computations. The upper level measurements are more representative of a true line average, because of the integrating effect of atmospheric motions, while the van observations

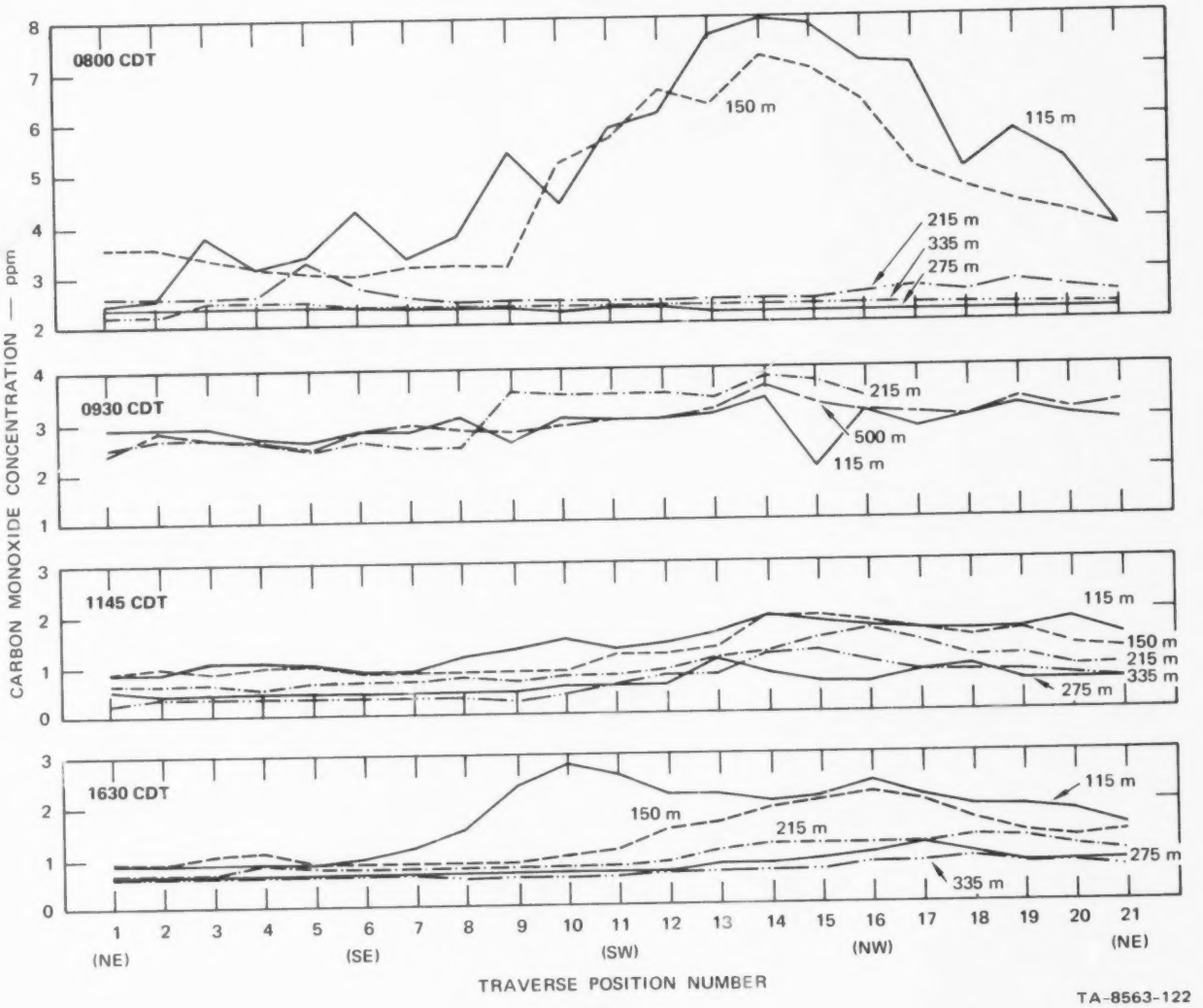

FIGURE 14 SPACE AND TIME VARIATION OF CO CONCENTRATION OVER DOWNTOWN ST. LOUIS, 31 AUGUST 1971

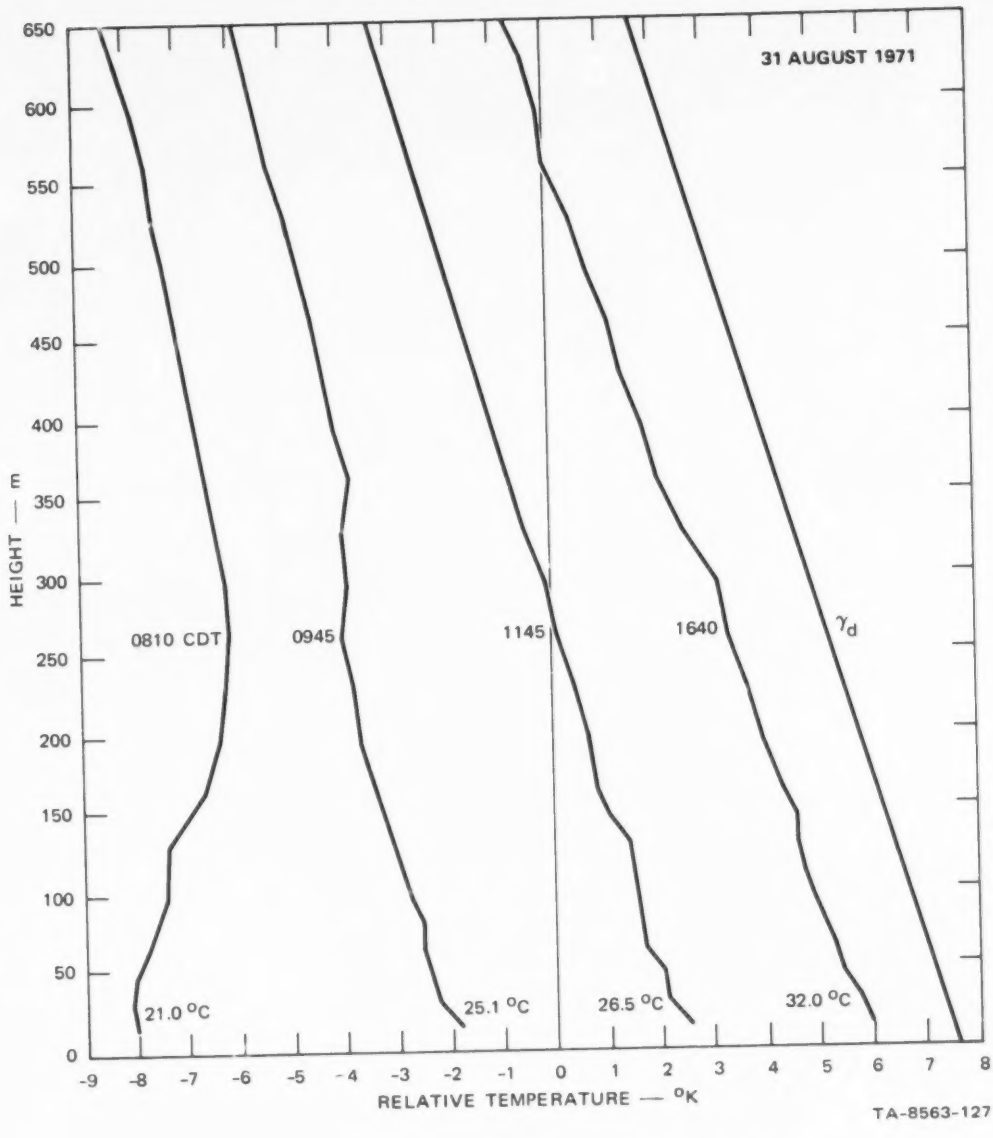

FIGURE 15 ST. LOUIS SUBURBAN TEMPERATURE PROFILES

can easily be biased by the influence of sources close to the sampling intake. This effect can deteriorate the quality of the cross-town gradient computed at the surface. Furthermore, it is necessary to limit the analyses to cases where the emissions and meteorological fields do not vary rapidly with time.

Observations made at 0800 CDT, 31 August satisfy these requirements sufficiently to permit a mass budget analysis for the estimation of the surface CO flux. The concentration and meteorological data are tabulated in Table 15 and the resulting fluxes are illustrated in Figure 16. The average surface emission rate of 571 gm (CO) sec^{-1} computed from the analysis is 2.5 times the value calculated from Eq. (4) using traffic data.

Another analysis was made using data collected during the evening rush period on 23 August (see Table 15). The surface flux computed from the budget analysis is about 75 percent of the value predicted by the submodel from the traffic data for the period. An interesting feature of the results of the analysis (Figure 17) is the net horizontal influx of CO in the bottom layer. The winds in that layer are a factor of 2-to-3 times larger than those in the previous case. Under these conditions, it is possible that there is a pronounced lifting of the air near the surface as it strikes the relatively dense face of the tall buildings in the urban core region. This could cause the higher upwind concentrations observed at the surface and the higher downwind values (as one would expect) aloft. A more striking example of this phenomenon is presented in the following analysis.

On the morning of 24 August, an interesting and unusual CO distribution pattern was observed: Street level concentrations observed by the mobile van were consistently high ($\sim$ 35 ppm) and decreased downwind across the study area; concentrations measured by the helicopter

Table 15

CARBON MONOXIDE AND WIND DATA
FOR BUDGET ANALYSES

Height (m)	CO Concentration (ppm)				Street-Oriented Wind Components		
	Broadway	Market	12th	Delmar	$u(m\ s^{-1})$	$v(m\ s^{-1})$	
0	23.7	22.1	22.6	22.7	-0.7	-0.8	
115	3.3	4.5	7.1	5.7	-1.4	+1.6	Case I:
150	3.3	3.9	6.5	4.8	-0.5	+2.2	0800 CDT
215	2.7	2.6	2.5	2.7	+0.9	+3.0	31 August
275	2.4	2.4	2.3	2.3	+1.6	+3.8	
335	2.4	2.4	2.4	2.4	+2.3	+4.5	
0	18.3	16.3	15.4	17.2	-1.0	+1.8	Case II:
115	2.0	2.3	1.8	2.5	-0.8	+3.2	1730 CDT
150	1.6	1.9	1.3	1.8	-0.8	+3.2	23 August
215	0.9	1.1	1.4	1.4	-0.8	+3.2	
275	1.0	1.1	1.4	1.8	-0.8	+3.2	
335	0.3	0.3	0.7	0.5			
0	37.0	34.6	34.8	34.4	-0.7	+1.9	
115	0.4	0.4	0.6	0.5	+1.4	+3.8	Case III:
137	0.4	0.6	0.8	0.6	+2.1	+3.7	0730 CDT
150	4.3	2.4	4.2	4.4	+2.6	+2.7	24 August
215	1.8	1.1	2.1	0.9	+3.5	+3.5	
275	0.5	0.5	0.5	0.5	+3.9	+3.9	
335	0.1	0.2	0.2	0.1	+4.2	+4.2	

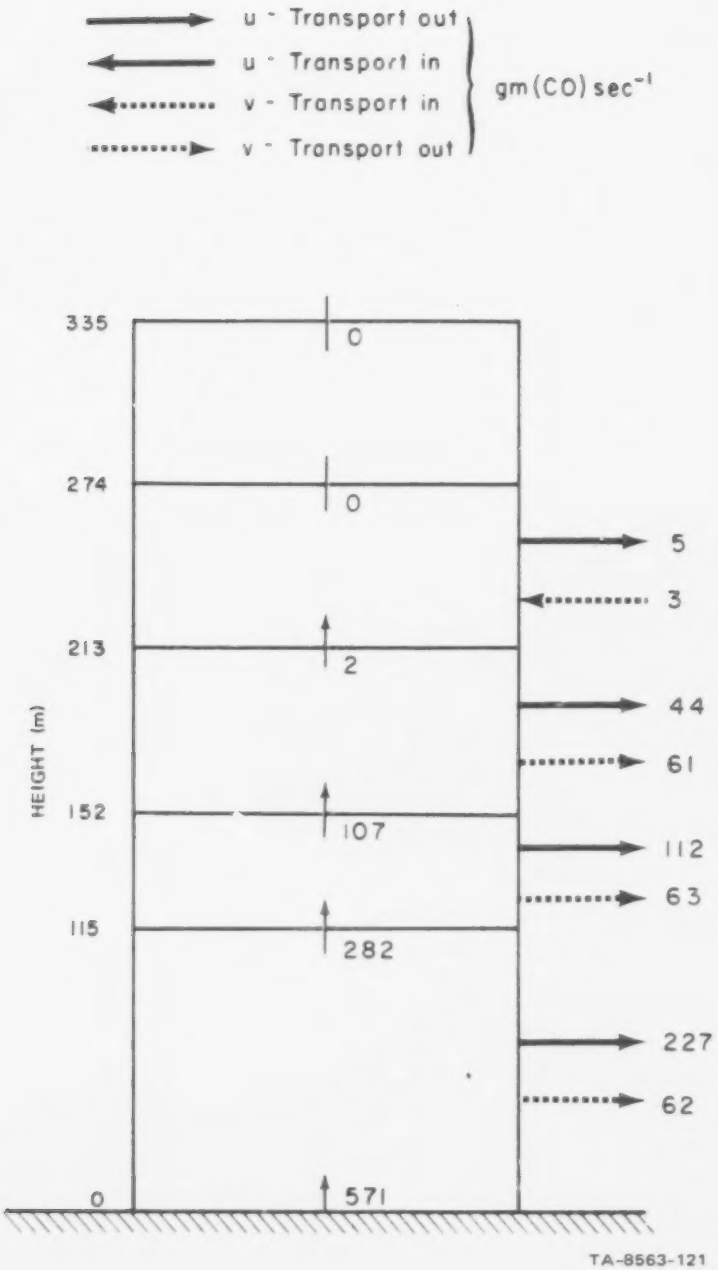

FIGURE 16 CARBON MONOXIDE MASS BUDGET ANALYSIS, ST. LOUIS
0800 CDT, 31 AUGUST 1971

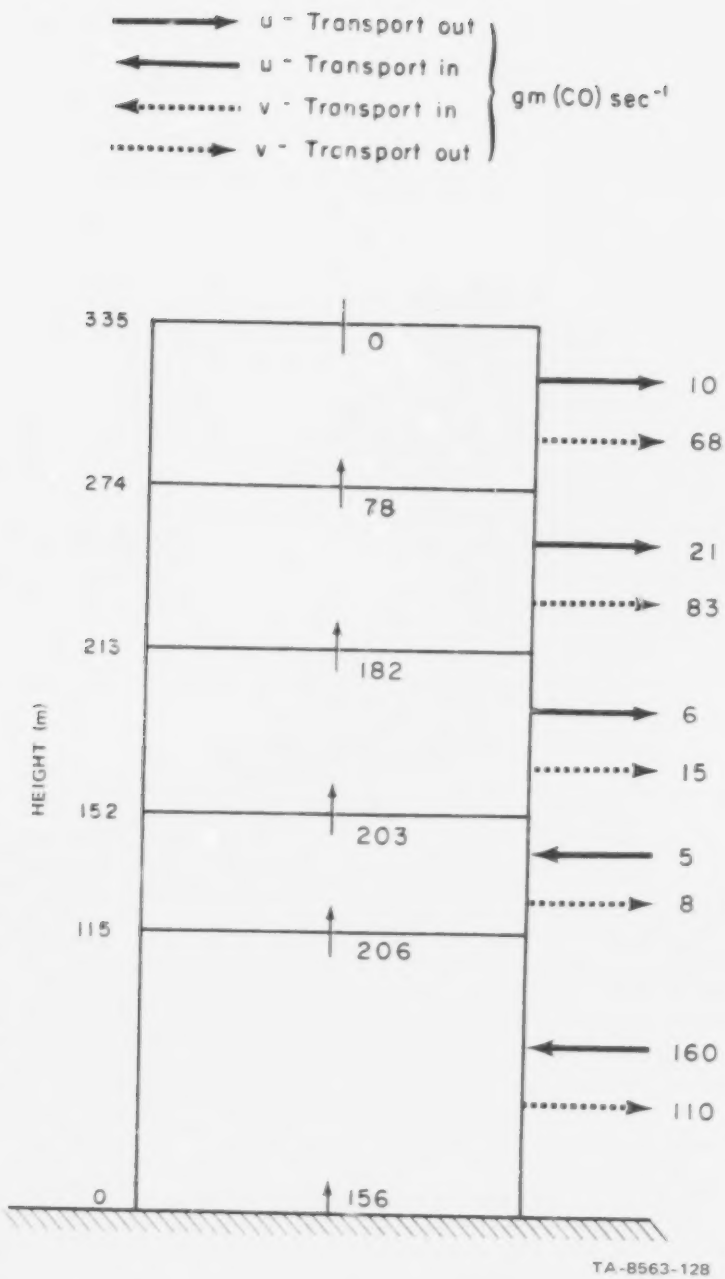

FIGURE 17 CARBON MONOXIDE MASS BUDGET ANALYSIS, ST. LOUIS 1730 CDT, 23 AUGUST 1971

were low and uniform at the 115-m and 135-m levels, but then increased dramatically at 150 m and remained high at 215 m, dropping again to consistently low values at 275 m and 315 m. These patterns are illustrated in Figure 18 together with the corresponding vertical profile of temperature; the wind and average CO values are summarized in Table 15. In spite of the stable conditions, the winds were moderately strong from the south through southwest. Again, the explanation for the pattern may be the "orographic" lifting of the air as it encounters the wall of buildings. This would have the effect of decreasing the surface concentrations downwind, while the tilt of the flow field could have the effect of raising the CO content of the air at the intermediate levels. It is, however, puzzling that only the two intermediate levels show the high concentrations. This pattern might occur if the tilt of the updraft were just right and the vertical diffusion sufficiently damped. These arguments are only offered in the way of conjecture, but the situation does illustrate some of the complexities of understanding and simulating urban dispersion.

Figure 19 illustrates the results of a budget analysis retaining the restriction of zero flux through the uppermost level, while Figure 20 is an alternative analysis where the zero-flux restriction has been modified to ensure no negative vertical fluxes. Traffic data were not yet available from the street experiment on this date and it has been assumed that conditions were similar to those experienced during the 0800 CDT case, one week later. Under the zero-flux assumption, the budget calculation is 25 percent of the submodel prediction; under the alternative analysis assumption, the submodel value is only 80 percent greater.

The budget analyses are interesting and serve to illustrate the features of urban-scale dispersion, but they have not provided data of sufficient quality to objectively analyze the performance of the emissions

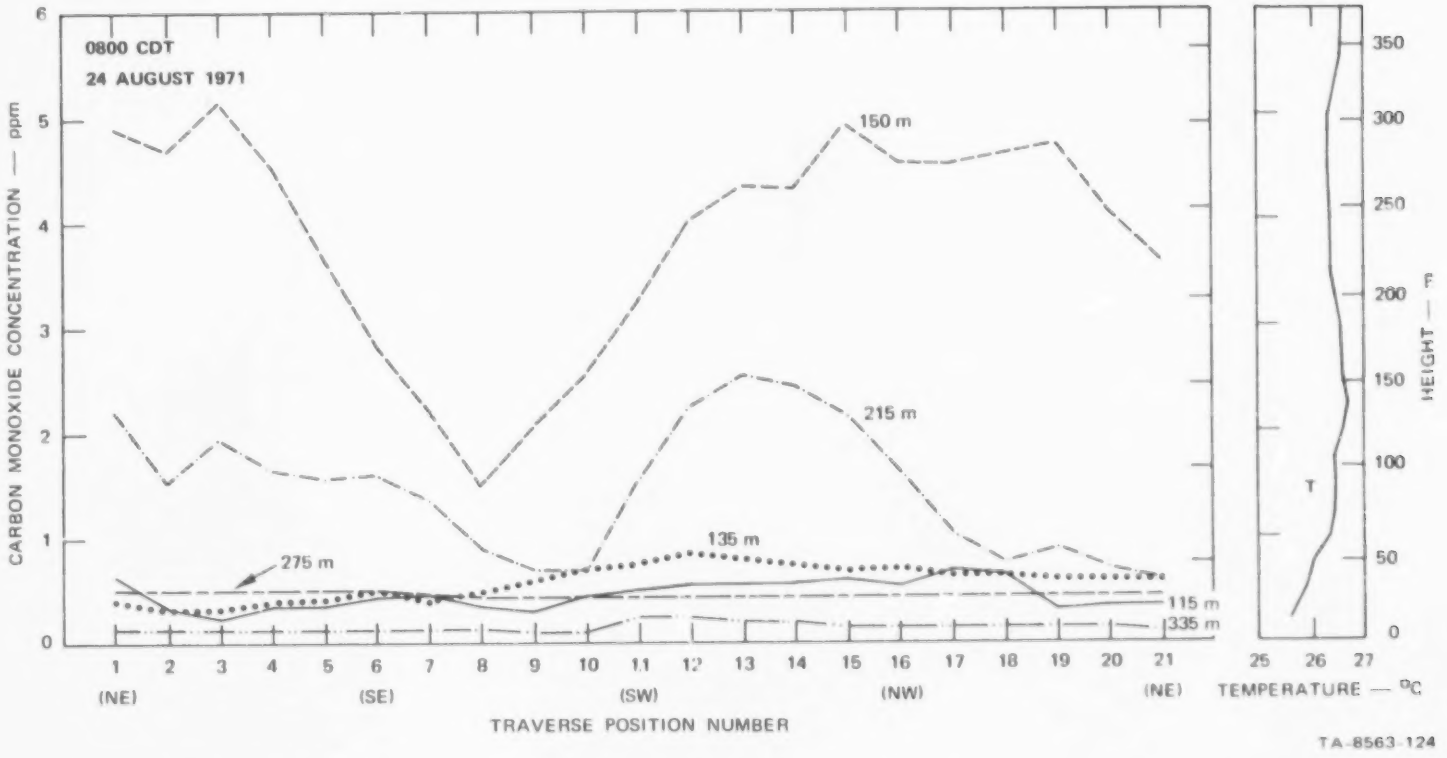

FIGURE 18 SPACE-VARIATION OF CO OVER DOWNTOWN ST. LOUIS, AND SUBURBAN TEMPERATURE PROFILE

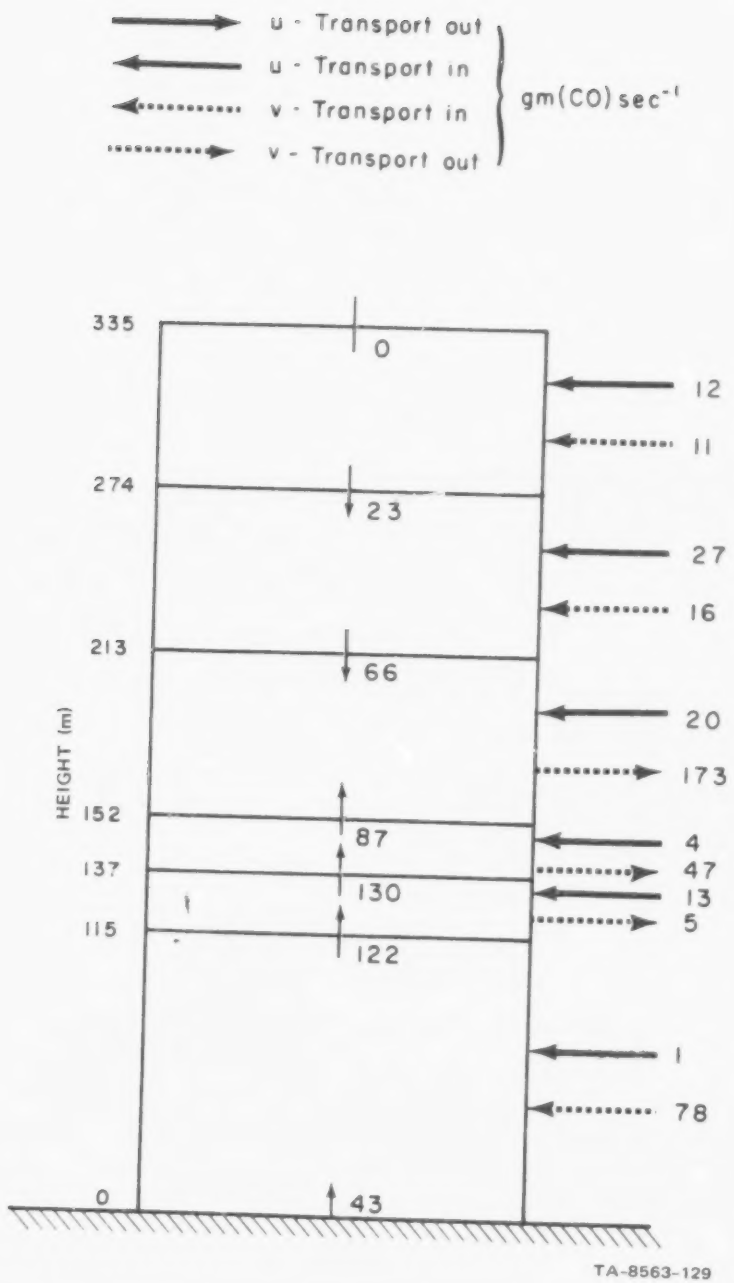

FIGURE 19 CARBON MONOXIDE MASS BUDGET ANALYSIS, ST. LOUIS
0730 CDT, 24 AUGUST 1971

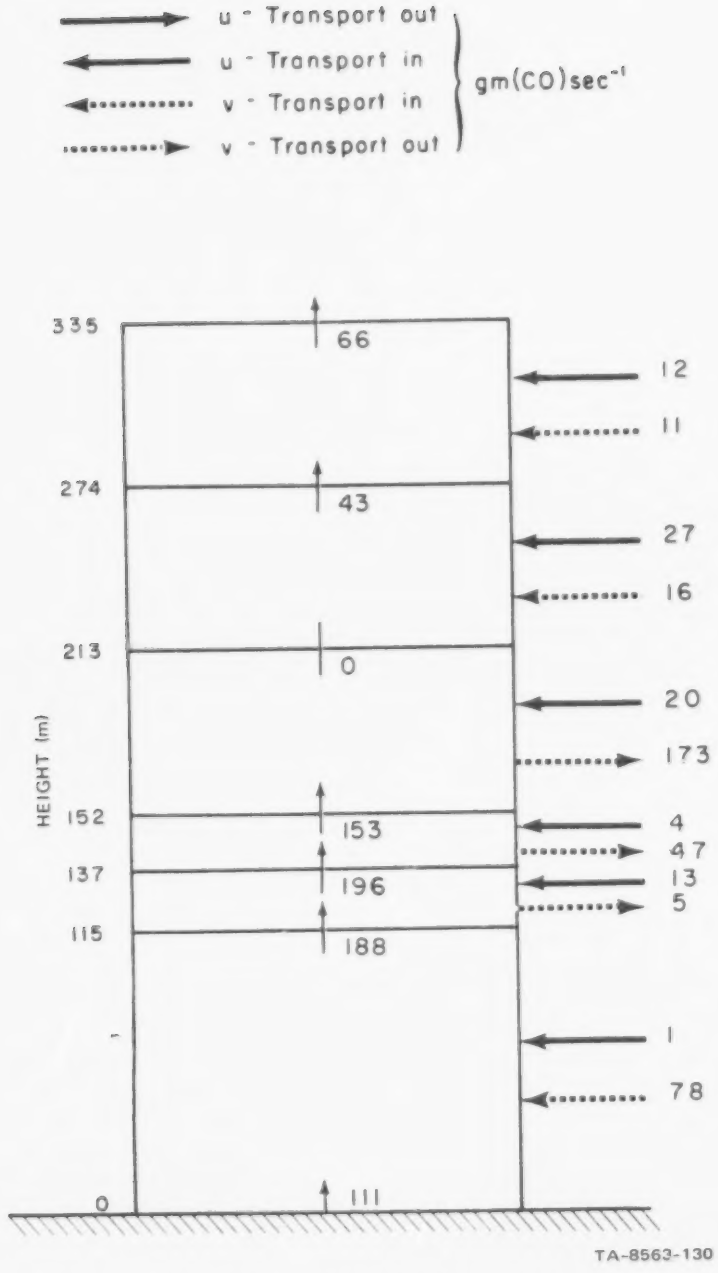

FIGURE 20 CARBON MONOXIDE MASS BUDGET ANALYSIS, ST. LOUIS 0730 CDT, 24 AUGUST 1971

submodel. To do this would require an experimental program where all the variables could be monitored with the precision necessary to fully describe the traffic and meteorological conditions and the resulting pollution concentrations.

D. Winds

Winds are an important input to many aspects of the model. The wind direction is used to determine those sources that will contribute to concentrations at the receptor. The direction is also used in the application of the street canyon effects submodel. Wind speed enters as a dilution factor in both the Gaussian and box model formulations; it is also required for the stability and street submodels.

Recognition of the importance of more detailed wind (and temperature) information for the prediction of atmospheric dispersion has prompted the National Weather Service to develop the EMSU program; as these data become available on a routine basis, additional model improvements can be anticipated. However, the current program is a limited one--measurements are made at only a few cities and even then on a relatively infrequent basis (twice daily on weekdays). Therefore, in formulating the model, we have assumed that winds measured at the airport will be the only measured values generally available for use with the model. These winds have been assumed to be uniform over the urban area. In this section, the validity of this assumption will be discussed. Much of this discussion is based on a recent study in St. Louis by Wuerch (1971).

Wuerch has compared airport winds with the "transport" winds computed from the EMSU radiosonde data obtained at the Gateway Arch. The radiosonde site is about 21 km southeast of Lambert Field. The transport winds are a vector-average of the winds in the mixing layer. The airport wind speed that is used for comparison is a scalar average over 1-hour time periods, and therefore differs somewhat from the data used as inputs to

the model. The model input data are the routine, subjective one-minute averages as determined by a weather observer.

Wuerch has studied the relationships between airport and transport winds at both dawn and midday. The dawn results are based on 134 sets of data collected during the period of November 1969 through June 1970. The midday results are based on 150 data pairs collected from September 1969 through June 1970.

For the midday cases, Wuerch found that the airport wind speed u_a was highly correlated (correlation coefficient, 0.82) with the transport wind speed u_t. The standard error of estimate was 1.8 m s^{-1} about the regression line,

$$u_t = 0.576 + 1.174\, u_a \quad . \qquad \text{(3, midday)}$$

The dawn cases were slightly less correlated (0.76) and had a somewhat greater standard error of estimate (2.1 m s^{-1}) about the regression line,

$$u_t = 2.421 + 1.179\, u_a \quad . \qquad \text{(4, dawn)}$$

The equations show that the airport wind speeds tend to be less than the mixing layer transport wind, as would be expected. Wuerch infers from the generally high correlations that the transport wind speed does not vary much between downtown and the airport. However, for low wind speeds in the morning, the differences may be more important.

The transport wind speed would be the appropriate speed for use with the box model, which assumes the pollutants to be spread through the mixing layer. The appropriate wind speed for the Gaussian model would be less, because for those regions to which that model is applied the pollutants have not yet mixed to the higher levels with their correspondingly larger wind speeds. Furthermore, in the lower layers over the city, the frictional effects of the rough urban surface will cause the wind speeds to be less than those observed at comparable heights over the smoother airport (rural) surface.

There are some very important computational advantages to the use of the same value of wind speed in both the box and Gaussian models. The wind speed can then be factored out of many of the expressions and the calculations that are required are greatly reduced, particularly when a long series of concentrations are to be determined (see, e.g., Ludwig et al., 1970, pp. 58-62 and 163-166). For this reason, it seems best to use only a single value of wind speed in the general model. In the absence of other information, the wind speeds measured at the airport seem to be the best compromise choice. They are also the most suitable for use to determine the stability category. For application of the street model, a wind speed of half the airport value has been found to give good results in the complete model. A minimum value of 0.75 m s^{-1} was used in this application.

The question of wind direction variability within the mixing layer was also addressed by Wuerch (1971). He compared the vector-averaged wind speeds in the layer with scalar averages; the greater the difference between these two averages, the greater the directional variability in the layer. On the basis of these comparisons, Wuerch concluded that changes of wind direction through the mixing layer are generally quite small at midday, but of greater significance during the morning.

The variation in wind direction between the airport and downtown was checked using the data collected on this program. The reported airport wind directions (excluding calm winds) were compared with those observed at the upper tower level. The root-mean-square difference between the directions measured at these two locations was 31^{o}. In assessing these results it should be remembered that the airport winds are reported to only the nearest 5^{o}; this fact accounts for at least a small part of the apparent differences. The aerodynamic influence of the tower (Dabberdt, 1968a,b) may also be a contributing factor. The variability of winds in the area should be better defined when the detailed studies

from the Metropolitan Meteorological Experiment (METROMEX) (Chagnon, 1971) become available. At the time of this writing, the analyses of the multi-balloon wind measurements in the St. Louis area are not yet complete.

E. Street Canyon

The data collected in the street canyon experiment were stratified according to wind direction and wind speed, because in our earlier studies in San Jose (Johnson et al., 1971) these two variables had been found to be very important. The stratifications were based on the winds measured at the upper tower level. Twelve 30^{o} wind classes were used and three wind speed classes. The wind speed categories were: 1 to 3 m s^{-1}, 3-6 m s^{-1}, and greater than 6 m s^{-1}. Sufficient data were available for analysis in all but one case (60^{o}, > 6 m s^{-1}). The resulting average CO concentrations were computer analyzed and the results are shown in Figures 21 and 22.

In the coordinate system used for the winds, Broadway is oriented along a 0^{o}-180^{o} line, and Locust along a 90^{o}-270^{o} line. The street canyon model predicts that cross-street CO gradients should be zero for winds parallel to the street, and concentration should decrease with height. For roof-level winds perpendicular to the street, street-level concentrations are expected to decrease in the downwind direction; the vertical gradients should be zero in front of the buildings that face the wind, while on the opposite side of the street the concentrations should decrease with height. In all cases, the gradients should be more pronounced on streets with greater traffic emissions than on lightly traveled streets. From this latter fact it can be deduced that the street canyon effects would be more pronounced on heavily traveled Broadway than on Locust, which generally has only about 40 percent the traffic that Broadway has.

The figures show that as expected, the gradients on Broadway are generally greater than those on Locust. In Figure 21, the Broadway results can be seen to show the features predicted by the model. The Broadway analyses for the 90^{o} and 270^{o} wind cases show the street-level concentrations increasing across the street in the proper sense. There is very little change of concentration with height in front of the buildings that face the wind. On the other side of the street, there are pronounced decreases of concentration with height. These same features are equally pronounced for winds from 30^{o} either side of the direction perpendicular to the street--with the exception of the 300^{o} case. At the lower wind speeds the 300^{o} case does not exhibit the expected features. Instead the concentrations are more like those that we would expect with winds parallel to the street.

For 180^{o} and 360^{o} winds, parallel to Broadway, the cross-street concentration gradients are much less than the vertical gradients. The gradients are generally seen to decrease with increasing wind speed as expected. For winds 30^{o} either side of the parallel directions, the CO distributions are of the parallel-wind type, with the exception of the 150^{o} and 210^{o} low-wind cases, which show considerable evidence of the effects of the cross-street wind component.

As already noted, the lighter traffic on Locust results in generally smaller concentration gradients. In many cases these smaller gradients make the expected features of the distribution less well defined. The parallel-wind cases, 90^{o} and 270^{o}, are much as expected with generally horizontal isopleths of concentration. The cases with winds within 30^{o} of the street alignment show more influence of the cross-street component than was found for Broadway. In fact, these analyses show the influence of the cross-street component for all cases except 90^{o}, 270^{o}, and 180^{o}. The last named direction is perpendicular to Locust Street, and at first it appears quite surprising that it does not show the typical pattern for

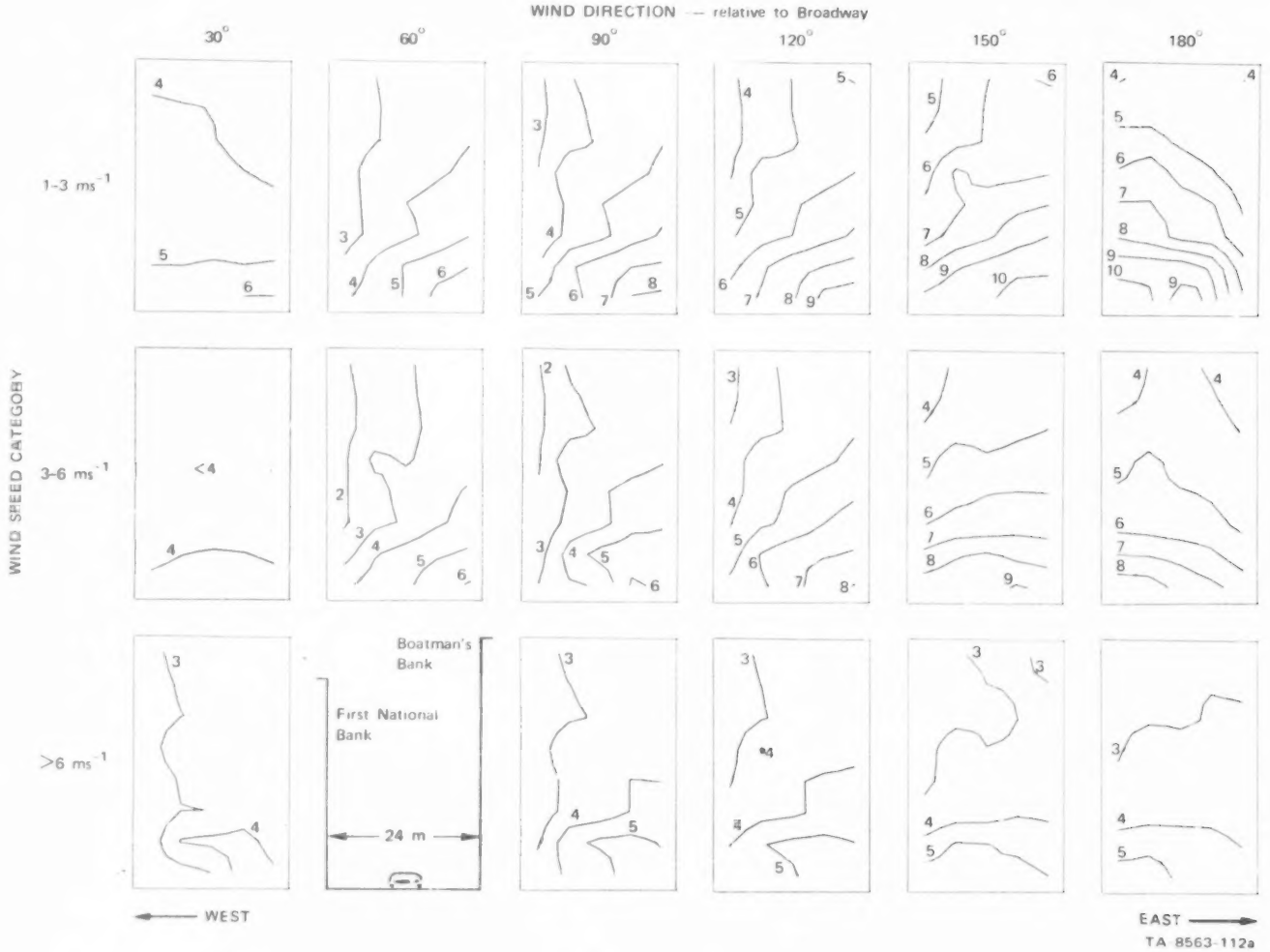

FIGURE 21 DISTRIBUTION OF CO CONCENTRATION IN BROADWAY STREET CANYON

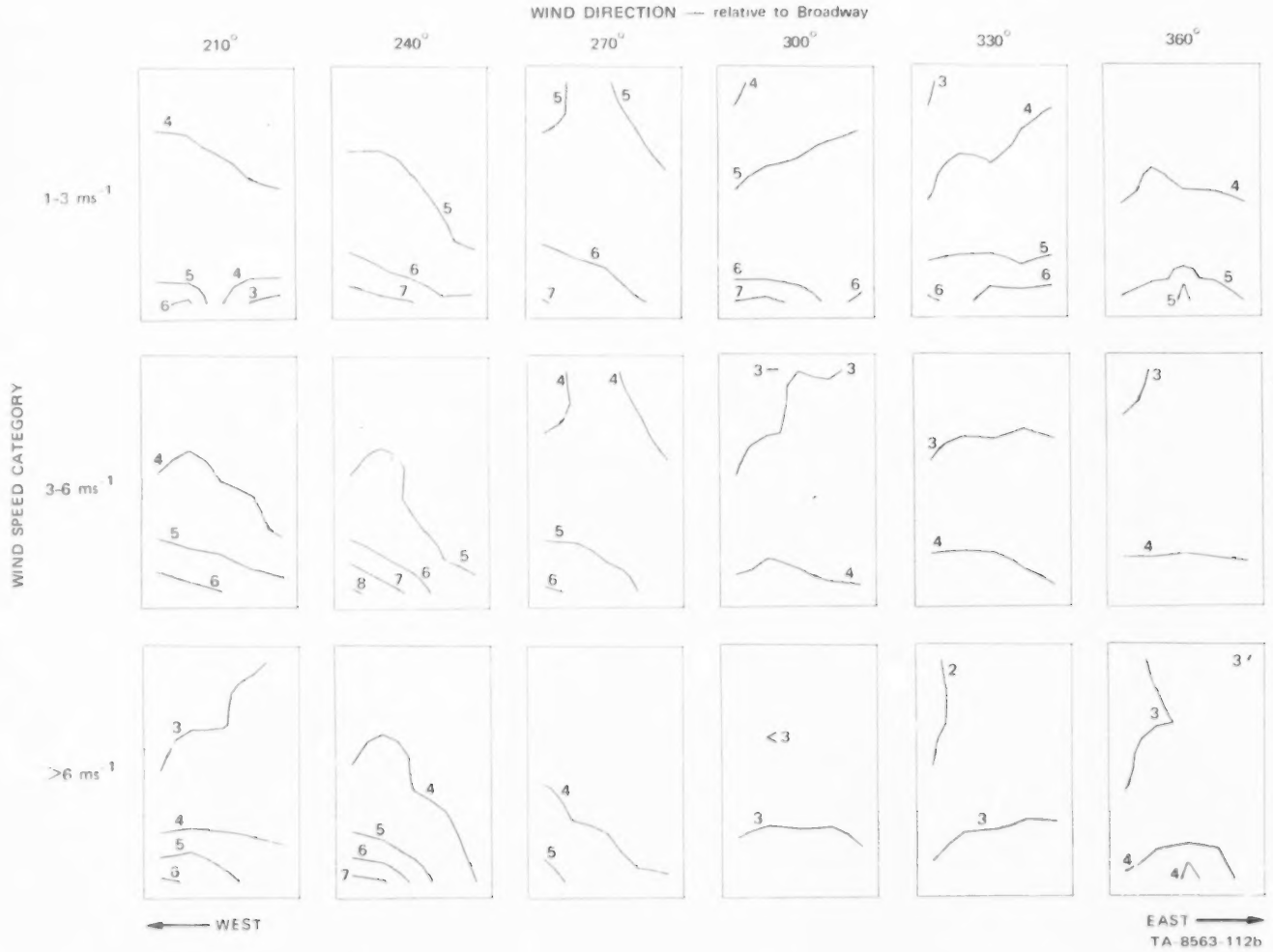

FIGURE 21 DISTRIBUTION OF CO CONCENTRATION IN BROADWAY STREET CANYON (Concluded)

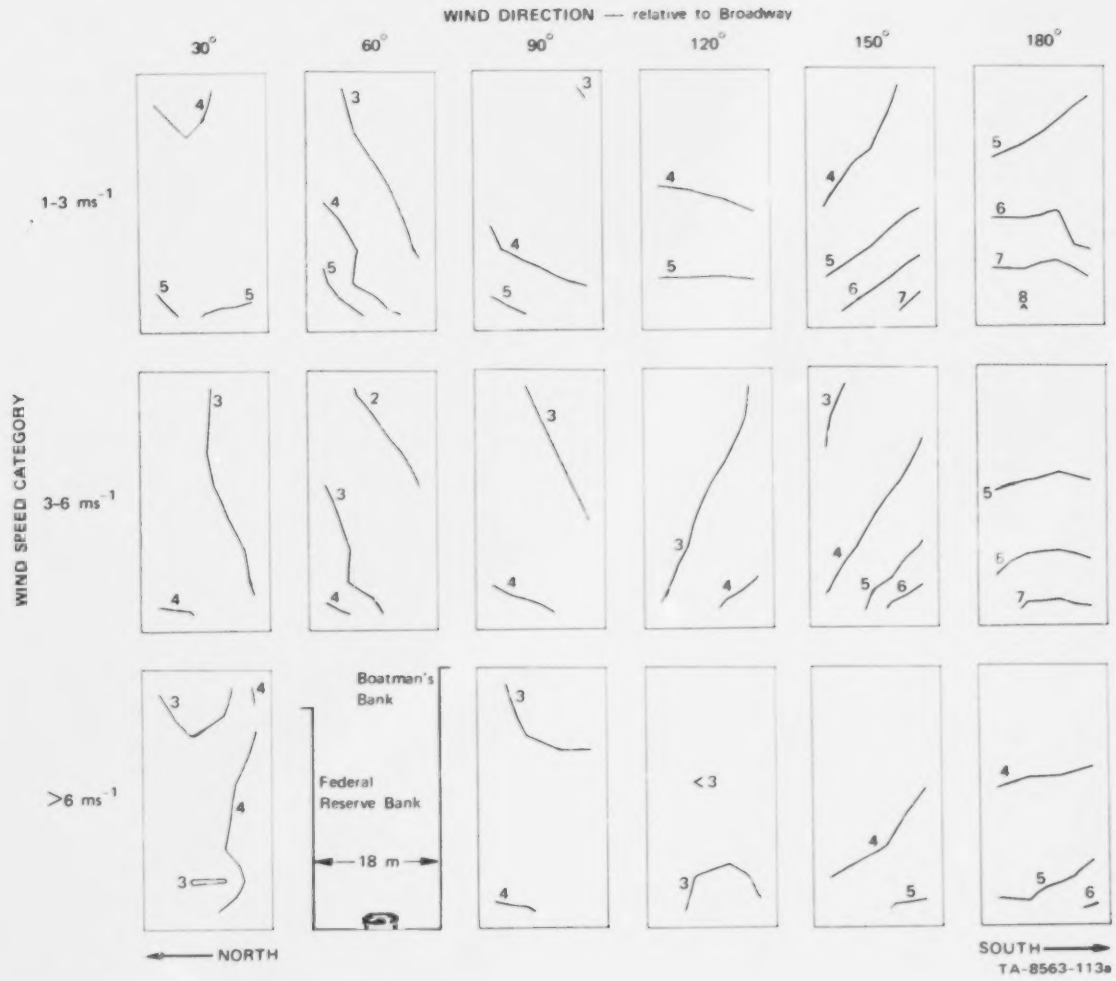

FIGURE 22 DISTRIBUTION OF CO CONCENTRATION IN LOCUST STREET CANYON

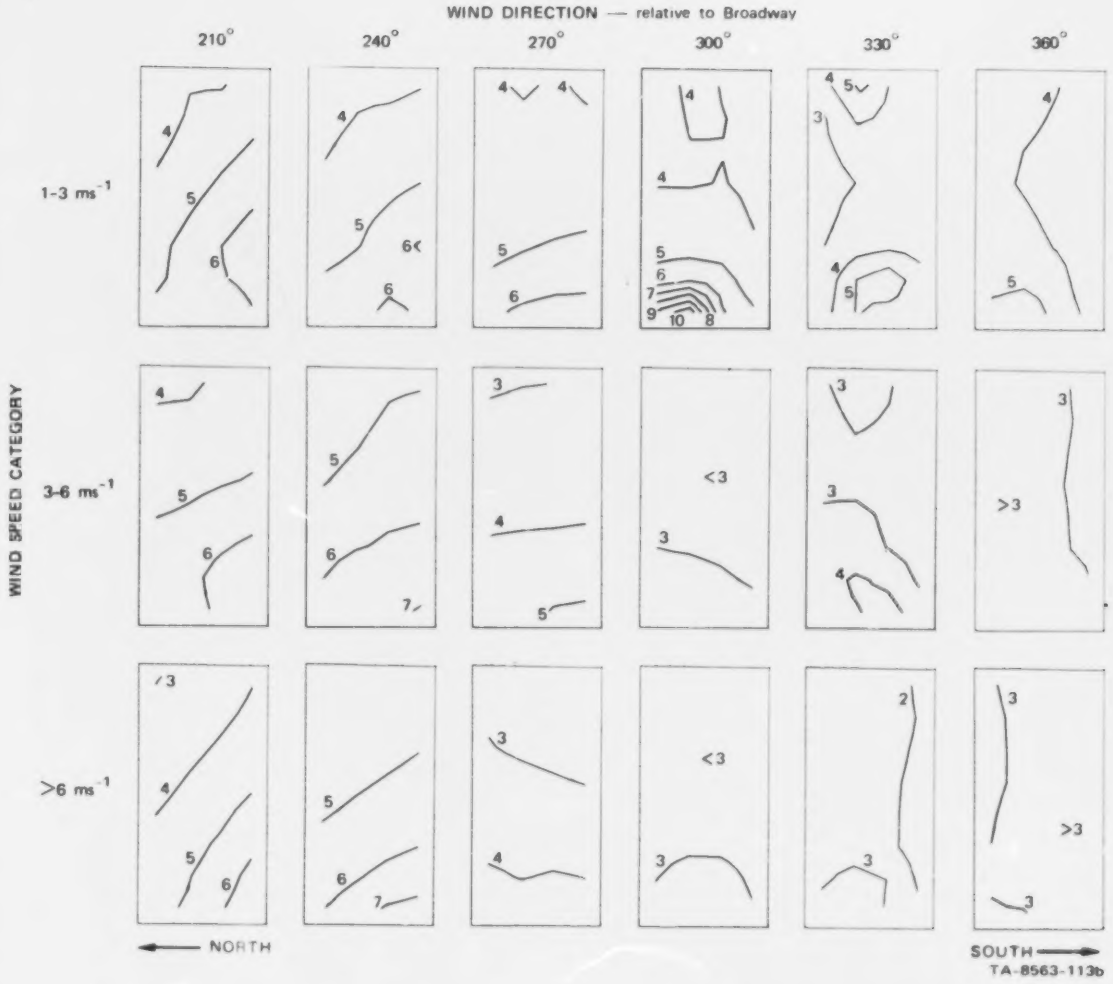

FIGURE 22 DISTRIBUTION OF CO CONCENTRATION IN LOCUST STREET CANYON (Concluded)

such cases. However, the observed patterns can apparently be explained by the distribution of buildings in the immediate area.

The south wall of the Locust Street canyon is formed by the Boatmen's Bank Building which is 11 stories high on Locust Street. The south half of this same building rises to 23 stories and thus forms a wall one-half block to the south that towers above the street canyon. The distribution of CO in the Locust Street canyon during south winds suggests that this wall deflects the air flow and causes eddies in its lee such that the expected south-to-north airflow across the canyon top does not occur. Without such flow there is nothing to initiate the helical circulation that produces the cross-street gradients. As a result, ordinary turbulent diffusion processes prevail and produce the vertical concentration gradients shown in the analyses. If the wind shifts as little as 30^{o}, the concentration patterns expected of cross-street winds are observed, as can be seen in the analyses for 150^{o} and 210^{o} winds.

The average CO distribution in the Locust Street canyon for 300^{o} winds and low wind speed is anomalous and deserves some comment. The distribution shown represents the average of about one hour total data and is therefore very subject to unmeaningful bias. In this particular case, the very high average concentrations occur near a bus stop. On occasion, when two or more buses stopped simultaneously, the exhaust from one of the buses would be below the lowest CO sampling inlet. In this small sample one or two such events would be enough to cause the observed bias. However, such occurrences were infrequent enough that they should not have seriously affected the other averages.

It has been suggested (Chang et al., 1971) that light winds with light turbulence can produce a double helical circulation with the two vortices rotating in opposite directions in a street canyon that is deeper than it is wide. This would lead to cross-street CO gradients at low levels that would be opposite to those expected with a single vortex. Furthermore,

since the transfer of surface-generated CO would be slow between the upper and lower vortices, a "concentration front" might be expected at the interface between the two circulations. There would be relatively uniform high concentrations at lower levels, then an abrupt drop between vortices to relatively uniform lower concentrations. None of the average CO distributions shown in Figures 21 and 22 substantiate the existence of a double helix. Nearly all are consistent with a single-helical circulation.

The air motion measurements in the street canyon do not always agree with the hypothesis of a single-helical circulation, but the agreement was found to be much better in St. Louis than it was in San Jose, and the observations are in better agreement with the single-helix hypothesis than with the double-. It appears, as it did in San Jose, that the lower sensors were located in a region of eddies near the "corner" of the street canyon. The expected low-level cross-street directions of flow were observed in a greater percentage of cases in St. Louis than in San Jose; this may reflect the fact that the sensors were located about one meter higher in St. Louis and were therefore somewhat less likely to be in the corner eddy. The upper sensors were located, of necessity, almost on a level with the building cornices and were therefore subject to all the eddies associated with airflow over these edges.

The evidence suggests that the street canyon submodel developed from the San Jose data (Johnson et al., 1971) is fundamentally correct and requires only relatively minor revision. Some revision is required because the results have shown that the air does not retain the same CO concentration from rooftops to street level as it flows down in front of the buildings facing the wind. Apparently there is substantial entrainment of recirculating polluted air and this leads to greater concentrations at lower levels. This feature was observed in San Jose also; the total body of data indicates that it is not anomalous and should be considered in the formulation of the model.

It is reasonable that the air in the down draft should be typified by a "box model" concentration as was done in the formulation of the street model. We have chosen to retain this feature. To incorporate the observed increase in concentration from roof level to street level, a term has been introduced that is linear with height. We have assumed that the CO augmentation of concentration from roof level to street level is the same as was given by the equation developed from the San Jose data (Johnson et al., 1971):

$$\Delta C_W = \frac{0.1\ KNS^{-0.75}}{W\ (u + 0.5)} \qquad \text{ppm}, \tag{5}$$

where ΔC_W is the CO added to roof-level values to account for street effects in front of the buildings facing the roof-level wind; K is a constant; S and N are the average traffic speed (miles per hour) and volume (vehicles per hour); W is street width (m); and u is wind speed ($m\ s^{-1}$) above roof level. The development of this parameterization has been discussed by Johnson et al. (1971) and will not be repeated here. If the value of ΔC_W is taken to be zero at roof level, and if its street-level value is given by the above equation (which is independent of height, z) a linear variation with height gives

$$\Delta C_W = \frac{0.1\ KNS^{-0.75}}{W\ (u + 0.5)} \cdot \frac{(H - z)}{H} \tag{6}$$

where H is the depth of the street canyon.

There is no evidence to justify changing the equation used to describe the augmentation of CO concentration (ΔC_L) by street effects on the opposite side of the street, i.e., in front of the buildings facing downwind. This equation, as developed by Johnson et al.,is

$$\Delta C_L = \frac{0.1\ KNS^{-0.75}}{(u + 0.5)\ [(x^2 + z^2)^{1/2} + 2]}\ , \tag{7}$$

where x is the horizontal distance to the nearest traffic lane. This formulation retains the same cross-street gradients given by the earlier pair of equations for small values of z, but the cross-street gradients at higher levels are greater than with the earlier version of the model.

For parallel winds the average of ΔC_L and ΔC_W is used for both sides of the street. The equation for winds parallel to the street is

$$\Delta C_I = 0.5\ (\Delta C_L + \Delta C_W)$$

$$= \frac{0.05\ KNS^{-0.75}}{(u + 0.5)} \left[\frac{1}{(x^2 + z^2)^{1/2} + 2} + \frac{H - z}{HW} \right] . \quad (8)$$

The value of the exponent of S is subject to change with changes in exhaust emission devices and the mixture of model years on the road. The value -0.75 is appropriate to a 50/50 mix of cars whose model years are before and after the 1968 introduction of exhaust emission control devices (1965 in California). The constant 0.1 in Eqs. (5) and (6) is also a factor that relates to automotive emission controls and the model year mix.

The distributions of CO concentrations shown in Figures 21 and 22 suggest that the helical circulation develops with rather small cross-street roof-level components and therefore the application of the parallel-wind equation for ΔC_I should be restricted to a smaller angular segment than was previously suggested. Ninety-degree segments were to be used for general applications; for wind directions within 45^o of the street direction, the "parallel" formulation would be used, and for other wind directions the "cross-wind" formulation. However, when the San Jose data were analyzed, the cross-wind cases prevailed over 120^o wind direction intervals and the parallel-wind over 60^o intervals for the two midblock street canyon stations. The sectors were not always symmetric about the parallel and perpendicular directions. This was ascribed to the effects of nearby buildings, which, as we have seen in the St. Louis data, can be important. However, the St. Louis

data also indicate that cross-wind patterns often develop with winds blowing at a relatively small angle to the street direction, and so it appears that 60^{o} wind segments are appropriate for application of the parallel-wind model. In lieu of other information, which would not be available for most general applications, the segments should be arranged symmetrically about the street direction.

The street submodel predicts the difference between roof-level and street-level CO concentrations. The submodel was applied to the data shown in Figures 21 and 22 to estimate its accuracy and to compare it with the version that had been developed from San Jose data. The anomalous case (300^{o} wind direction, low wind speed) was excluded from the data set. The upper-tower average winds, and the average traffic volumes were used as inputs for application of the submodel. The average traffic volumes vary from 90 to 384 vehicles per hour on Locust and 211 to 904 vehicles per hour on Broadway, so a wide range of traffic conditions is represented.

An average vehicle speed of 8.5 mph was used for the Broadway calculations. This value comes from the measurements discussed in an earlier section. For Locust Street a value of 5 mph was used. This low speed was chosen because there is a stop sign at the end of the short block where the measurements were made and vehicles enter the block after stopping for another stop sign, so the average speeds must be less than on Broadway.

The original and the revised street model were applied to the averaged data, and the calculated values of ΔC were compared with the corresponding observed differences between street- and roof-level CO concentrations. The correlation coefficients and root-mean-square differences (RMSD) between observed and calculated values were determined for several values of K between 3 and 10. Both the original and the revised street submodels showed minimum RMSD's between observed and calculated ΔC's for K approx-

imately equal to 7, the same as used in San Jose. Using this value, the RMSD for the original submodel was 1.4 ppm. For the revised model, the RMSD was 1.1 ppm. The respective correlation coefficients were 0.55 and 0.60; the revisions have improved the performance of the model somewhat.

The RMSD's and correlations were also determined for the observed and calculated differences between concentrations measured on opposite sides of the street at roof level and at street level. Since the original and revised models give virtually the same cross-street differences at street level, whatever differences there are between the two versions of the model must arise from their performances in predicting cross-street differences at roof level. The revision in the submodel reduces the predicted cross-street CO concentration differences. The original model predicts the cross-street differences with an RMSD of 1.12 ppm and a correlation coefficient of 0.57. The revised model's RMSD is 1.07 and its correlation coefficient is 0.63. As with the calculations of ΔC there has been an improvement in the performance of the submodel.

In order to avoid the complications of wind circulations that may exist in the immediate vicinity of intersections, the fixed wind and CO installations were located at midblock. However, we also made measurements of the along-street variability of CO concentrations in order to assess the general applicability of the midblock analyses. The mobile van system was used for this purpose; the van was parked during 13 daytime periods of up to 7 hours each at a variety of locations on Locust Street and Broadway as shown in Figure 23. Hourly van concentrations were computed for comparison with the 4-m CO observations made at the fixed installation on the same side of the block. Figure 24 shows the results of the comparisons for those periods during which both van and fixed-station CO data were available; the horizontal wind components measured at the 4-m level are also shown. We could not use a larger variety of sites due to local parking restrictions, but there are still enough sites to warrant confidence in the results.

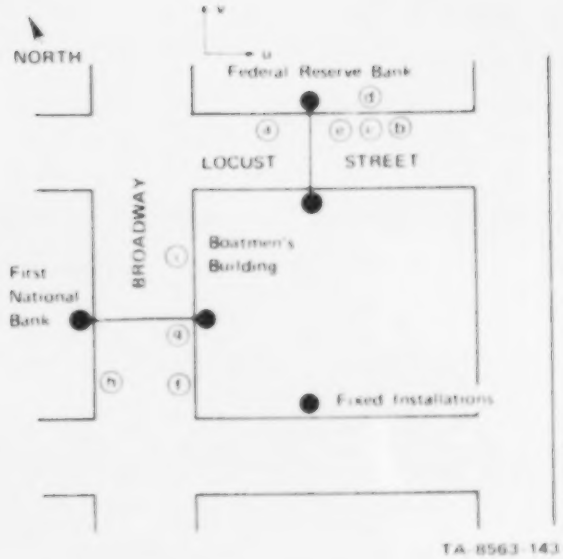

FIGURE 23 LOCATIONS OF ALONG-STREET CO MEASUREMENT SITES

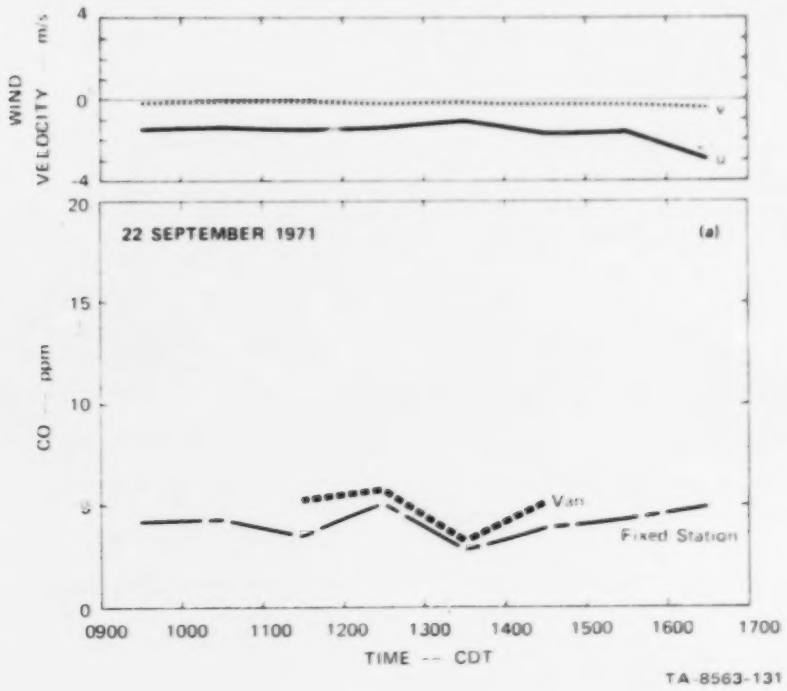

FIGURE 24 COMPARISON OF ALONG-STREET CO CONCENTRATIONS WITH MIDBLOCK, 4-m OBSERVATIONS OF CO AND WINDS. Locations of along-street measurement sites are given in Figure 23.

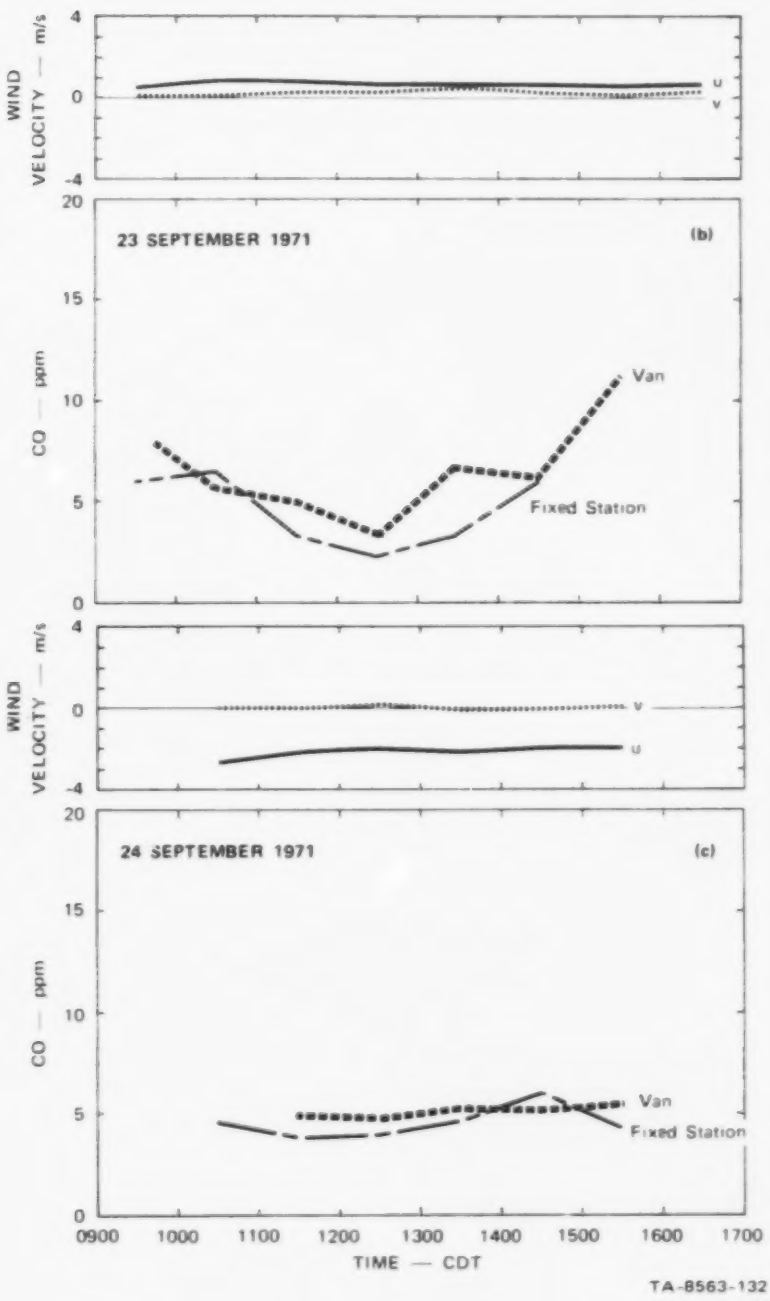

FIGURE 24 COMPARISON OF ALONG-STREET CO CONCENTRATIONS WITH MIDBLOCK, 4-m OBSERVATIONS OF CO AND WINDS. Locations of along-street measurement sites are given in Figure 23. (Continued)

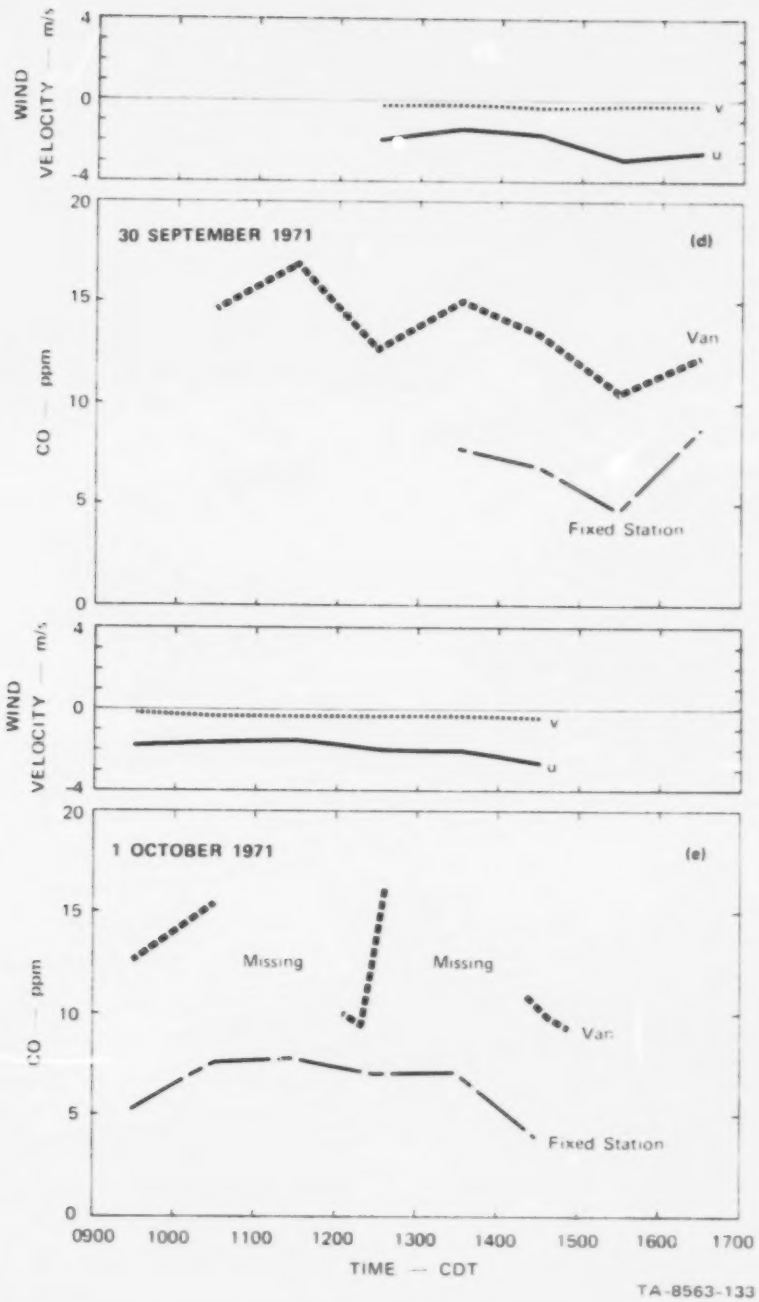

FIGURE 24 COMPARISON OF ALONG-STREET CO CONCENTRATIONS WITH MIDBLOCK, 4-m OBSERVATIONS OF CO AND WINDS. Locations of along-street measurement sites are given in Figure 23. (Continued)

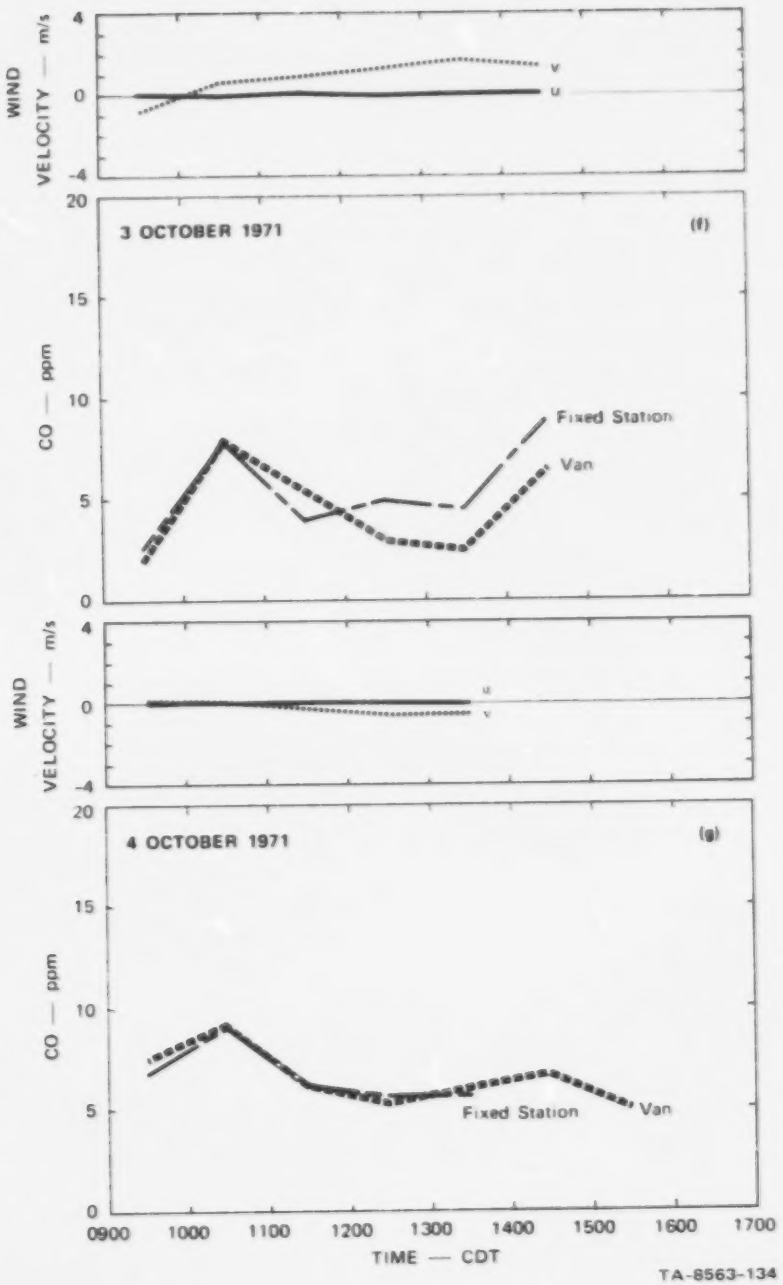

FIGURE 24 COMPARISON OF ALONG-STREET CO CONCENTRATIONS WITH MIDBLOCK, 4-m OBSERVATIONS OF CO AND WINDS. Locations of along-street measurement sites are given in Figure 23. (Continued)

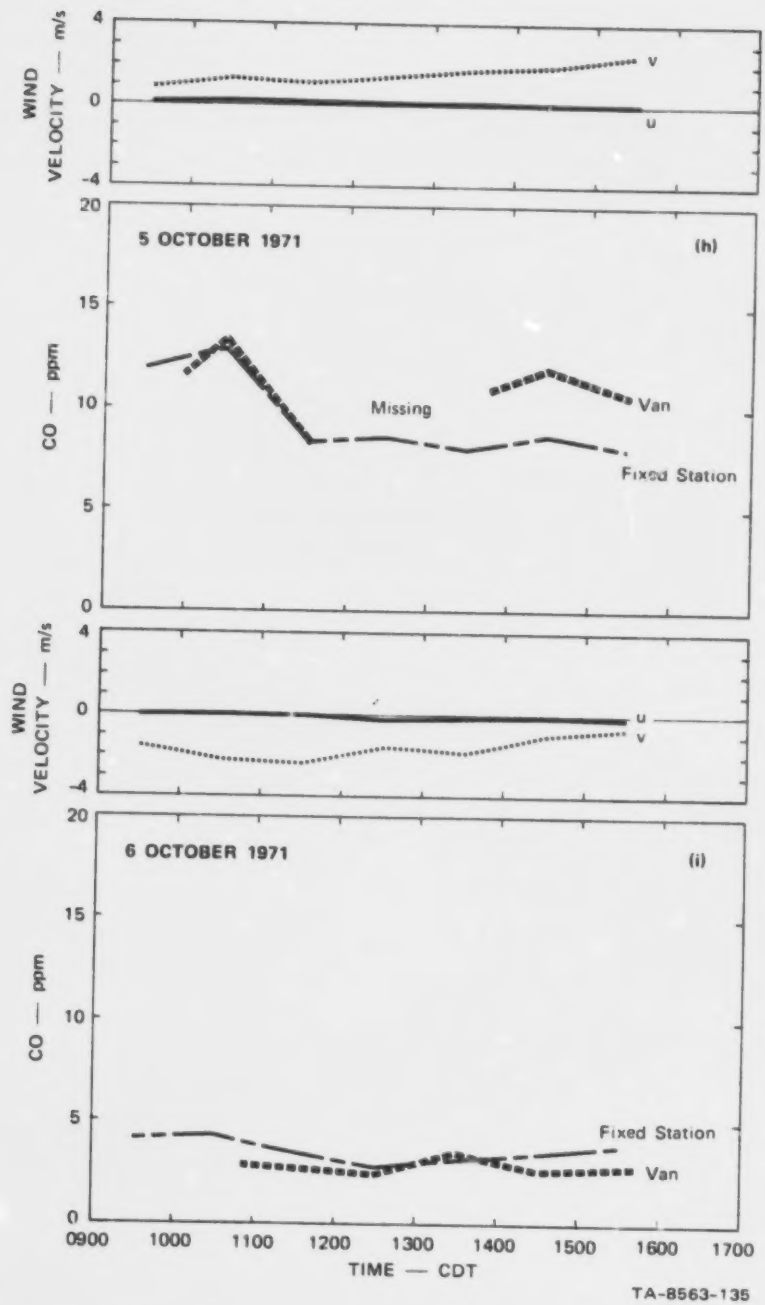

FIGURE 24 COMPARISON OF ALONG-STREET CO CONCENTRATIONS WITH MIDBLOCK, 4-m OBSERVATIONS OF CO AND WINDS. Locations of along-street measurement sites are given in Figure 23. (Concluded)

Agreement between the van and fixed-station measurements is generally quite good; the two usually agree within 1-2 ppm and show no systematic differences. This agreement may, in part, be attributable to the along-street uniformity of the source. This, together with the generally larger wind components parallel to the street, will tend to minimize the along-street gradients, as opposed to the cross-street gradients which can be appreciable, as the discussions on the preceding pages have shown.

Two cases of relatively large along-street variations were found. These are shown in Figure 24(d) and (e) where systematically larger values (on the order of 6 ppm) were measured with the van. Correlation with the fixed-station measurements, however, is quite good. We can offer no explanation for this phenomenon, but several observations may be in order. The differences do not appear to be a peculiarity of the site. The observations illustrated in Figure 24(b) and (c) were made in the same area (see Figure 23), yet show good agreement. In all four cases, the magnitude of the cross-street wind component was less than 0.5 m s^{-1}, while the along-street component ranges from 0.5 to 3.0 m s^{-1}. Furthermore, the case of good and the case of poor agreement were observed on the same day of the week, thereby minimizing effects of traffic differences. The only systematic difference is that during the periods of large differences in concentrations measured at van and fixed sites, the cross-street wind was consistently from the north, while good agreement was achieved for zero and southerly cross-street winds. Finally, in view of the good correlation observed during the periods of poor absolute agreement, the question of instrument malfunction cannot be ruled out entirely, although calibrations of both the fixed and van systems were made routinely. Figure 24(g) is an example of the correspondence that can be expected between the two different measuring systems. On this day, the van intake was approximately 1 m from that of the fixed installation. The differences ($\leq$ 0.5 ppm) are within the uncertainties of the two measurement systems.

In summary, we may conclude that the midblock observations are quite representative of conditions throughout the block. These data show that the street effects submodel is capable of predicting CO concentrations in the street canyon with an accuracy that is comparable to the observed variations of CO along the street.

F. Freeway

In order to assess the potential application of the model to areas in the immediate vicinity of major roadways, the mobile van monitoring system was used to make selected observations of CO concentrations downwind of the six-lane Daniel Boone Expressway at Forest Park (see Figure 5). Specifically, these measurements were of four types: (1) temporal observations at a fixed location, (2) horizontal profiles immediately downwind of the freeway, (3) vertical profiles adjacent to the roadway, and (4) mobile measurements in the park area to a distance of about 1 km downwind of the freeway.

There are a number of questions that need to be answered with regard to the source characteristics of a modern, multilane freeway. In the first approximation, the freeway may be treated as an infinite line-source with an effectively constant emission rate for periods up to one hour. More realistically, the modern freeway is better represented by two roadways--one in each direction of travel--with significantly different emission rates and traffic patterns. The mechanical turbulence induced by the usually fast moving vehicles disperses the emissions quite rapidly at the source, thereby effectively creating an extended volume source. Other roadway characteristics must also be considered, such as the height displacement of the roadway with regard to the surrounding terrain. The mobile van facility was used for a preliminary investigation of the manifestations of these features on the resulting distribution of CO near a major, ground-level freeway.

Observations made during two early morning, peak traffic periods are illustrated in Figures 25 through 27; meteorological conditions derived from the near-simultaneous EMSU data are also presented. Figure 25 illustrates the temporal variation of CO observed during a half hour period at a height of 3 m and at a distance of about 3-4 m downwind of the nearest (westbound) traffic lane; traffic during this period is a factor of about three times heavier in the more distant, eastbound lanes. Atmospheric conditions were slightly stable during the period and the winds were steady and nearly perpendicular to the roadway, although the speed was estimated to be about half the value of 6 m s^{-1} reported at the EMSU station. The observed CO concentrations ranged from about 12 to 22 ppm. Five-minute average concentrations differed by about 3 ppm over the period; during the last 20 minutes there was only 1.5 ppm variation.

When a single monitoring system is used to obtain horizontal CO profiles immediately downwind of the freeway, care must be exercised to separate the horizontal gradients from temporal variations. To minimize this difficulty, horizontal profiles were made by moving the van in discrete steps toward the source during a period when the source strength could be expected to decrease and the turbulent diffusion to increase with time. The horizontal profile obtained in this manner to a distance of 200 m is shown in Figure 26. Five-to-seven minute observation periods were made at each site, except for the near-freeway site, where two consecutive observations were made. Both the absolute value and the standard deviation of the concentrations decrease in an exponential fashion with distance from the source. Qualitatively, the data are as expected, but the lack of information on ambient CO levels and temporal emission trends, as well as the lack of micrometeorological data, precludes quantitative analysis.

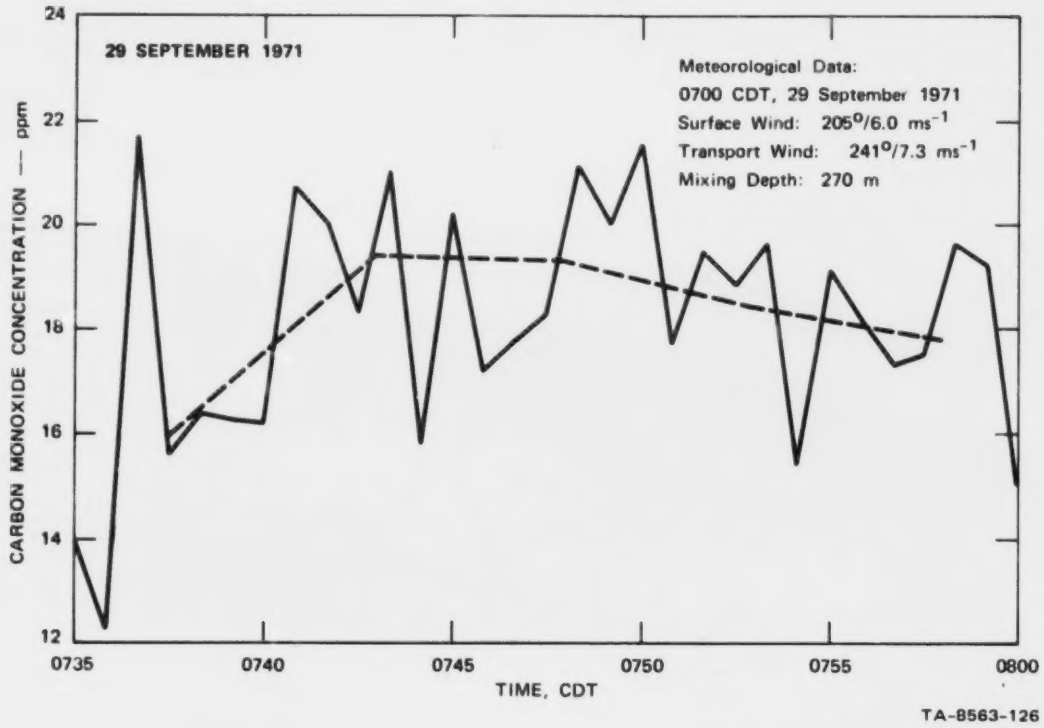

FIGURE 25 TEMPORAL VARIATION OF CO CONCENTRATION ADJACENT TO THE DOWNWIND EDGE OF THE SIX-LANE DANIEL BOONE EXPRESSWAY AT FOREST PARK, ST. LOUIS

Figure 27 is an illustration of the vertical structure of CO concentration at the near-freeway site; the data were collected sequentially at the various levels over a 65-minute period under meteorological conditions similar to those given above. Concentrations were measured at five levels from 3 m to 11 m. The observations began and ended with measurements at the 3-m level. The 3-m measurements (which differed by 3 ppm) were used to establish the temporal trend by linear interpolation. The observations at other heights were referenced to the interpolated 3-m values. The significant feature of these observations is the apparent pronounced elevated CO maximum at 5 m. Two arguments may be offered

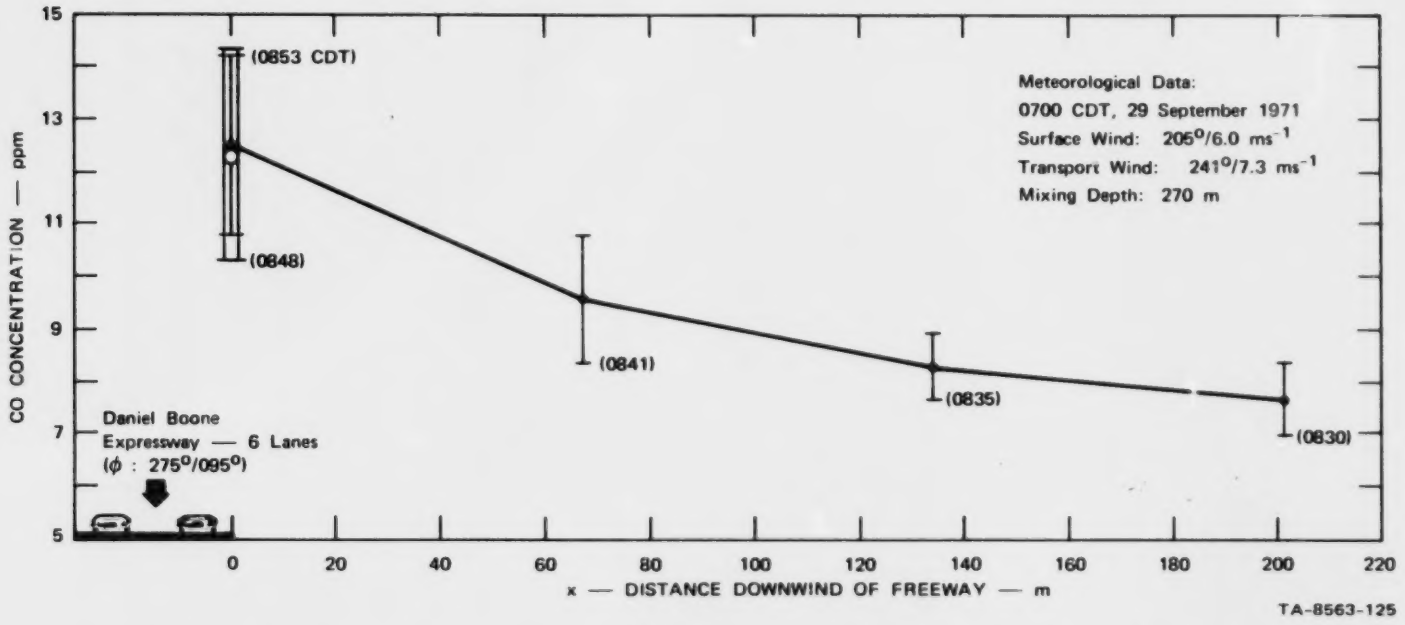

FIGURE 26 DISTRIBUTION OF CO CONCENTRATION AT 3-m HEIGHT DOWNWIND OF THE DANIEL BOONE EXPRESSWAY AT FOREST PARK, ST. LOUIS

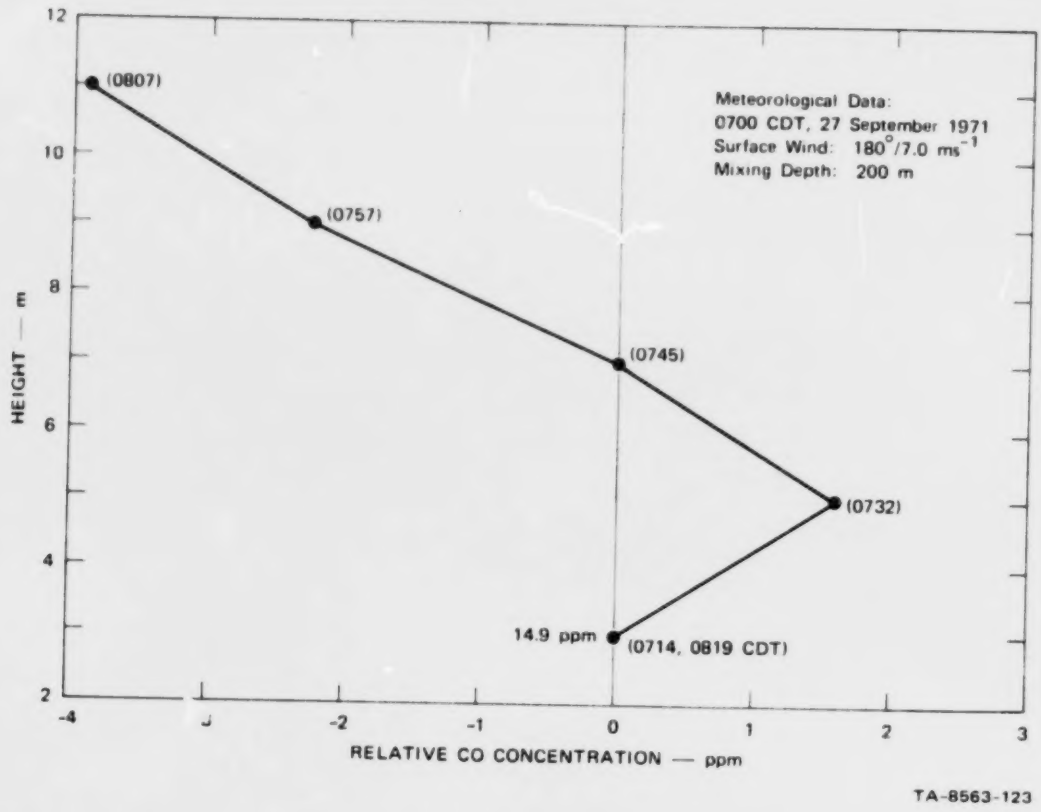

FIGURE 27 HEIGHT VARIATION OF CO CONCENTRATION ADJACENT TO THE DOWNWIND EDGE OF THE SIX-LANE DANIEL BOONE EXPRESSWAY AT FOREST PARK, ST. LOUIS

that this feature is an artifact caused by: (1) temporal variations of the emissions and/or meteorological fields which were not accounted for by the interpolation, or (2) aerodynamic effects of the van structure. The observations presented in Figures 25 and 26, as well as the personal evaluation of the observers, indicate that conditions did not change significantly with time. The latter, however, may be significant in that the body of the van could have caused a tilting of the local wind trajectories. However, in view of the relatively light winds, it is somewhat doubtful that this is the total cause of the phenomenon. Alternatively, one may suggest some characteristic of the freeway itself. In this regard, air flowing from one side of the roadway to the other may encounter a shelterbelt effect of the "wall" of vehicles in the

downwind lanes. Also, the strong mechanical turbulence induced by the traffic movement causes the emissions to be rapidly dispersed into some effective volume near the source, thereby increasing the effective height of the source.

These limited freeway observations serve to illustrate the complexity and large variability of the distribution of vehicle-generated pollutants in the freeway corridor. Additional research is indicated to better define concentration patterns near major roadways and to evaluate the applicability of the APRAC-1A model in these areas. The situation is somewhat similar to the importance of street effects in the downtown area, and an analogous freeway submodel may be required.

IV PERFORMANCE OF THE MODEL

In the preceding section, the various components of the composite model were examined. Their initial outputs were compared with values of the corresponding parameters obtained in St. Louis by different and independent methods, and in some cases minor revisions were made. The algorithm for obtaining the stability index was changed slightly on the basis of the St. Louis data, as was the street-effects submodel. Also, the emissions model now uses a new diurnal traffic cycle for downtown streets, both arterial and freeway. This is not a fundamental change, but simply reflects the availability of better data.

The changes resulting from the St. Louis studies have not been major; the major changes in the model were made at the conclusion of the San Jose study. In that experiment, the traffic data were not used to apply the model in its complete form. Concentrations resulting from emissions at distances greater than 2 km from the receptor were not calculated. Instead, measured concentrations were used to simulate this part of the model. The San Jose evaluations used winds specially measured in the downtown area for the application of the model and its submodels; also special measurements had been used to determine the wind direction sectors where the helical street canyon circulation developed. All these factors should have given the model somewhat better performance than would be expected if it used a complete traffic network, airport meteorological measurements, and the standard street model wind direction sectors.

For this report, the model has been applied in the manner that would be employed by its potential users. The extensive traffic network for St. Louis that was used in our earlier studies (Ludwig et al., 1970) has been updated using the most recent data available to us (Missouri State

Preceding page blank

Highway Department, 1970). Hourly airport meteorological observations and the routine radiosonde measurements from Salem, Illinois have been used. When the model is applied in this way and the results are compared with the special CO measurements made in downtown St. Louis, its capabilities can be accurately defined.

Figure 28 shows the observed hourly average CO concentrations for the operating periods at the four low-level street canyon sites; these values were measured at heights of about 3 and 4 m from the building faces. This same figure shows the concentrations calculated with the model using hourly meteorological data. The calculated values are shown for all hours, but the observations were not always made continuously (see Table 4). It is obvious that the model generally reproduces the observed trends very well.

Figure 29 shows the scatter diagrams where the observed CO concentrations are plotted against those calculated with the model. The root-mean-square differences between the observed and the calculated CO concentrations range from 2.9 ppm at the east side of Broadway to 3.9 ppm at the west side of Broadway. At roof level the observed (the average of the four measurements at the top of each street canyon) and the calculated concentrations have root-mean-square differences of 2.5 ppm. These values compare quite favorably with the 3-ppm accuracy found in San Jose using special data. They certainly exceed the performance of the model before it was revised. In earlier studies (Ludwig et al., 1970) using St. Louis CAMP station data, the original model was found to have root-mean-square differences with the observations of 5 to 9 ppm. The model revisions made on the basis of the San Jose and St. Louis field studies have resulted in considerable improvements in the performance of the model.

As demonstrated earlier (Ludwig et al., 1970), the results can be improved considerably if special statistical regressions are undertaken.

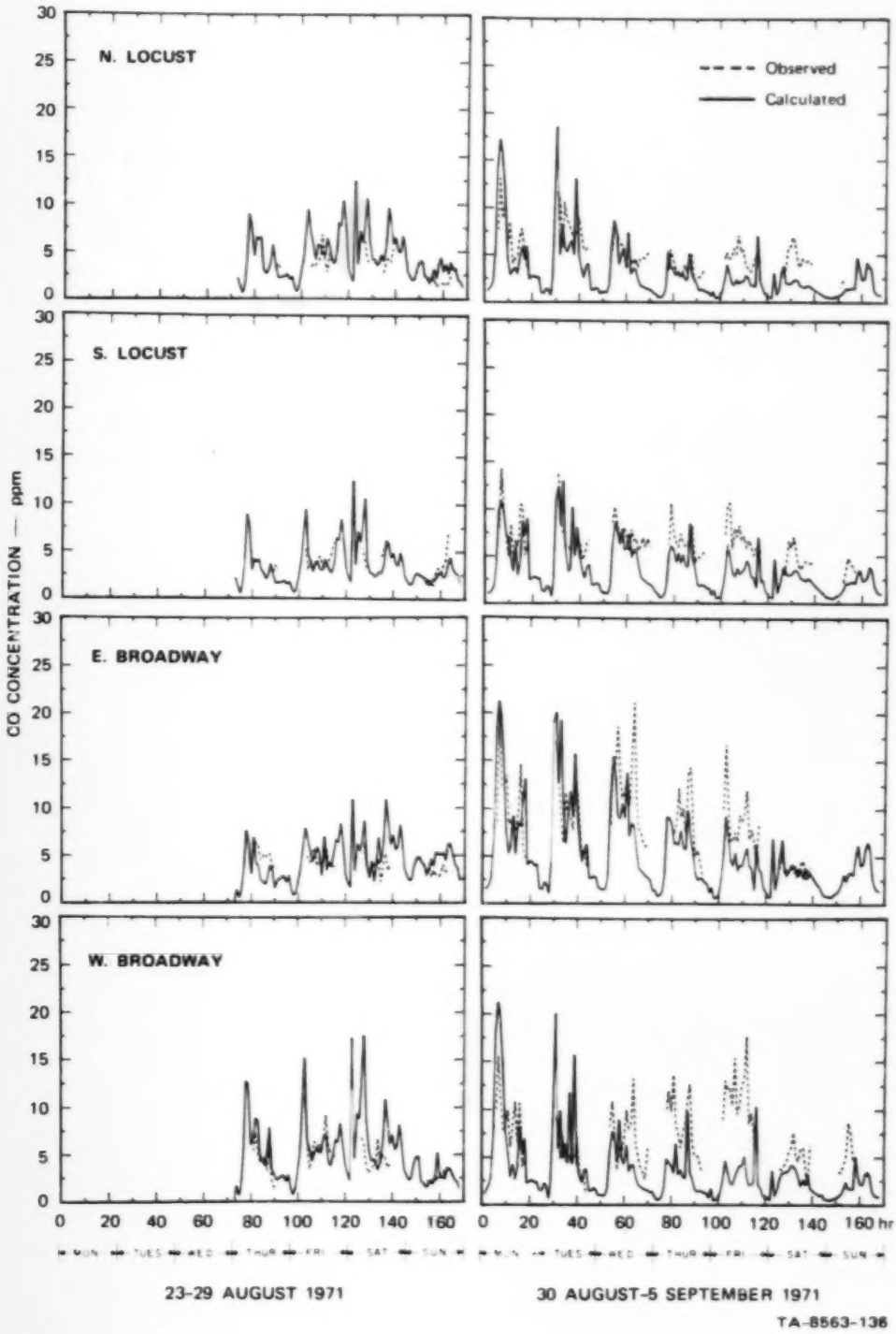

FIGURE 28 OBSERVED AND CALCULATED CO CONCENTRATIONS AT 4 m

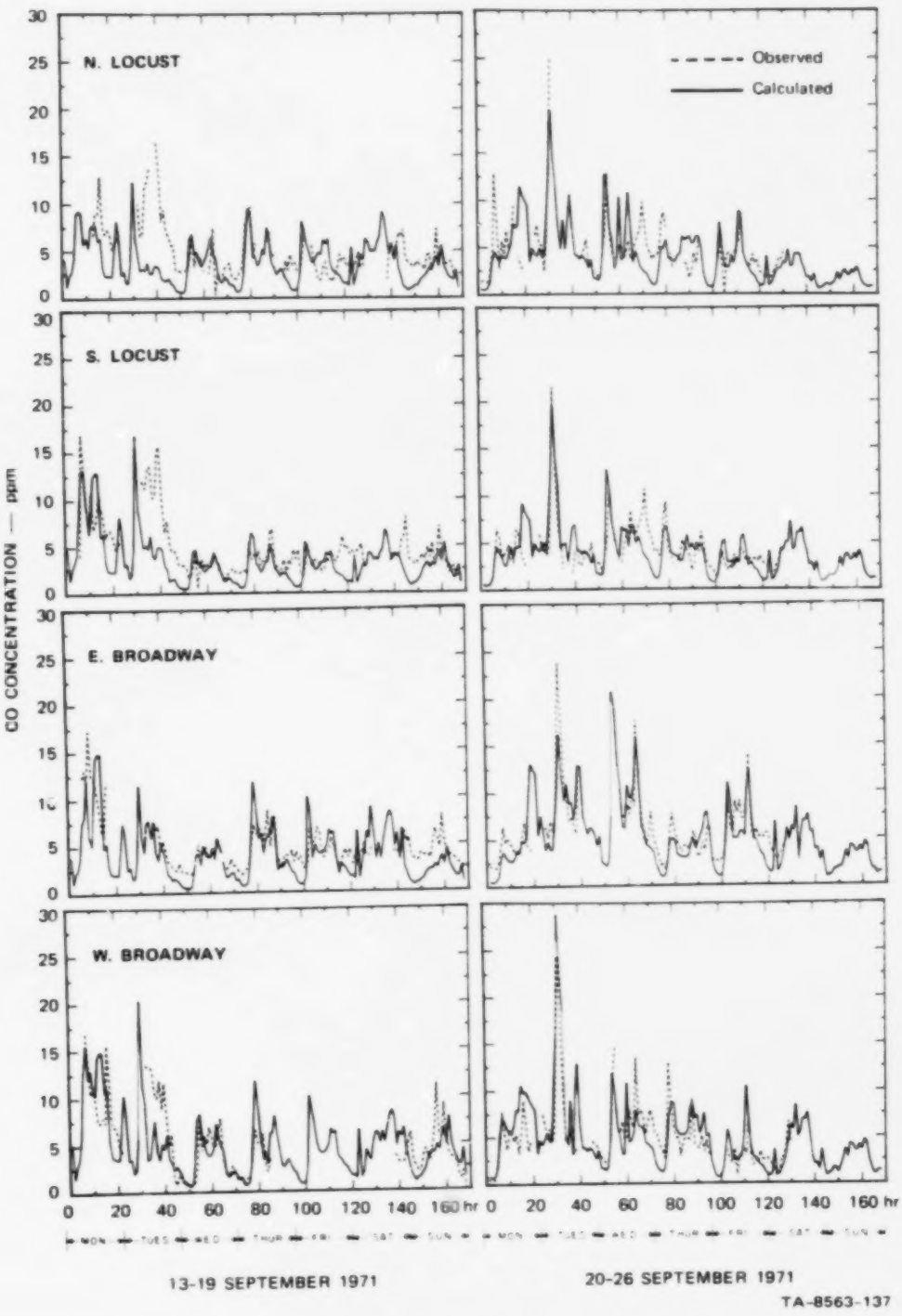

FIGURE 28 OBSERVED AND CALCULATED CO CONCENTRATIONS AT 4 m (Continued)

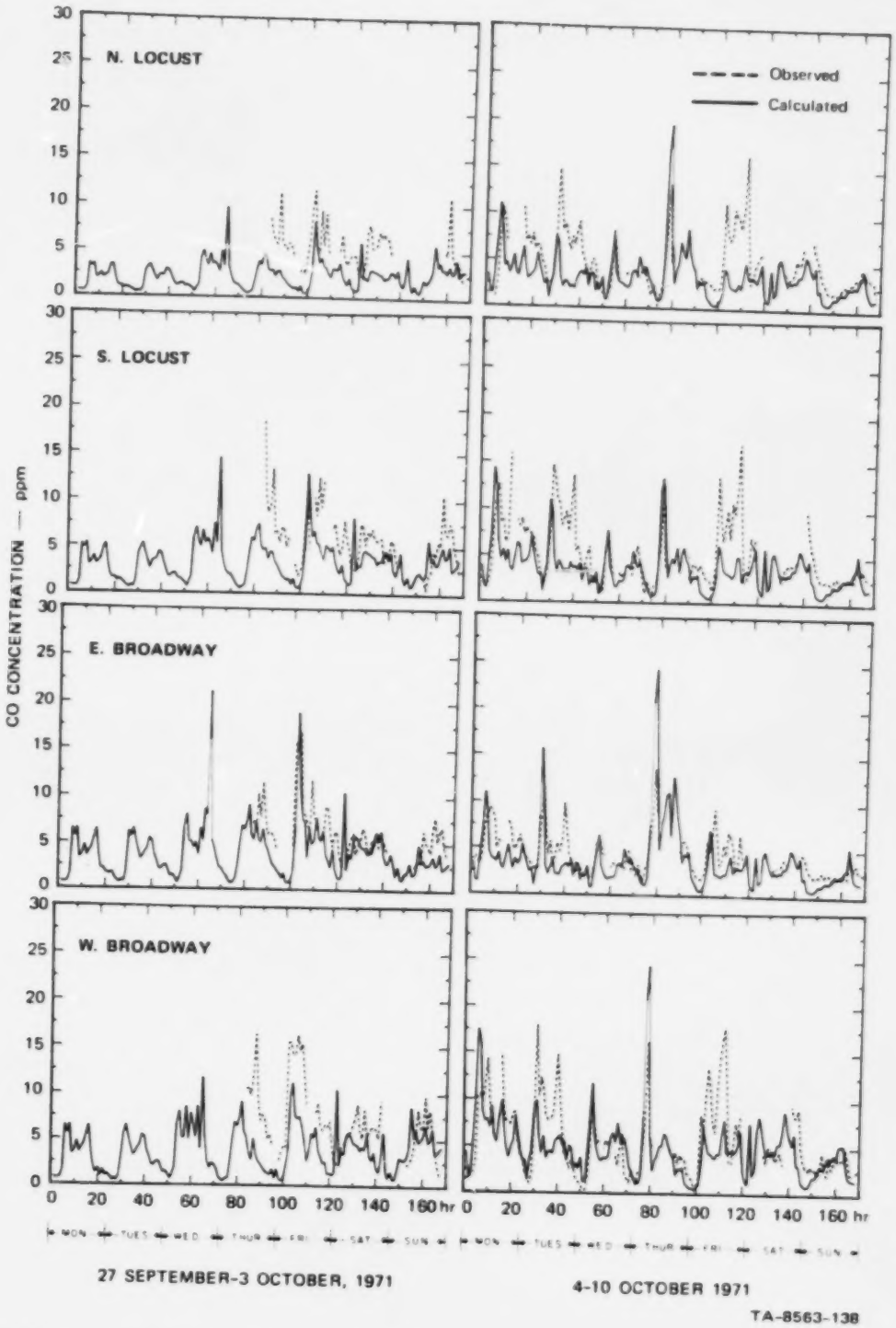

FIGURE 28 OBSERVED AND CALCULATED CO CONCENTRATIONS AT 4 m (Continued)

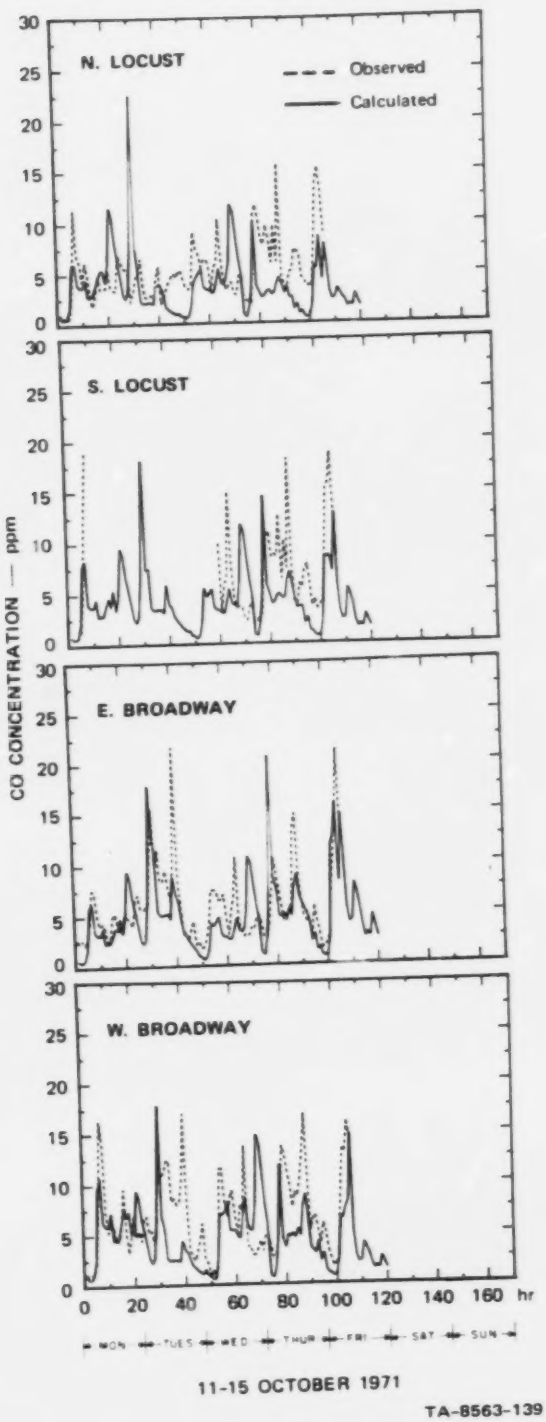

FIGURE 28 OBSERVED AND CALCULATED CO CONCENTRATIONS AT 4 m (Concluded)

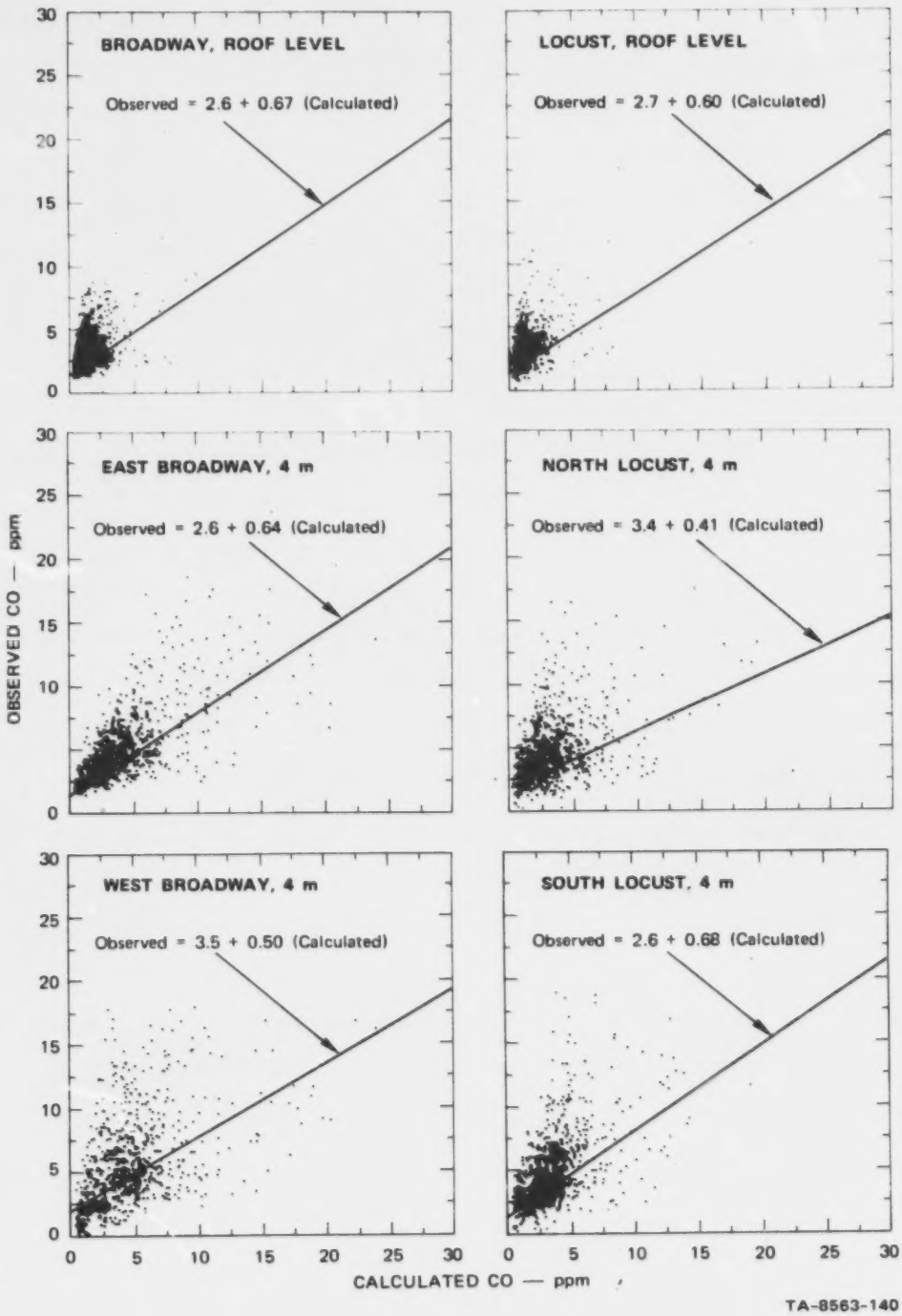

FIGURE 29 SCATTER DIAGRAMS SHOWING OBSERVED CO CONCENTRATIONS VERSUS THOSE CALCULATED WITH THE MODEL

However, special regressions cannot be depended upon to apply to all cities or sets of conditions, only those for which they were derived. Since the model was developed from physical principles, the error figures in the preceding paragraph should be a good indication of the model's general applicability. The revisions and additions that have been made to the model have brought its accuracy to a point where it is comparable to the ± 2-to-4-ppm values achieved earlier only through special fitting processes (Ludwig et al., 1970).

In some special situations, reliable measurements are available, and these could be used as a basis for statistical regressions appropriate to certain locations. Such relationships developed from the data collected in St. Louis are shown in Figure 29. Use of these relationships would reduce root-mean-square errors somewhat. At street levels, the relationships shown in Figure 29 reduce the root-mean-square errors on the east side of Broadway to 2.5 ppm (from 2.9) and on the west side to 3.3 ppm (from 3.9); these are the extremes. At roof level, the regression lines reduce the errors to 1.6 ppm (from 2.5).

The correlation coefficients between calculated and observed values of CO concentration vary from 0.40 for the North Locust site to 0.67 for the East Broadway site. Although these values are not as high as we would like, they do represent an improvement over the values found in our earlier St. Louis comparisons. These earlier values varied from 0.16 to 0.45 for the months studied. For comparison, the earlier correlations for the months of August through October 1964 ranged from 0.16 to 0.27.

Figure 29 shows certain systematic differences between the observed CO concentrations and those calculated with the model. The model generally underestimates concentrations below about 7 or 8 ppm and overestimates those at the higher values. The overestimation of high concentrations may reflect a systematic inadequacy in the treatment of conditions conducive

to high concentrations. If the source of error were the use of a minimum effective wind speed during periods of observed calm, then the data suggest that a slightly larger minimum wind speed would be more appropriate. Another likely source of bias is the emissions model. High concentrations are frequently found during periods of peak traffic. The model presumes that the average speeds during peak traffic periods are 85 percent of the average speeds at other hours. If this were an underestimate or if the exponent used in the emission equation [see Appendix A, Eq. (A-4)] were incorrect, then emissions might be overestimated during periods of high concentration; overestimates of the emissions would lead directly to overestimates of the concentration.

The fact that the model underestimates CO concentration when the concentration is low may be attributable to the effects of sources beyond 32 km from the receptor. Virtually all the important sources in the St. Louis metropolitan area are within this distance and should be accounted for, so it seems unlikely that differences of about 2.5 ppm would arise from CO entering the area from the rural regions. If the emission model overestimates the emissions for high emission situations, it may also underestimate for the low emission situations that account for many of the periods of observed low concentration. The tests that have been conducted to check the performance of the emissions model have not been sufficiently sensitive to detect errors of the magnitude that might be associated with the observed differences between calculated and observed concentrations.

Figures 30 and 31 illustrate the model's ability to predict the frequency distributions of hourly average CO concentrations. The model does well; median values have been defined within about 2 ppm of the observed values. Ninety- and 98-percentile values are within about 3 and 2-1/2 ppm, respectively. The tendency of the model to overestimate high concentrations and underestimate low is reflected in these figures. Since

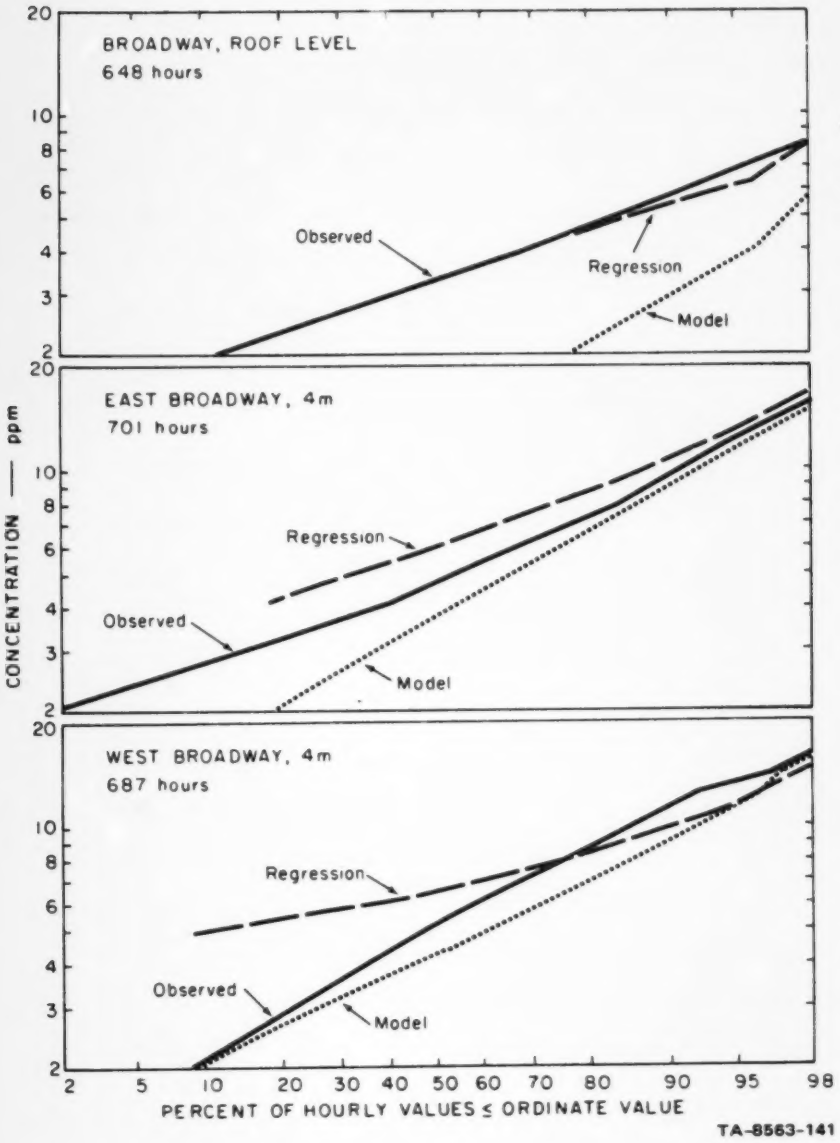

FIGURE 30 CUMULATIVE FREQUENCY DISTRIBUTIONS OF HOURLY CO CONCENTRATIONS ON BROADWAY

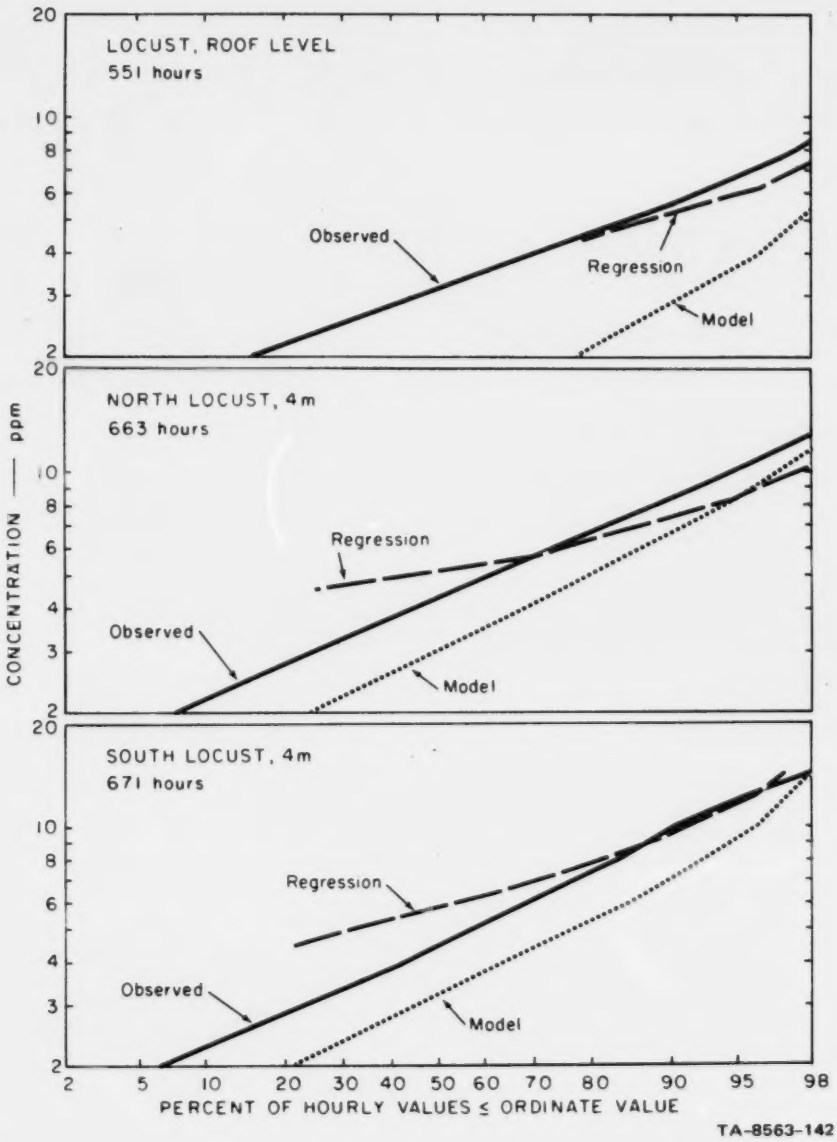

FIGURE 31 CUMULATIVE FREQUENCY DISTRIBUTIONS OF HOURLY CO CONCENTRATIONS ON LOCUST

there are many more low concentration cases than there are high, the curve based on the model calculations falls consistently below the observed values. However, because of the model's tendency to overestimate at the higher concentrations, the model curves have steeper slopes than the observed and approach them at the higher cumulative percentages.

Figures 30 and 31 show the importance of the emissions within the street canyon, particularly at higher concentrations. Comparisons of the 90-percentile concentrations at roof and street level indicate that the street-level concentrations are nearly twice those at roof level; the differences in the medians are not so pronounced, but still show that the local street emissions are of considerable importance in determining the observed CO concentrations at street level.

The curves marked "regression" in Figures 30 and 31 indicate the improvements that can be achieved through the use of the linear regression equations shown in Figure 29. Use of these relationships halves the errors in specifying the median and 90-percentile values; observed concentrations and those calculated with the regression equations have root-mean-square differences of only about 1.3 ppm.

V CONCLUDING REMARKS

A. General

The results of the St. Louis experimental and analysis program for the validation of the APRAC-1A urban diffusion model are extremely encouraging. The model had been refined and evaluated earlier during the San Jose program, with good success in predicting urban levels of CO concentration as a function of the meteorological conditions, traffic characteristics, and geographical location. On the basis of these results, the St. Louis study was formulated to evaluate the model in a significantly different environment. Specifically, the following objectives of the study have been accomplished: (1) analysis of the street canyon-flow and pollution-concentration regimes in conjunction with the evaluation of the street-effects submodel, (2) analysis of the representativeness of airport wind data, (3) further evaluation of the procedure for the estimation of urban stability and mixing depth, and (4) validation of the emissions submodel. This study has shown that the street-effects, stability, and mixing-depth submodels perform very well, but we are less certain of the performance of the emissions submodel.

On the basis of the results of the evaluation programs, it is concluded that the APRAC-1A urban diffusion model is suitable for use as an operational tool by air pollution control personnel, city planners, traffic engineers, and the like. The model has demonstrated its capacity to predict the distribution of concentrations of vehicle-generated, inert pollutants (e.g., CO) on both the urban mesoscale and the street-canyon microscale. It may therefore be used to evaluate objectively the impact of variations of meteorological conditions, vehicle emission levels, and traffic distributions, either singly or in combination.

Even with these highly significant capabilities, the APRAC-1A model provides the answers only to some, but not all, questions of vehicle-generated pollution. Three areas exist where additional development is required: (1) the distribution of pollutants on the near-freeway microscale, i.e., within the freeway corridor; (2) evaluation of vehicle emissions for traffic patterns on the local scale, i.e., of the applicability of the standard composite test route to local conditions; and (3) consideration of chemically reactive pollutants.

As the basic APRAC-1A model is currently structured, the best spatial resolution available is on the order of 65 m. This is sufficient to account for variations on the urban scale, but it may be inadequate to simulate large microscale variations in the immediate vicinity of strong emission sources. It was for this reason that a submodel was developed for street canyon effects. Similar work appears necessary for the near-freeway situation. This need is acknowledged by the federal requirements for environmental impact statements to assess in detail the effect of freeway development on air quality within the freeway corridor (a lateral distance of 350 m), as well as the mesoscale effect. Although the model can handle the latter, additional work is required to simulate the microscale structure.

Another area where additional refinement may be required is the emissions formulation. The current submodel for emissions is based on a relationship that uses average speed over a composite urban route as the independent variable. This composite route speed includes idling time at intersections as part of the average speed and, therefore, appears to give high readings for emissions along a relatively uncongested freeway. A potential for improvement of the emission rate model has been suggested by Curry and Andersen (1971). In their emission model, emission rates for CO and hydrocarbons are presented as functions of average traffic speed

over a short uniform highway segment, and corrections to the rates are presented that account for signal stops and for speed changes caused by congestion.

As currently structured, the APRAC-1A model predicts only the distribution of CO, although the treatment of other vehicle-generated pollutants is both desirable and feasible, especially on a limited scale. The very small size of the lead particulates found in the urban atmosphere and in the vicinity of freeways (Ludwig and Robinson, 1965; Robinson and Ludwig, 1967) means that they will be dispersed much like the relatively inert gas CO. For the short travel distances in the freeway corridor, the hydrocarbons should also disperse similarly to CO, in that many of them react quite slowly (Ott, 1971). On the other hand, NO, NO_2, and O_3 react very rapidly, and additional research about their distribution in the immediate vicinity of the freeway would be desirable. Qualitative analysis of these chemical reactions suggest that the problem is reasonably simple on the freeway microscale, and a solution for this special case appears tractable.

Additional research in these several areas would expand the scope of the problems to which the model can be applied but would not invalidate the usefulness of the model in the areas for which it has been developed and tested.

Appendix A

GENERAL DESCRIPTION OF THE MODEL

Appendix A

GENERAL DESCRIPTION OF THE MODEL

I. Introduction

The basic nature of the APRAC-1A diffusion model has not changed appreciably since it was first formulated (Ludwig et al., 1970). However, there has been considerable refinement in a number of areas. The model has been developed to be applied in virtually any city. As a result a number of submodels have been formulated to convert conventional, readily available meteorological data into the specialized inputs required by the model. The results of this program are intended primarily to be used as tools in planning activities for predicting the pollution patterns in any urban region that will result from planned traffic changes from predicted growth, or to be used in an operational mode for short-term predictions.

Because of the emphasis on traffic-generated pollutants, it has also been necessary to develop a submodel to describe the behavior of these effluents in the street canyons where they are often generated. Since a substantial portion of the public is exposed to pollution in these street canyons, it is quite important that the effects of the localized air circulations found in them be understood. One of the major achievements of the second phase of the research (Johnson et al.,1971) was the development of a method of describing these effects.

The current model is appropriate to quasi-inert traffic-generated pollutants. The submodel that is used to convert traffic data to emissions is for the specific pollutant carbon monoxide (CO). In principle, another submodel could be substituted that would be appropriate to another pollutant such as lead aerosol.

Preceding page blank

The modular nature of the model is one of its important features. It has been designed for relative ease in incorporating new findings without requiring complete reorganization of the model. Thus when better methods or better data are available for determining atmospheric stability, mixing depth, or other parameters, they can be used to design submodels to replace the submodels now used.

This Appendix describes the model in general terms. The detailed development of the equations is given in the earlier reports (Ludwig et al., 1970; Johnson et al., 1971) and in the body of this report. The listing of the computer programs that actually constitute the APRAC-1A model is given in the user's manual (Mancuso and Ludwig, 1972).

2. General Organization of the Model

a. The Basic Model

The model uses a combination of the "Gaussian plume" and "box model" diffusion formulations. Basically, the Gaussian plume model assumes that the vertical concentration profile from a cross-wind line source is Gaussian in shape as shown in Figure A-1. The spread of this vertical concentration distribution is described by its standard deviation, σ_z. On the basis of experimental data, the vertical diffusion parameter σ_z is taken to have the form

$$\sigma_z = ax^b \quad , \qquad (A\text{-}1)$$

where x is the downwind distance and the parameters a and b depend upon atmospheric stability. The functions used in the model are based on the analysis of urban tracer tests (see Johnson et al., 1971). Figure A-2 shows how σ_z varies with x and atmospheric stability. The curves in the figure represent conditions from extremely unstable (A) to moderately stable (E).

When vertical mixing is inhibited, the box model is applied to emissions from sources relatively distant from the receptor. The receptor

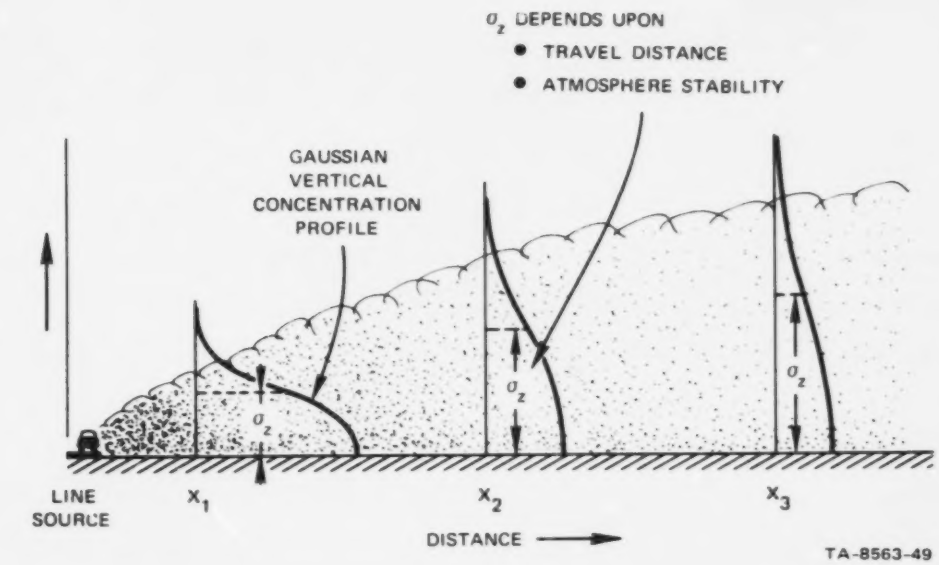

FIGURE A-1 VERTICAL DIFFUSION ACCORDING TO GAUSSIAN FORMULATION

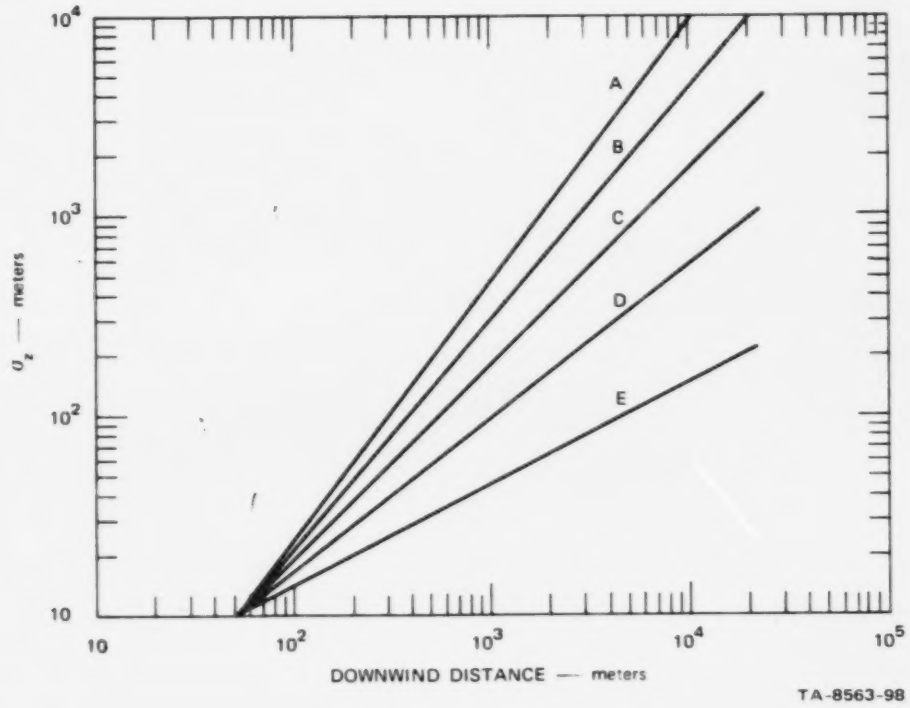

FIGURE A-2 VERTICAL DIFFUSION AS A FUNCTION OF TRAVEL DISTANCE AND STABILITY CATEGORY, AS REVISED FOR URBAN CONDITIONS

is the point for which the concentrations are being calculated. Emissions tend to become uniformly distributed in the vertical up to the limiting mixing height after sufficient travel has taken place.

The models are applied to ten area sources, each of which is assumed to have source emissions spread uniformly throughout. These area sources are oriented in the upwind direction as shown in Figure A-3. The logarithmic spacing of the area boundaries allows the nearby sources to be considered in greater detail than the farther sources, whose individual contributions tend to be merged during their longer travel. The contributions of each of the ten area sources to the CO concentration at the receptor are computed individually with one of the simple formulations given below. For the closer segments the Gaussian formulation is used to obtain the concentration C_i resulting from emissions in the i^{th} segment:

$$C_i = \frac{0.8\, Q_{Ai}}{u\, a_j} \left(1 - b_j\right)^{-1} \left(x_{i+1}^{1-b_j} - x_i^{1-b_j}\right) , \qquad \text{(A-2)}$$

where Q_{Ai} is the average area emission rate (g m^{-2} s^{-1}), u is the transport wind speed (m s^{-1}), and a_j and b_j are the constants appropriate to the segment and atmospheric stability class j. The x's are the distances to the closest boundary of the segment designated by the subscript, i.

The model changes from the Gaussian formulation to the box model at a distance where the two (in their respective line source formulations) give equal surface concentration values. The box model concentration is given by the following equation:

$$C_i = Q_{Ai} \frac{x_{i+1} - x_i}{u_t h} , \qquad \text{(A-3)}$$

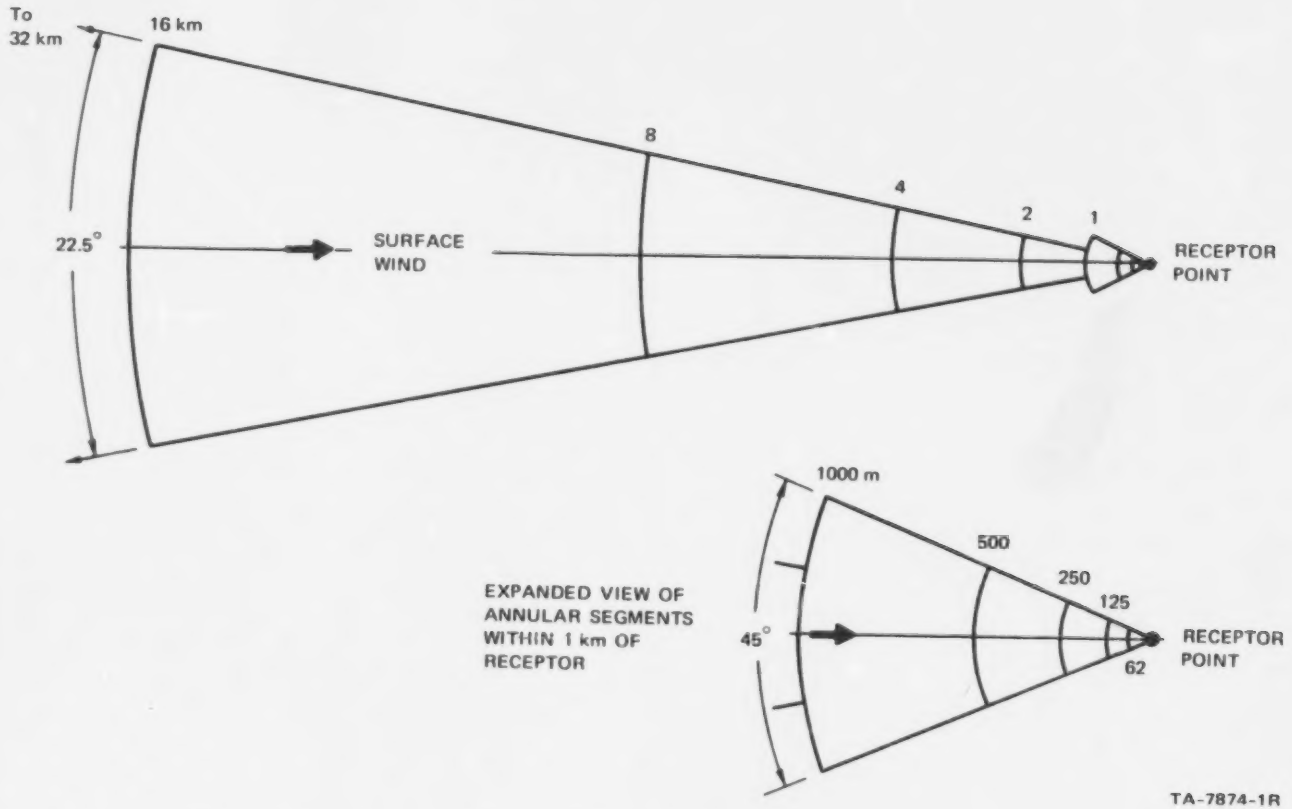

FIGURE A-3 DIAGRAM OF SEGMENTS USED FOR SPATIAL PARTITIONING OF EMISSIONS

where h is the mixing height. The contributions of the emissions in each segment, as determined from Eqs. (A-2) and (A-3), are summed to obtain the concentration at the receptor.

The input variables required for application of the basic model are: (1) traffic emissions, (2) mixing height, (3) atmospheric stability type, and (4) transport wind speed and direction. The model is designed to be applicable to any city, where traffic data and conventional (airport) weather observations are available. None of the required input variables are directly observed. The airport surface wind speed and direction have been applied as a first approximation to the transport wind, but suitable adjustments need to be made to account for urban effects. Separate submodels had to be developed to estimate mixing depths and stability categories from the available airport observations, and emissions from the daily traffic volumes on the major city streets.

The basic model treats the dispersion process only on the urban mesoscale, whereas concentrations at specific locations may be strongly influenced by microscale effects. One of the principal accomplishments of this program has been the development and validation of a street-scale submodel that describes microscale effects and thereby substantially improves the performance of the overall model.

b. Emissions Submodel

Instead of an emissions inventory, such as is used for other pollutants, the CO model uses a traffic inventory. An example of a network of traffic "links," in this case for Chicago, is shown in Figure A-4. Each straight road segment, or link, is assigned an average daily traffic volume, based on historical or forecast data. Each link is identified in the computer memory by its length and the geographical locations of its endpoints and is designated as a particular road type. To calculate emissions for a given time, daily traffic volumes are

FIGURE A-4 COMPUTER DISPLAY OF TRAFFIC LINKS FOR CHICAGO

multiplied by a temporal adjustment factor to obtain traffic volumes for a particular hour. Then the emission rate, E (g-CO vehicle-mi^{-1}), is estimated from the mean vehicle speed, S (mi h^{-1}), by an empirical equation of the form

$$E = \alpha S^{-\beta} \quad . \qquad \text{(A-4)}$$

Here α and β are constants that depend on the characteristics of the emission control devices installed and the mixture of old and new model cars on the road. For the calculations given in this report α was taken to be 700 and β to be 0.75. These values are appropriate to a mixture of about half pre-1968 (1966 for California) and half newer cars (Johnson et al., 1971). For cars produced since 1968, the value of β has been 0.48. Existing and potential legislation requires α to decrease with time, as shown in Table A-1. For future years, the effective values of α and β for use in Eq. (A-4) have to be determined on the basis of the fraction of the total cars represented by each model year.

Table A-1

VALUES OF α FOR CARS PRODUCED AFTER 1970

Model Years	α
1972 - 1974	160
1975 - 1979	16
After 1980	8

The values of S in Eq. (A-4) are based on the road type and the time of day (whether during peak or off-peak traffic conditions). The total hourly CO emission for a given traffic link is the product of three factors: the emission rate, the length of the link, and the hourly traffic volume. The emissions from all the links and parts of links that fall within one of the segments in Figure A-3 are summed to determine the average emission rate for that segment.

c. Mixing Height Submodel

The determination of mixing height is based on the physical characteristic that a mixed layer of the atmosphere has an adiabatic lapse rate. Thus, by using the observed morning lapse rate obtained from the nearest National Weather Service radiosonde station and the surface temperature at a given hour during the day, it is possible to determine at which height a parcel of air lifted adiabatically would reach a temperature observed by the radiosonde. This is the mixing height, and the method of determination is the one commonly used (e.g., Holzworth, 1967).

During the daylight hours the observed surface temperatures at the airport observing site are used as a basis for the determination of mixing height. During the predawn hours the airport temperatures are augmented by an amount determined from an empirical relationship that accounts for urban heat island effects. During the post sunset hours the model interpolates between the afternoon mixing depth and that for the predawn hours of the following morning.

d. Stability Submodel

In order to select the proper function to use for σ_z, it is necessary to categorize the atmospheric stability. Pasquill (1961) in originally proposing the Gaussian plume approach to describing atmospheric diffusion, suggested that wind fluctuation data be used. Wind fluctuations are not routinely measured and cannot be used as inputs for a model designed for widespread practical application. Therefore, the stability submodel has employed an alternative approach suggested by Pasquill; this alternative method makes use of wind speed, cloud cover, and intensity of insolation. The last factor is not measured, but the St. Louis experiments indicate that it can be estimated with sufficient accuracy from solar elevation angle and opaque cloud cover.

In essence, the submodel consists of a table wherein daytime stability class is related to five classes of surface wind speed and three classes of insolation strength. Nighttime stability is tabulated according to wind speed and two classes of cloud cover. In general, daytime stability increases with wind speed and decreases with increased solar heating. At night, the stability increases with the increased surface cooling that accompanies clear skies. Higher nighttime winds will diminish the effectiveness of the cooling and reduce the stability. The table used by the model reflects these effects. It is based on Pasquill's table which summarizes the interpretation of numerous field tracer studies.

e. Winds

The model's treatment of the winds that advect the pollutants is quite simple, of necessity. First, the wind is taken to be uniform in speed and direction over the entire urban area. This assumption is dictated by the fact that many cities have only one wind measurement site. For areas of relatively simple geography, it does not appear to be a serious shortcoming. It is most serious for areas that are subject to land-sea breeze circulations.

Two wind speeds are used with the model; both can be derived from the airport value. The first wind speed is the transport wind speed, or the average wind speed through the mixing layer. This has been found in St. Louis to be reasonably well correlated with airport measurements (Wuerch, 1971) and for reasons given in the body of the report we have chosen to use the value measured at the airport. The other wind speed that is important in the model is the "roof-level" wind. It tends to be less than the airport wind, but it is relatable to it (Johnson et al.,1971; Schnelle et al.,1969). The roof-level wind affects the dilution and small-scale transport of pollutants released within the street canyons and serves as one of the inputs to the street canyon effects submodel discussed below.

f. Street Canyon Effects Submodel

The street canyon effects submodel was developed as a result of studies in San Jose, California. These studies indicated that CO concentrations could change by a factor of 2, or several parts per million from one side of the street to the other. With such large gradients, it is apparent that the effects must be included if reliable comparisons are to be made with observed concentrations in such areas.

Observations have shown that when the roof-level wind blows within about $\pm 60^{o}$ of the cross-street direction, a helical circulation develops in the street. At street level the cross-street component is opposite the roof-level wind direction, causing a down flow of relatively clean air in front of the "downwind" buildings that face the roof-level wind, and an upflow across the street. Resulting low-level CO concentrations in front of the downwind buildings are appreciably less than those observed across the street. When winds are approximately parallel to the street, cross-street gradients of CO are quite small.

A simple model based on physical principles is used to describe the observed distribution of CO in the street canyon. First, the model assumes that the emissions from the local street traffic are added to the CO already present in the air that enters from roof level. These additive concentrations are proportional to the local street emissions, Q_L(g m^{-1} s^{-1}), and inversely proportional to the roof-level wind speed u (m s^{-1}), augmented by a small amount (0.5 m s^{-1} has been found to work well) to account for the mechanically induced air movement caused by traffic.

In front of the downwind buildings the air begins its downward flow at roof-level concentration. Pollutants are gradually entrained as the air sinks toward street level, so CO concentrations on this side of the street increase slightly in the downward direction. The CO that is added should be inversely proportional to the width of the street W and

the wind speed u, because these two factors govern the volume of air available for dilution of the emissions from the vehicles in the street. The added pollutants should be directly proportional to the rate Q at which these emissions are released. Entrainment has been assumed to vary linearly with height z through the depth (H) of the street canyon. Thus the amount of CO that is added to the roof-level concentrations is given by the following equation for the side of the street on which the buildings face the wind:

$$\Delta C = K \frac{Q_L}{W(u + 0.5)} \quad \frac{H-z}{H} \quad . \qquad \text{(A-5)}$$

On the upwind side of the street the model uses box model reasoning. The volume into which the emissions are mixed is limited by the air circulation toward the buildings and upward. As the air moves from the street-level source, the volume into which the pollutants are mixed increases, so the concentration is taken to be inversely proportional to the slant distance, r, between the receptor and the nearest traffic lane. For concentrations in front of the upwind buildings, the equation is:

$$\Delta C = K \frac{Q_L}{r(u + 0.5)} \quad . \qquad \text{(A-6)}$$

The constant, K, is the same for both equations. When the wind blows nearly parallel to the street, the additive concentration, ΔC, is described by the average of the values from the above two equations and is the same on both sides of the street. The development of these equations is discussed in greater detail in Johnson et al. (1971) and in the body of this report.

3. Uses of the Model

a. General

The model has several available outputs, each designed to satisfy particular needs. Hourly concentrations for a few locations can be calculated as a function of time. Certain simplifications can be incorporated so that hourly concentrations can be calculated for periods of time up to several years. This provides a basis for determining frequency distributions and other statistical features of the calculated concentrations for the location. Finally, the concentrations can be calculated for various locations in a geographical grid, using current or forecast meteorological data. From such calculations detailed horizontal concentration patterns can be developed for operational or planning purposes.

The model can be applied to current or forecast traffic patterns. Thus, there is the very important capability to determine in advance what the effects of planned highways will be. These effects can be determined as an area-wide pattern for specific meteorological conditions, or on a climatological basis for a limited number of arbitarily chosen special points. In the following sections some examples are given of these various applications.

b. Hourly Concentration Sequences and Climatological Outputs

Figures A-5 and A-6 are examples of calculated concentrations for extended periods; Figure A-5 is for conditions in San Jose using an earlier version composite model, while results from the first version of the basic model are shown in Figure A-6 for Cincinnati. Figure A-6 also shows observed winds and cloud amounts and the mixing heights and stabilities determined by the model. This type of calculation is most useful for evaluating the performance of the model

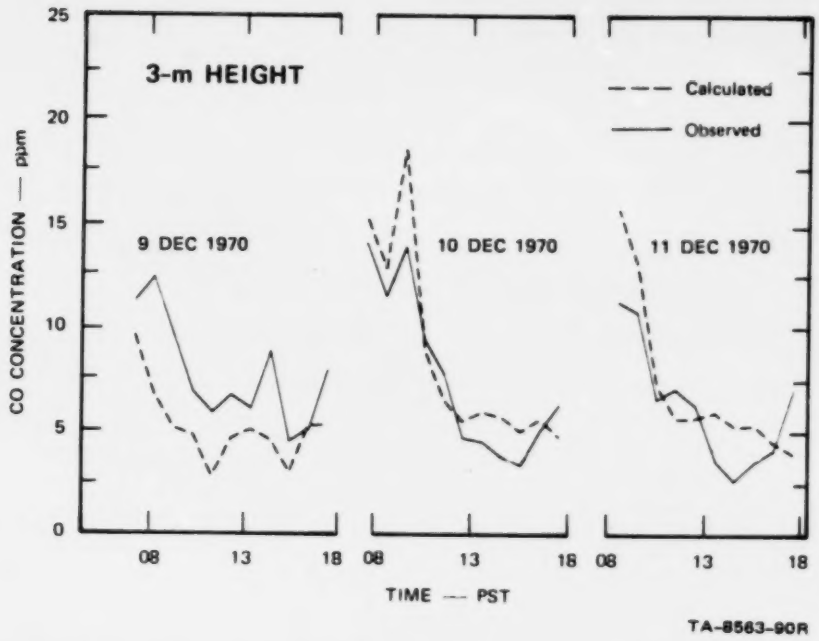

FIGURE A-5 CALCULATED AND OBSERVED CO CONCENTRATIONS FOR A MIDBLOCK LOCATION IN SAN JOSE

and comparing it with the observed patterns. If such calculations are applied to several years of weather data, then the results can be interpreted as shown in Figure A-7. This figure shows the calculated frequency distribution of CO concentration for weekdays, Saturday, and Sunday for a downtown St. Louis location with 1965 traffic conditions.

If the model is reapplied in the same manner, but with emissions appropriately projected for traffic conditions at some future time, then frequency distributions can be forecast. Figure A-8 shows the results for the same St. Louis location, using a forecast of 1990 traffic and assuming that the auto population has the emission controls that can be anticipated from current federal regulations. This figure also shows the effects of changing the averaging time. As the averaging time is increased, the spread of the frequency distribution decreases.

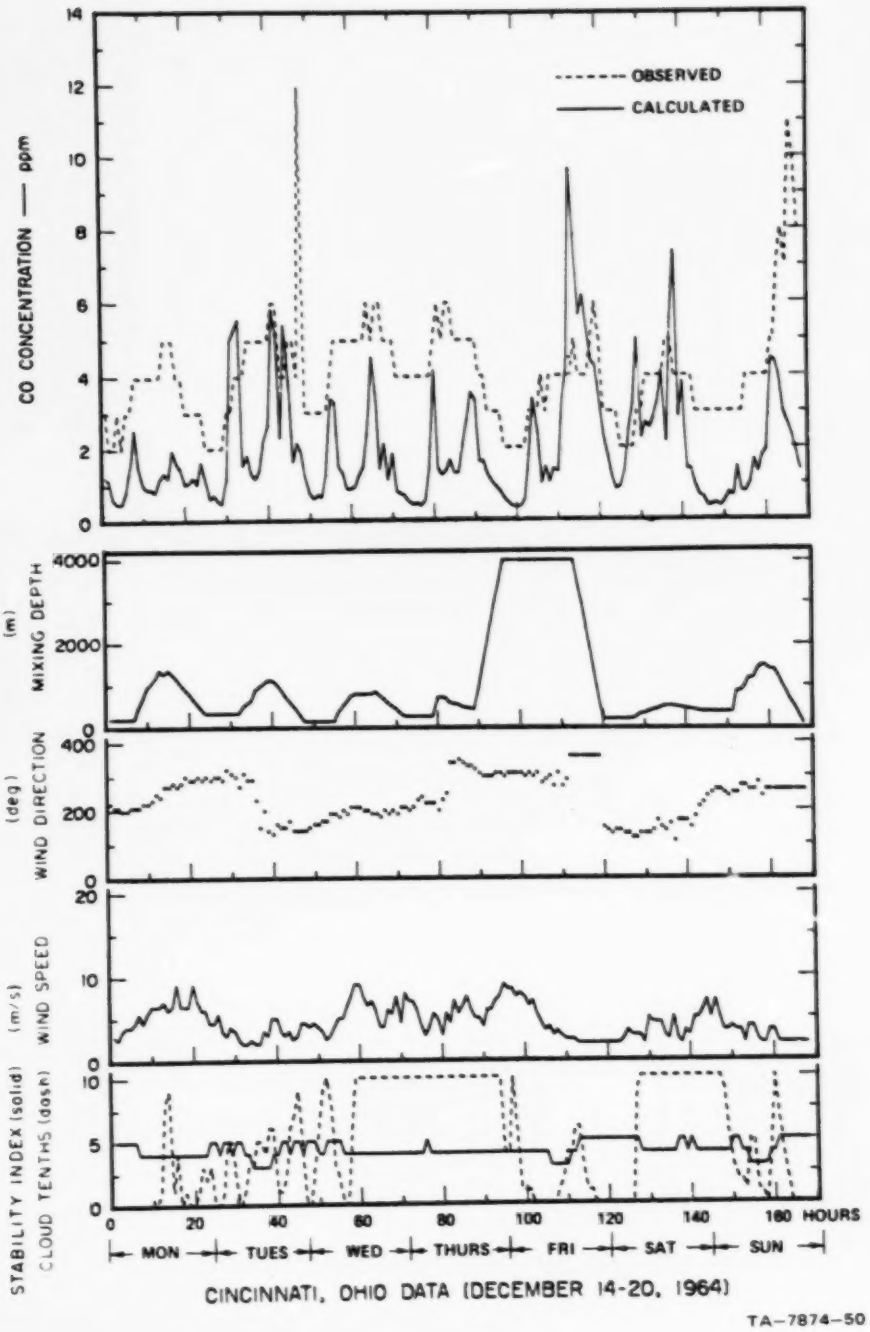

FIGURE A-6 OBSERVED AND CALCULATED CO CONCENTRATIONS AT THE CINCINNATI CAMP STATION, 14-20 DECEMBER 1964

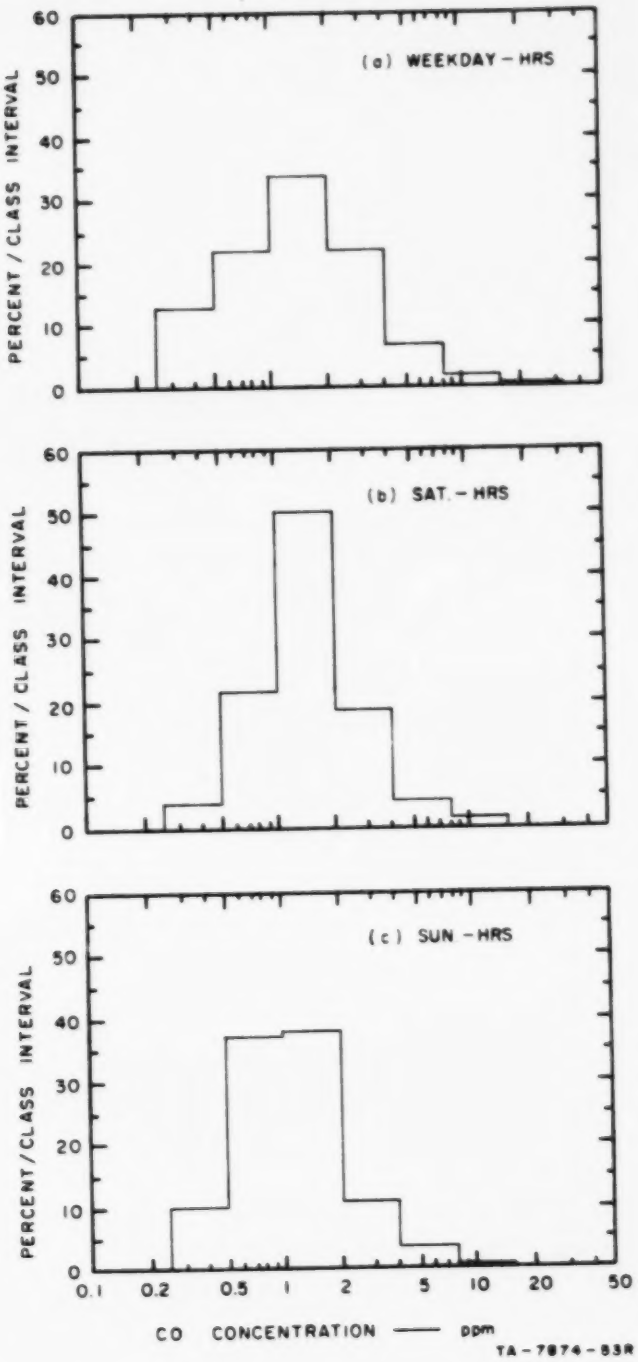

FIGURE A-7 CALCULATED ST. LOUIS CAMP STATION CO CONCENTRATION FREQUENCY DISTRIBUTION FOR 1965 TRAFFIC CONDITIONS— WEEKDAY, SATURDAY, AND SUNDAY HOURS

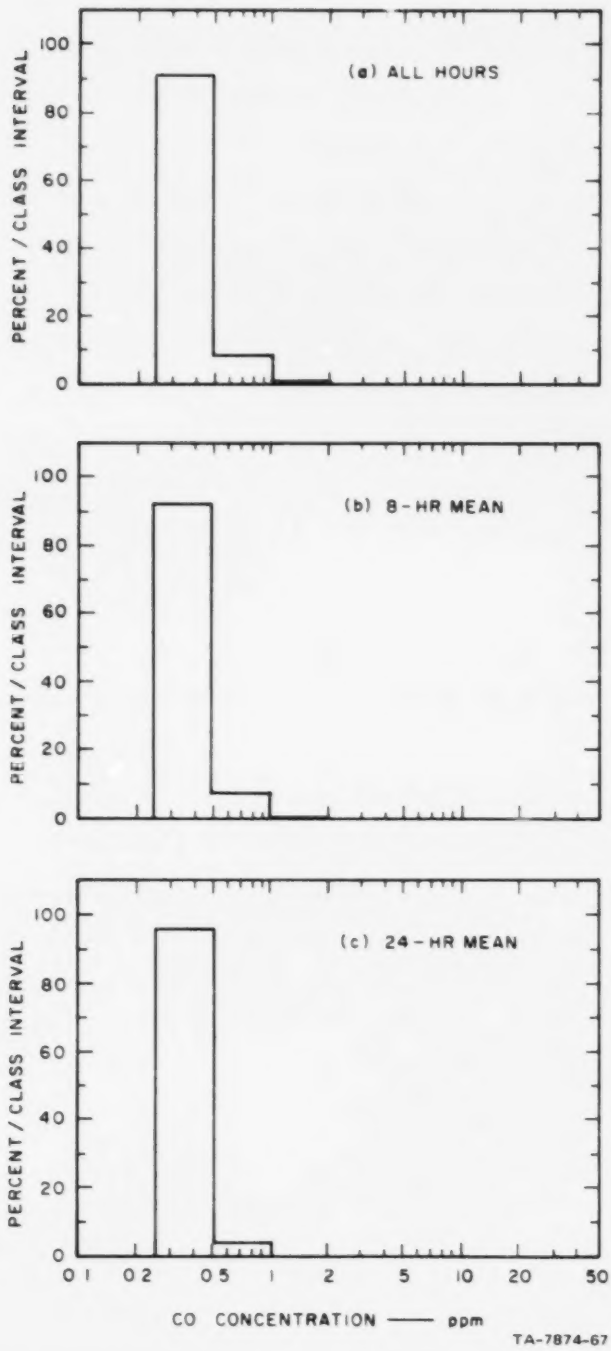

FIGURE A-8 CALCULATED ST. LOUIS CAMP STATION CO CONCENTRATION FREQUENCY DISTRIBUTION FOR 1990 TRAFFIC CONDITIONS— 1-HOUR, 8-HOUR, AND 24-HOUR AVERAGES

c. Maps of Concentration Distribution

For operational applications, the ability of the model to produce a map of expected CO concentration in an urban area is quite useful. This capability is illustrated in Figure A-9. This figure also illustrates the ability of the model to calculate results for different grid spacing. In the upper part of the figure, concentrations at 625 grid points spaced at 1-mile intervals were calculated, and from these the computer analysis that is shown was prepared. The calculations were repeated for a smaller area with smaller grid-point spacing resulting in the more detailed picture of CO distribution shown in the lower part of the figure.

The grid-point calculations can also be used for planning purposes. Figure A-10 shows the results of applying the model for three different emission fields while maintaining the same meteorological inputs. In this case, the three fields were calculated for morning rush hour traffic, relatively stable atmospheric conditions, a mixing height of 120 m, and a 2 m s^{-1} west wind. Figure A-10(a) shows the field for 1964 traffic; Figure A-10(b) shows the field for 1990 traffic with no emission controls on the vehicles; and Figure A-10(c) illustrates the effects of introducing the anticipated emission control devices.

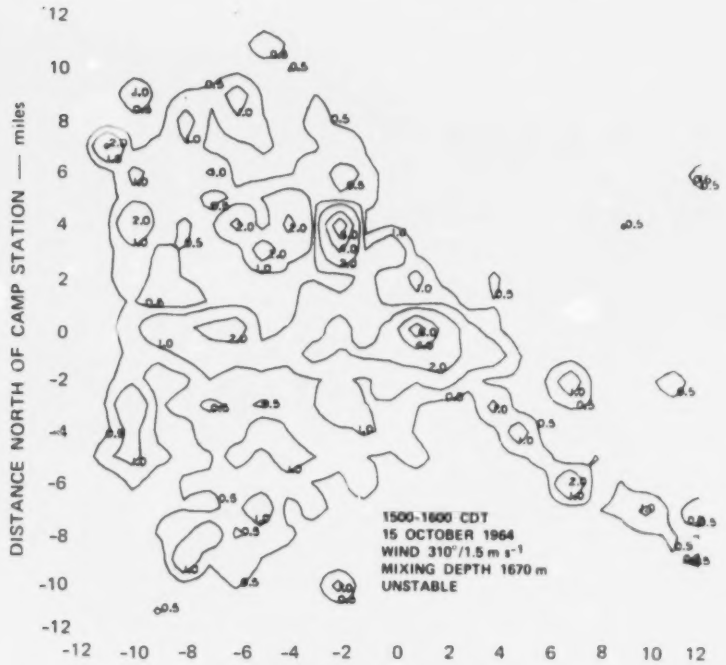

(a) 1-MILE (1.6 km) GRID SPACING

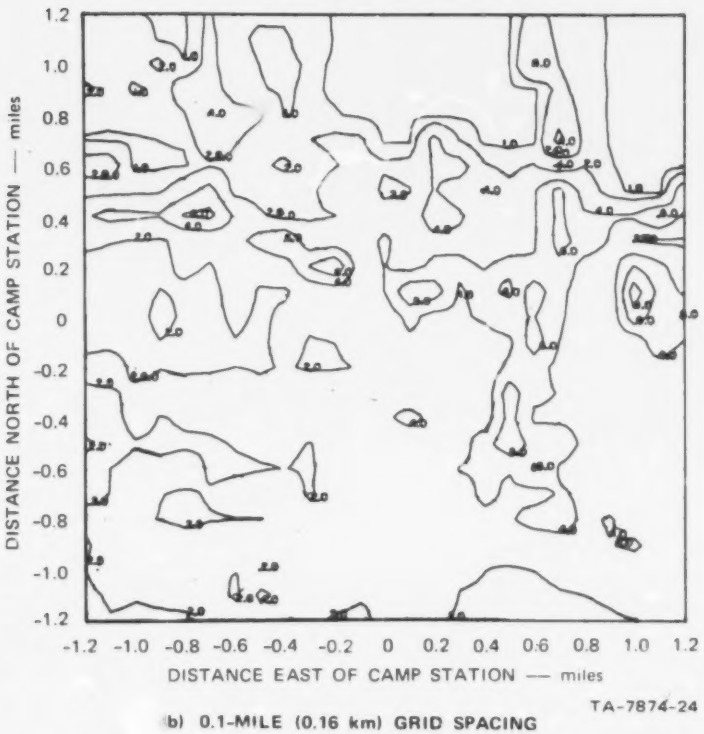

(b) 0.1-MILE (0.16 km) GRID SPACING

FIGURE A-9 CALCULATED ST. LOUIS CONCENTRATION PATTERNS FOR TWO GRID SIZES

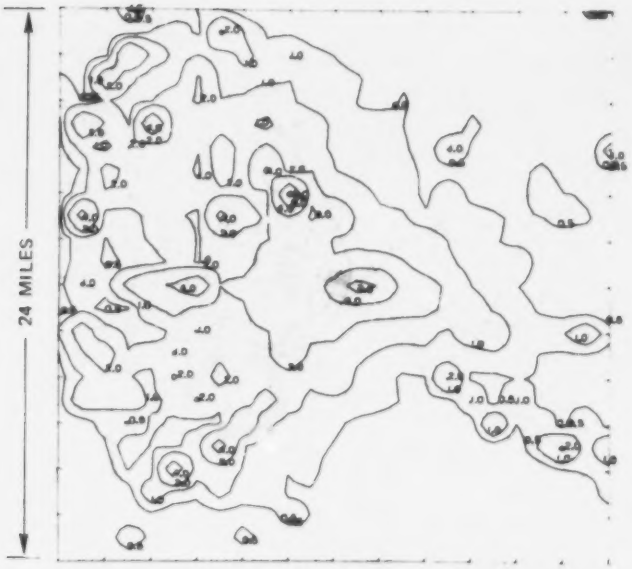

(a) 1964, BASED ON HISTORICAL TRAFFIC DATA

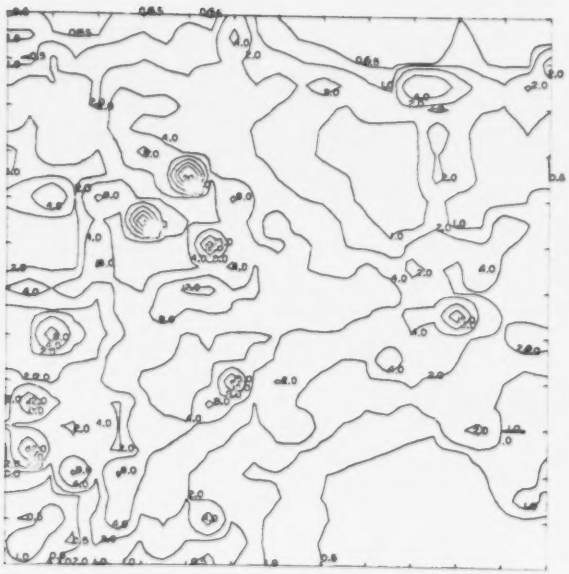

(b) 1990 FORECAST TRAFFIC WITHOUT EMISSION CONTROLS

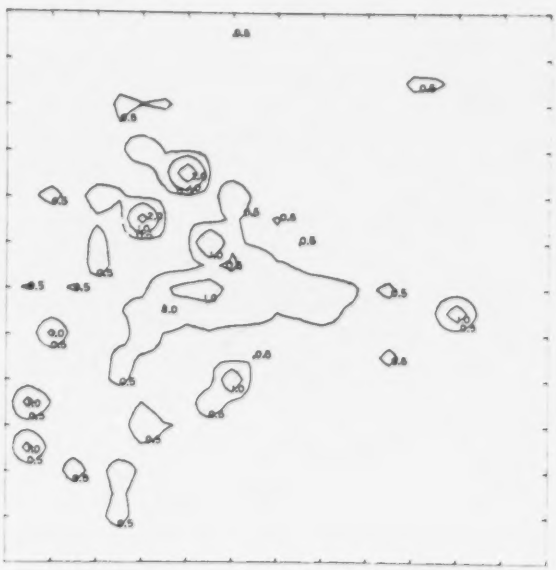

(c) 1990 FORECAST TRAFFIC WITH EMISSION CONTROLS

TA-653583-16

FIGURE A-10 CALCULATED CO CONCENTRATIONS IN ST. LOUIS FOR HISTORICAL AND FORECAST TRAFFIC CONDITIONS

Appendix B

LIST OF SYMBOLS

Appendix B

LIST OF SYMBOLS

Symbol	Unit	Definition	Equation Number(s)
a, a_j	m	Coefficient used in representing the vertical dispersion coefficient (for stability class j) as an exponential function of travel distance from source	(A-1), (A-2)
b, b_j	Dimensionless	Exponent used in representing the vertical dispersion coefficient (for stability class j) as an exponential function of travel distance	(A-1),(A-2)
C, C_i	gm m^{-3}	CO concentration arising from emissions in the i^{th} segment (see Fig. A-3)	(A-2),(A-3)
c	ppm	Term used to correct for zero offset in CO instrumentation	(1)
d	Dimensionless	Coefficient used to correct for span changes in CO instrumentation	(1)
E	gm(vehicle-mile)$^{-1}$	CO emission rate	(A-4)
H	m	Depth of street canyon	(6),(8),(A-5)
h	m	Mixing height	(A-3)

Preceding page blank

Symbol	Unit	Definition	Equation Number(s)
K	Dimensionless	Proportionality constant used in street canyon submodel. K found to equal 7 in San Jose and St. Louis	(5),(6),(7),(8), (A-5),(A-6)
N	Vehicles hr^{-1}	Traffic volume	(5),(6),(7),(8), (A-5),(A-6)
N	Dimensionless	Fraction of sky covered by opaque clouds	(2)
Q_{Ai}	gm m^{-2} s^{-1}	Area source emission rate for i^{th} segment	(A-2),(A-3)
Q_L	gm m^{-1} s^{-1}	Line source emission rate	(A-5),(A-6)
r	m	Straight-line distance between receptor and nearest traffic lane	(A-6)
S	mi hr^{-1}	Average vehicle speed on traffic link	(5),(6),(7),(8), (A-5),(A-6)
u	m s^{-1}	Wind speed at roof level	(5),(6),(7),(8), (A-4)
u_a	m s^{-1}	Wind speed measured at airport	(3),(4)
u_t	m s^{-1}	Transport wind speed in mixing layer	(3),(4),(A-2), (A-3)

Symbol	Unit	Definition	Equation Number(s)
u,v,w,	$m\ s^{-1}$	Wind components measured in street canyon experiment; u, parallel to Locust Street, positive toward east; v parallel to Broadway positive to north; w positive upward (see Fig. 3)	
W	m	Street width	(5),(6),(8), (A-5)
x	m	Travel distance from source to receptor	(A-1)
x	m	Cross-street distance from receptor to nearest traffic lane	(7),(8)
x_i	m	Distance from receptor to nearest boundary of the i^{th} segment (see Fig. A-3)	(A-2),(A-3)
z	m	Height of receptor	(6),(7),(8), (A-5)
α	$gm(vehicle\ mi)^{-1}$	Coefficient in exponential equation describing automotive emissions as a function average vehicle speed	(A-4)
α	Degrees	Solar elevation angle	(2)
β	Dimensionless	Exponent in equation describing automotive emissions as a function of average vehicle speed	(A-4)

Symbol	Unit	Definition	Equation Number(s)
ΔC	ppm	Concentration at receptor minus roof level concentration	(A-5),(A-6)
ΔC_I	ppm	Some as ΔC, but specifically for winds within 30^o of the street direction	(8)
ΔC_L	ppm	Same as ΔC, but for receptors in front of buildings facing in the direction the roof-level wind is blowing	(7),(8)
ΔC_W	ppm	Same as ΔC, but for receptors in front of buildings facing toward the roof-level wind	(5),(6),(8)
σ_z	m	Vertical dispersion coefficient (see Fig. A-1)	(A-1)
Φ	Dimensionless	Insolation parameter	(2)

REFERENCES

Chagnon, S. A., Jr., 1971 Operational Report for METROMEX, Argonne National Laboratory, University of Chicago, Illinois State Water Survey, and University of Wyoming.

Chandler, T. J., 1965: The Climate of London, Hutchison and Co., Ltd., London, 292 pp.

Chang, P. C., P. N. Wang, and A. Lin, 1971: Turbulent diffusion in a city street, Air Pollution, Turbulence and Diffusion Symposium, December 7-10, 1971, New Mexico State University, Las Cruces, New Mexico.

Curry, D. A., and D. G. Andersen, 1971: Procedures for estimating highway user costs and air and noise pollution effects, Final Report, Highway Research Board Project 7-8, Stanford Research Institute, Menlo Park, California.

Dabberdt, W. F., 1968a: Tower-induced errors in wind profile measurements, J. Appl. Met., 7, 359-366.

Dabberdt, W. F., 1968b: Wind disturbance by a vertical cylinder in the atmospheric surface layer, J. Appl. Met., 7, 367-371.

Holzworth, G. C., 1967: Mixing depths, wind speeds, and air pollution potential for selected locations in the United States, J. Appl. Met., 6, 1039-1044.

Johnson, W. B., W. F. Dabberdt, F. L. Ludwig and R. J. Allen, 1971: Field study for initial evaluation of an urban diffusion model for carbon monoxide, Comprehensive Report for Coordinating Research Council and Environmental Protection Agency, Contract CAPA-3-68 (1-69), Stanford Research Institute, Menlo Park, California, 240 pp., National Technical Information Service No. PB 203469.

Junge, C. E., 1963: Air Chemistry and Radioactivity, Academic Press, New York, 392 pp.

Ludwig, F. L., 1970: Urban air temperatures and their relation to extraurban meteorological measurements, paper presented at Semiannual Meeting of the American Society of Heating, Refrigerating and Air-Conditioning Engineers, January 19-22, 1970, San Francisco, California.

Ludwig, F. L., W. B. Johnson, A. E. Moon, and R. L. Mancuso, 1970: A practical multipurpose urban diffusion model for carbon monoxide, Final Report, Coordinating Research Council Contract CAPA-3-68, National Air Pollution Control Administration Contract CPA 22-69-64, Stanford Research Institute, Menlo Park, California, 184 pp., National Technical Information Service No. PB 196003.

Ludwig, F. L., and J. H. S. Kealoha, 1968: Urban Climatological Studies, Final Report, Contract CD-DAHC-20-67-C-0136 (Work Unit 1235A), Stanford Research Institute, Menlo Park, California, 195 pp., National Technical Information Service No. AD 672 071.

Ludwig, F. L., and E. Robinson, 1965: Size distribution studies with the aerosol spectrometer., J. Air Poll. Cont. Assoc., 15, 102.

Mancuso, R. L., and F. L. Ludwig, 1972 (in preparation): User's Manual for the APRAC-1A Diffusion Model Computer Program, Coordinating Research Council and Environmental Protection Agency, Contract No. CAPA-3-68(1-69), Stanford Research Institute, Menlo Park, California.

McElroy, J. L., and F. Pooler, Jr., 1968: St. Louis dispersion study, Vol. II--Analysis, 51 pp., National Air Pollution Control Administration Publication No. AP-53, 51 pp.

Missouri State Highway Department, 1970: Traffic map of St. Louis, St. Louis County and St. Charles City.

Ott, Wayne, 1971: An urban survey technique for measuring the spatial variation of carbon monoxide concentrations in cities. PhD thesis, Dept. Civil. Eng., Stanford University, Stanford California 153 pp.

Pasquill, F., 1961: The estimation of the dispersion of windborne material, Meteorological Mag. (London), 90, pp. 33-49.

Pooler, F., 1966: A tracer study of dispersion over a city, J. Air Poll. Contr. Assoc., 11, pp. 677-681.

Robinson, E., and F. L. Ludwig, 1967: Particle size distribution of urban lead aerosols, J. Air Poll. Cont. Assoc., 17, 664.

Schnelle, K. B., F. G. Ziegler, and P. A. Krenkel, 1969: A study of the vertical distribution of carbon monoxide and temperature above an urban intersection, APCA Paper No. 69-152, Air Pollution Control Association.

Slade, D. H. (ed.), 1968: Meteorology and Atomic Energy, U.S. Atomic Energy Commission, Oak Ridge, Tennessee.

Smith, M. (ed), 1968, Recommended Guide for the Prediction of the Dispersion of Airborne Effluents, American Society Mechanical Engineers, New York.

Smithsonian Institution, 1951: Smithsonian Meteorological Table, 527 pp.

Stanford University Aerosol Laboratory and The Ralph M. Parsons Co., 1953a: Behavior of aerosol clouds within cities, Joint Quarterly Report No. 3, January-March 1952, Contracts DA-18-064-CML-1856 and DA-18-064-CML-2282, DDC No. AD31711.

Stanford University Aerosol Laboratory and The Ralph M. Parsons Co., 1953b: ibid; Joint Quarterly Report No. 4, April-June 1953, DDC No. AD31508.

Stanford University Aerosol Laboratory and The Ralph M. Parsons Co., 1953c: ibid; Joint Quarterly Report No. 5, July-Sept., 1953, 238 pp., DDC No. AD31507.

Stanford University Aerosol Laboratory and The Ralph M. Parsons Co., 1953d: ibid; Joint Quarterly Report No. 6, Vol. I, October-December, 1953, DDC No. AD31510.

Stanford University Aerosol Laboratory and The Ralph M. Parsons Co., 1953e: ibid; Joint Quarterly Report No. 6, Vol. II, October-December 1953, DDC No. AD31711.

Turner, D. B., 1964: A diffusion model for an urban area, J. Appl. Met., 3, 83-91.

Wuerch, D. E., 1970: A comparison of observed and calculated urban mixing depths, Environmental Sciences Services Administration Technical Memorandum WBTM CR-36.

Wuerch, D. E., 1971: An investigation of the resultant transport wind within the urban complex, National Oceanic and Atmospheric Administration Technical Memorandum NWS CR-44.